Exploring the roles of seasonality and demography in tick borne disease dynamics

Asena Goren

Dissertation presented for the degree of
Philosophiae Doctor (PhD)
2024

Centre for Ecological and Evolutionary Synthesis (CEES)
Department of Biosciences
Faculty of Mathematics and Natural Sciences
University of Oslo

Series of dissertations submitted to the
Faculty of Mathematics and Natural Sciences, University of Oslo
No. 2741

ISSN 1501-7710

Cover: UiO.
Print production: Graphic center, University of Oslo.

Table of Contents

Summary (English summary) I

Sammendrag (Norwegian summary) V

List of Papers VIII

Acknowledgments XI

Introduction 1

Seasonal Ecology 1

Seasonality and Disease 2

Lyme disease 4

Climate Change in Norway 7

Aims 10

Study System 11

Lyme Disease Emergence 11

Clinical Manifestations 12

Tick Vectors 14

Hosts 17

Pathogens 17

Methods 19

Analysis of Lyme Disease Surveillance Data 19

Matrix Population Models 20

Main Results 22

Discussion 24

Shifting Seasons as a Driver of Disease Emergence 24

Case Seasonality Analysis 26

Demography and Sociological Features 28

Insights from Mathematical Models 30

Bibliography 35

Summary (English summary)

The most common vector borne disease in the Northern Hemisphere is Lyme disease, a bacterial infection vectored by ticks. Recent changes in climate, land use, and wildlife communities have resulted in the rapid emergence (increased incidence) of Lyme disease, which is both spreading in geographic extent and exhibiting increased incidence in many areas where the disease is already established. Climate change has been observed to disrupt the timing and duration of seasonal cycles, impacting ecosystems globally by changing species distributions, abundances, and phenology (timing of periodic life events). Disruptions of the phenological synchrony between interacting species, termed phenological mismatch, is known to impact population and evolutionary dynamics. However, the importance of phenological relationships for disease dynamics has not been well explored. A more in-depth understanding of phenological synchrony is crucial in the field of vector-borne disease ecology, where complex interactions between multiple host and vector species drive the circulation of pathogens in ecosystems. In this thesis, I use Lyme disease as a case study to explore the effects of changing seasonality on tick borne disease ecology. In **Papers 1** and **2**, surveillance data is used to investigate seasonal and demographic trends in Lyme disease cases, while in **Paper 3** a mathematical model is used to explore phenological and demographic effects on pathogen transmission between a small mammal host and tick vector.

In **Paper 1**, statistical analysis of surveillance data from Norway quantified changes in the seasonal timing and annual incidence of Lyme disease over a 25-year study period (1995-2019). The surveillance data captures disease emergence at the expanding northern biogeographical edge of Lyme disease in Europe. A modern Bayesian statistical framework was used to fit a flexible seasonal model across the entire study period to measure changes in

the peak incidence week. This analysis demonstrated a six-week advancement in case timing accompanying an increase in incidence across regions of Norway. The change in timing of plant greening, derived from Normalized Difference Vegetation Index (NDVI), was used as a yardstick to contextualize the magnitude of the seasonal shift in case timing. While following a similar pattern, the shift in case timing outpaced a concurrent advancement of peak spring greening by around two weeks.

In **Paper 2**, the Norwegian Lyme disease surveillance data is used to explore demographic patterns in patient clinical manifestations and case timing. This analysis identified a bimodal pattern of incidence across patient age, with children and seniors having disproportionately high incidence rates. Youth presented with a higher proportion of neuroborreliosis cases than adults, and among adults the proportion of arthritis cases was higher in males than females. Case timing was found to be consistently around 4.4 weeks earlier in youth than in adults, independent of clinical manifestation. Both youth and adults exhibited a similar advancement in case timing over the study period.

In **Paper 3**, a theoretical SI (Susceptible-Infected) model for structured populations of ticks and hosts is presented for exploring pathogen dynamics on a monthly timescale. In the mathematical model, the size of the tick population is regulated by the availability of hosts, specifically, a reservoir competent small mammal host with seasonal variations in fertility and survival, and a reservoir incompetent large mammal host with stable abundance across seasons. The model was used to explore how the seasonal density of infected questing ticks depends on tick questing phenology and demographic turnover (change in demographic composition) in the small mammal host population. Pathogen dynamics were sensitive to phenological synchrony between tick questing and small mammal reproduction in the model,

because host demographic turnover rapidly diluted pathogen prevalence during periods of high reproduction.

These three papers together advance our understanding of the Lyme disease system in a way that is both novel and aligned with prior empirical and theoretical work. **Paper 1** is the among the first to identify a consistent, long-term shift in the timing of a tick borne disease. In light of this finding, **Papers 2** and **3** aim to identify possible causes and mechanisms that could underlie a shift in case timing. **Paper 2** extends the statistical analysis from **Paper 1** to investigate how case timing varied based on patient demography and clinical manifestation. **Paper 3** employs a mathematical model to explore relationships between host and vector phenology and disease dynamics. In the face of an incredibly complex puzzle that global change poses to human and wildlife health, combining epidemiological and ecological methods enables a deeper understanding of the underlying dynamics of vector borne diseases required for confronting emerging health challenges.

Sammendrag (Norwegian summary)

Den vanligste vektorbårne sykdommen på den nordlige halvkule er borreliose, en bakteriell infeksjon overført av flått. Endringer i klima, arealbruk og sammensetning av vertsdyrbestander har resultert i den raske fremveksten av borreliose, som både øker i geografisk utbredelse og viser økt forekomst i mange områder der sykdommen allerede er etablert. Klimaendringer skifter tidspunktet og varigheten av sesongmessige sykluser i miljøet, og påvirker økosystemer globalt ved å endre utbredelse, antall og fenologi, dvs. når på året aktivitet foregår. Forstyrrelser av den fenologiske synkroniteten mellom trofisk koblede arter, kalt fenologisk «mis-match», er kjent for å påvirke dynamikken både på økologisk og evolusjonær tidsskala. Imidlertid har ikke betydningen av fenologi blitt godt undersøkt når det kommer til sykdommer. En mer dyptgående forståelse av fenologisk synkroni er avgjørende for å forstå dynamikken til vektorbårne sykdommer, der komplekse interaksjoner mellom flere vertsdyr og vektorarter driver sirkulasjonen av patogener i økosystemene. I denne oppgaven bruker jeg borreliose som et eksempel for å utforske interaksjoner mellom sesongvariasjoner og økologien til flåttbårne sykdommer. Paper 1 og 2 bruker overvåkingsdata for å undersøke sesongmessige og demografiske trender i borreliose-data hos mennesker, mens Paper 3 bruker en økologisk matrise-modell for å utforske sesongmessige og demografiske effekter på patogenoverføring mellom en liten pattedyrvert og flåttvektor.

I **artikkel 1** brukes overvåkingsdata fra Norge for å kvantifisere endringer i det sesongmessige tidspunktet og årlig forekomst av borreliose over en 25-årig studieperiode (1995-2019). Overvåkingsdataene fra Norge fanger opp økt forekomst ved den nordlige utbredelsen av borreliose i Europa. En fleksibel sesongmodell ble implementert over hele studieperioden for å måle endringer i høyeste ukentlige forekomst av borreliose ved å bruke et

moderne Bayesiansk statistisk rammeverk. Denne analysen viser en seks ukers tidligere forekomst sammen med en økning i forekomst på tvers av regioner i Norge. Endringen i tidspunktet for plantegrønning, avledet fra «Normalized Difference Vegetation Index» (NDVI), ble brukt som en målestokk for å skalere omfanget av sesongskiftet i forekomst av borreliose. Selv om NDVI fulgte et lignende mønster med tidligere start på plantevekst over tid, skiftet det tidligere startpunkt på høyeste ukentlige antall borreliose-tilfeller med to uker mer enn det tilsvarende skifte i start på plantevekst.

I **artikkel 2** brukes overvåkingsdataene for borreliose for å utforske demografiske mønstre i pasientens kliniske manifestasjoner og sesongvariasjonen i forekomst. Denne analysen identifiserte et bimodalt mønster for forekomst med hensyn på pasientalder, med barn og eldre med uforholdsmessig høy forekomst. Barn hadde en høyere andel tilfeller av nevroborreliose enn voksne, og blant voksne var andelen tilfeller av artrose høyere hos menn enn kvinner. Sesongvariasjonen i tidspunktet for forekomst ble funnet å være konsekvent rundt 4,4 uker tidligere hos barn enn hos voksne, uavhengig av klinisk manifestasjon. Både barn og voksne viste et lignende skifte med et tidligere tidspunktet for høyeste forekomst i løpet av studieperioden.

I **artikkel 3** presenteres en modell for å utforske patogendynamikk i en flåttvektor og en liten pattedyrvert på en månedlig tidsskala. I modellen er størrelsen på flåttpopulasjonen regulert av tilgjengeligheten av verter, som inkluderer en reservoarkompetent liten pattedyrvert med sesongvariasjoner i reproduksjon og overlevelse, og en reservoarinkompetent stor pattedyrvert med stabil bestand gjennom året. Modellen brukes til å utforske hvordan den sesongmessige tettheten av infiserte flått på jakt etter vert avhenger av fenologi og demografisk sammensetning hos små pattedyrverter. Smittesyklusen er følsom for fenologisk synkronisering mellom flått på jakt etter vert og reproduksjon av små pattedyr,

fordi høyt antall unge småpattedyr (som ikke er infisert) raskt fortynner patogenprevalens i perioder med høy reproduksjon.

Disse tre artikkelene som helhet fremmer vår forståelse av borreliose på en måte som er både ny og konsistent med tidligere empirisk og teoretisk arbeid. **Artikkel 1** er blant de første som identifiserer et skifte i tidspunktet for forekomst av en flåttbåren sykdom. I lys av dette funnet, tar **artikkel 2 og 3** sikte på å identifisere mulige årsaker og mekanismer som kan ligge til grunn for endring i tidspunktet for sykdomsforekomst. **Artikkel 2** tar en statistisk tilnærming til å forstå disse endringene basert på demografiske og kliniske trender i overvåkingsdata. **Artikkel 3** bruker en teoretisk tilnærming ved å bruke en populasjonsmodell for å utforske sammenhenger mellom verts- og vektorfenologi og sykdomsdynamikk. I møte med et komplekst puslespill som global endring utgjør for menneskers og dyrs helse, muliggjør kombinasjonen av epidemiologiske og økologiske metoder en dypere forståelse av den underliggende dynamikken til vektorbårne sykdommer som kreves for å møte nye helseutfordringer.

List of Papers

Paper 1 | Goren, A., Viljugrein, H., Rivrud, I. M., Jore, S., Bakka, H., Vindenes, Y. & Mysterud, A. (2023). The emergence and shift in seasonality of Lyme borreliosis in Northern Europe. *Proceedings of the Royal Society B*, *290*(1993), 20222420.

Paper 2 | Goren, A., Mysterud, A., Jore, S., Viljugrein, H., Bakka, H. & Vindenes, Y. (2023). Demographic patterns in Lyme borreliosis seasonality over 25 years. *Zoonoses and Public Health*, *70*(7), 647-655.

Paper 3 | Goren, A., Mysterud, A. & Vindenes, Y. Modeling the effects of seasonality in tick questing behavior and host demographic turnover on Lyme disease hazard. Manuscript.

Image generated by Stable Diffusion (https://stablediffusionweb.com), a free and open-source latent text-to-image diffusion model, using the text prompt: “humanity revolving around the sun”

Acknowledgments

Over the past four years, I have often been asked why I have elected to study Lyme disease. After all, most people dislike the very idea of ticks, and Lyme disease is often a rather controversial topic. I find pathogens interesting to study because they teach us about how ecosystems function. Tracing the transmission of a pathogen between populations highlights the interconnectedness between species, locations, climate, and natural and built environments. It would make me quite happy if this thesis soon appears retrospective because a safe, effective, and affordable vaccine halts the emergence of Lyme disease. However, even if Lyme disease were wholly eradicated, I believe that this would do no more than cast a sepia tone on these pages, as the goal of this research extends beyond the case study of Lyme disease to explore fundamental questions about seasonal ecology, population demography, and pathogen transmission cycles. I hope that this thesis, in addition to conveying our findings and methods, will spark interest in disease ecology research as a fascinating way to study interactions between components of the natural world and an enduring interface between civilization and nature.

It is a privilege to express my gratitude to the many incredible individuals who have supported me during my research journey and contributed to the work included in this thesis. First and foremost, the immeasurable support and scientific contributions of my four amazing supervisors, Professor Yngvild Vindenes, Professor Atle Mysterud, Dr. Hildegunn Viljugrein, and Dr. Solveig Jore, cannot be overstated. I would be hard pressed to identify a more supportive and brilliant group of supervisors than those I have been so fortunate to have guiding me on this journey. I cherish all the time we have spent working together over the past four years, all our conversations, and all the insight and expertise you have shared with me throughout the creation of this dissertation. My co-authors, Dr. Haakon Bakka and Dr.

Inger Maren Rivrud have made great contributions to the work included in this thesis and went above and beyond to aid me in the development of my skills as a researcher.

Having had the experience of traveling over 3000 miles in the middle of a global pandemic to start my PhD, I have an especial depth of gratitude for the solidarity and supportiveness of my research team and community at the University of Oslo in the weathering of these challenging times. I thank Gry Gundersen, Tore Wallem, Erland Nettum, Nina Holtan, and the entire administrative staff of CEES and ISMO for their unwavering support from the moment I was hired all the way through my stay at the University of Oslo. The extent to which these individuals have gone above and beyond the call of duty to provide assistance is an incredible demonstration of personal integrity and dedication to the university community.

For all the friends and colleagues who have enriched my PhD experience, and shared with me wisdom, knowledge, laughter, and joy, I am so thankful. The mentorship and friendship of Dr. Christie Le Coeur, Dr. Jason Lee Anders, Dr. Håkon Lund, Dr. Emma Whittington, Dr. Kyrre Kausrud, Dr. Stefaniya Kamenova, and Dr. Eric de Muinck has meant so much to me. I cherish the support, laughter, and great conversations with my amazing office mates, Tilde Hjermann, Lars Lindsø, and Dr. Kaixing Dong. It has been a great fortune to enjoy the friendship of so many brilliant, kind, and exceptional researchers that have been my colleagues and classmates at the University of Oslo. To Astrid Bragstad Gjelsvik, Katarina Andersen, Benedicte Garmann-Aarhus, Tara Jane Daughton, Marianne Strand Torvanger, Lauren Louise Cobb, Emma Falkeid Eriksen, Anders Isaksen, Julie Bommerlund, Francesco Giannelli, Lydia Furness, Dabao Sun Lü, Lea Frank, Aurélie Boilard, Gunnar Thorsen Liahjell, Oliver Kersten, Inga Kjesbu Ottersland, Marius Maurstad, Robin Araya, my fellow

doctoral candidates at Grad Forum, my students, and many other wonderful colleagues, many thanks for the brightness you bring to UiO.

I am very grateful for the financial support awarded to me by the Kristine Bonnevie Travel Stipend to support my research stay at Princeton University. During my visit to Princeton, I was continuously amazed by the warmth and inclusiveness with which I was received. For the incredible experience of spending time in the lab and the many hours of research discussions, I am profoundly grateful to my host Professor Jessica Metcalf. I am also thankful to Professor Bryan Grenfell, Professor Gabriel Vecchi, Professor Andrea Graham, Holly Burrows, Burcu Tepekule Müller, Qiqi Yang, Justin Sheen, Daniel Park, Arthur Menezes, Ruby An, Fidisoa Rasambainarivo, Inga Holmdahl, Nicole Nova, Jamie Caldwell, and the entire Disease Ecology Group for your welcoming friendship and many inspiring conversations.

I may have never started my PhD journey without the inspiration and support from my previous supervisors, each of whom have played important roles in my development as a person and as a scientist, Professor Ian Tetlow, Professor Daniel Ashlock, Professor R. Larry Peterson, Professor Sam Zeeman, Dr. Ivano Brunner, Dr. Arthur Rogers, Dr. Jen Shuter, Dr. Roujing Wang, Janine Maruschak, Carol Zepatos, Dr. Gregory Guderian, and Louis Spinelli.

To end on the highest of notes, I cannot overstate the boundless support from my parents, my brother Tolga, and partner Ryan who have stood by my side every step of every path I have taken.

To all of you, I am grateful.

Introduction

Seasonal Ecology

Changes in seasonality resulting from climate change are already documented in most regions globally, with wide-ranging physical, ecological, and societal impacts, that are predicted to exacerbate in coming decades (Environmental Protection Agency, 2021; Ernakovich et al., 2014; Ramachandran, 2011; Suepa et al., 2016). Although seasonal environments are often associated with temperate and arctic regions with high annual fluctuations in temperature and day length, climate seasonality is found across biomes (Mellard et al., 2019), including tropical regions where changes in rainfall seasonality have been ecologically and socially important (Feng et al., 2013). The effects of climate seasonality have been shown to be important across vertebrate (Paul et al., 2007) and invertebrate (Lawrence & Soame, 2004; Zagatto et al., 2017) species of enormous variety in size, life history, and trophic level, including such diversity as fungal endophytes (Oita et al., 2021), soil microorganisms (Wang et al., 2023), insect parasitoids (Tougeron et al., 2020), zooplankton (Varpe et al., 2009), birds (Jenni & Kéry, 2003), and mammals (Bronson, 2009). All of these species have evolved life history strategies for coping with seasonal variation in resource availability and environmental conditions through a variety of strategies including: diapause, dormancy, hibernation, timing of reproduction and growth, pacing of growth, energy storage, and migration (Varpe, 2017).

The evolution of annual cycles and the phenological plasticity of these cycles are adaptations to climate seasonality which will shape biological responses to climate change (Varpe, 2017). The extent to which organisms have adapted to use predictable cues, such as photoperiodism, versus variable, climate-driven cues, such as temperature, to time life events, is an important component in determining the plasticity of a phenological response (Coppack

et al., 2003; Saikkonen et al., 2012; Tsai et al., 2020; Walker et al., 2019). There is increasing empirical evidence for pathways that integrate environmental cues, such as photoperiod and temperature, to signal physiological cycles (Abrieux et al., 2020; Flynn & Wolkovich, 2018; Wood et al., 2020).

Seasonality and Disease

Infectious diseases provide well-documented examples of the role of seasonality in shaping population dynamics, as many human and animal diseases exhibit conspicuously seasonal fluctuations in incidence (Altizer et al., 2006). Common examples of seasonality of infectious diseases in humans include increases in influenza in winter, measles with school terms, and malaria with seasonal rains (Altizer et al., 2006; Becker et al., 2016). Seasons can influence contact rates, infectivity of pathogens, host demographic structure, host immunity, and other factors that alter the spread and persistence of infectious diseases (Altizer et al., 2006). Understanding the causes of seasonal fluctuations in infectious diseases can yield insight into the functioning of the disease system, elucidate potential linkages between the disease system and climate, and ultimately inform public health actions and control measures (Altizer et al., 2006).

Diseases that are vector borne are particularly sensitive to abiotic conditions because they impact the population dynamics of arthropod disease vectors, the survival and replication of pathogens inside vectors, host distributions, and vector-host contact rates (Gage et al., 2008). The seasonality of many vector-borne human diseases is often largely driven by vector activity patterns (Gage et al., 2008). However, it can be challenging to predict how disease dynamics vary across seasons because it depends on many different components of the pathogen, vector, and host life cycles (Khong et al., 2023). Seasonal oscillations in

temperature and humidity can impact survival, fecundity, and phenology of the vector, pathogen, and host, as well as vector-host interactions, sometimes in opposing directions (Harvell et al., 2009; Khong et al., 2023; Medeiros et al., 2016). In addition to impacting disease ecology, changing climate seasonality can alter the duration and timing of human exposure to vectors (Mora et al., 2022). For ticks, shifting climate seasonality can alter vital rates, interstadial development, and the timing and duration of environmental suitability for questing (Levi et al., 2015; MacDonald et al., 2020; Ogden et al., 2020; Ogden & Lindsay, 2016). The timing and duration of tick questing can influence host contact rates, which determine tick abundance through survival and/or reproductive success, and the probability of encountering an infected host (MacDonald et al., 2020).

Generally, it is predicted that climate change will lengthen the transmission season of many vector-borne diseases, but many projections fail to fully capture how climate will shape seasonal vector borne disease patterns (Caminade et al., 2019). Dry springs and milder winter conditions are thought to increase the risk of West Nile virus transmission in the United States (Epstein, 2001). Milder winters and prolonged spring and autumn seasons in Europe are thought to have increased the seasonal activity and geographical range of *Ixodes ricinus,* the main tick vector of Lyme disease and several other tick borne infections (Medlock et al., 2013). Generalizations of the impact of seasons under climate change on vector borne diseases are limited because predictions are highly sensitive to regional and disease specific features (Khong et al., 2023). Limited availability of long-term, high quality disease and vector data, and a tendency to oversimplify the mechanisms by which climate change impacts disease transmission, have hindered our ability to determine exactly how shifting climate seasonality has already impacted vector borne disease systems and predict the effects of future climate change (Kovats et al., 2001). It remains an open question whether climate-driven

shifts in phenology could create novel disease emergence by introducing contact between groups of hosts, vectors, and pathogens that did not formerly interact (Altizer et al., 2013).

Lyme disease

Lyme disease, also known as Lyme borreliosis, is a bacterial infection caused by spirochetes in the *Borrelia burgdorferi* sensu lato complex, vectored by several species of hard-bodied ticks in the genus *Ixodes*. The *B. burgdorferi* sl complex contains several genospecies which are known to cause Lyme disease in humans (Stanek & Reiter, 2011). Lyme disease is the most common vector borne disease in the Northern Hemisphere, with a broad geographic distribution across Europe, North America, and Asia (Kilpatrick et al., 2017; Rizzoli et al., 2011). The current distribution and recent geographical expansion of Lyme disease is partially driven by the current and expanding distribution of tick vectors, although in some regions where vectors are present, Lyme disease incidence is low and possibly absent (Burtis et al., 2022; Eisen, Eisen, & Beard, 2016; Mysterud et al., 2016). Lyme disease vectoring ticks are generalists that can use a wide range of vertebrates as hosts, including mammals, birds, and lizards, that represent a wide range of reservoir competency for *B. burgdorferi* and also a broad range of life history traits and ecological niches (Brunner et al., 2008; Ostfeld et al., 2014).

The epidemiology of Lyme disease is based on an interplay of seasonal interactions between ticks, hosts, and humans. Figure 1 illustrates the overlapping timelines of tick questing phenology, host reproduction seasonality in an example small mammal host, and periods of peak infection risk for hosts and humans. This illustration is based on a northern European ecosystem as represented in **Paper 3**, and the timelines would be different in other regions with different climates and host and vector species. In this example, tick adults and

nymphs quest from March to November, with the peak questing period from April through June. Larvae start questing a little later, in April, and have peak activity in May and June. Oviposition by fed adult females occurs from July until November. Peak infection risk for hosts and humans is during the period of maximum nymphal questing. The small mammal in this example, based on the bank vole, reproduces from May to October, with peak reproduction from June through August. For humans, early symptom onset typically occurs within a month from the time of infection, but it could take several months for the infection to disseminate and be diagnosed.

The Lyme disease surveillance data from Norway used in **Paper 1** and **Paper 2** provide an excellent resource for exploring questions with relevance beyond the region from which the data are collected. The uniformity, quality, and long duration of surveillance makes the data from Norway a valuable resource for exploring long term trends and difficult-to-capture signals, such as changes in patient demography and case seasonality. Furthermore, Norway spans a large latitudinal range (57°58′–71°08′ N), comprised of distinct eco-regions with differences in climate and host composition unified under a single-surveillance umbrella (Mysterud et al., 2016; Mysterud et al., 2017). The Norwegian data also provides an excellent case study for the geographic spread of Lyme disease because it is situated at the expanding northern edge of the biographical range of Lyme disease in Europe (Mysterud et al., 2018).

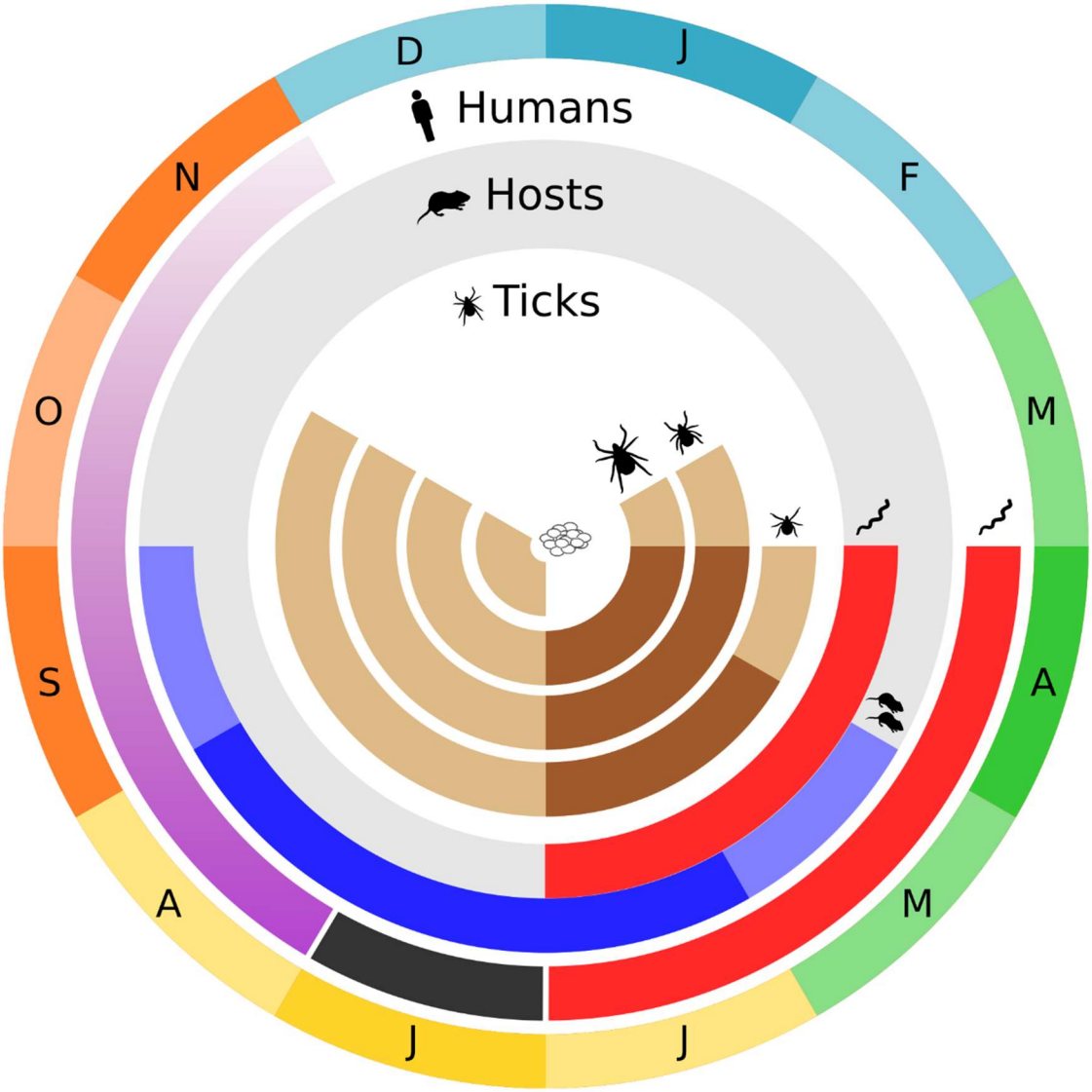

Figure 1. An illustration of the interplay of seasonal interactions underlying Lyme disease ecology. This illustration includes only a single small mammal host as an example, although Lyme disease is a multi-host system. The outermost circle represents the calendar months of the year, with the letters indicating the names of the months and the colors representing seasons. The innermost circle represents tick activity patterns layered from the center outward for eggs, adults, nymphs, and larvae, based on a northern European ecosystem (as described in Paper 3). The light brown arcs represent the questing period for larvae, nymphs, and adults, and the timing of oviposition, with the dark brown areas indicating peak questing activity. The next ring outward represents seasonality in a small mammal host, such as the bank vole, in a northern European ecosystem (as described in Paper 3). Peak host infection risk occurs during the peak of nymphal questing activity, and is represented by the red arc. The blue arc represents host reproduction, with the dark blue area indicating the time at which peak

reproductive output occurs. The seasonal infection dynamics of the host population are explored in Paper 3. The next ring outward illustrates human infection seasonality. As with the hosts, peak infection risk, represented by a red arc, overlaps with nymphal questing, although infection can happen at any time that ticks are active and cases are diagnosed throughout the year. The month following is filled in with a black arc to illustrate a lag between the onset of symptoms from the time of infection, which is usually around 2 to 30 days. The purple arc represents the timing over which disseminated symptoms and diagnosis would typically follow after the delay in initial symptom onset.

Climate Change in Norway

While it can be methodologically challenging to directly attribute disease burden to climate change, there is a growing body of evidence that climate change has impacted the geographic range, seasonality, and transmission of infectious diseases (Semenza & Menne, 2009). Lyme disease has been shown to be climate sensitive in both Europe (Semenza & Paz, 2021) and North America (Ebi et al., 2017). Over recent decades, Norway has experienced a marked and well-documented change in climate patterns that includes warming temperatures and increased precipitation in most regions (Hanssen-Bauer et al., 2009; Ketzler et al., 2021). **Paper 1** and **Paper 2** include regional analyses of Lyme disease surveillance data, following designations from prior studies (Mysterud et al., 2016; Mysterud, Heylen, et al., 2019). Across these study regions, long term climate trends have been similar, with a general pattern of increasing temperature and precipitation that has been ongoing since 1950 (Figure 2). Over the 25-year study period (1995-2019) used in **Paper 1** and **Paper 2**, the warming trend is predominantly discernible in Spring (March through May) and is very similar across regions (Figure 3). Precipitation shows considerable inter-annual variability, and a slight increase in summer, over the study period (Figure 4).

The warming pattern observed in spring leads to the prediction that ticks may be able to quest earlier in the year, resulting in advanced timing of Lyme disease cases. If host

availability is different for ticks questing earlier in the year, the timing of tick-host interactions could impact infection prevalence in ticks, and thereby provide an ecological explanation for the observed increase in the number of human cases occurring each year. While the different regions of Norway have considerably different climates, primarily due to differences in topography and coastal effects (Mysterud, Heylen, et al., 2019), the change in climate over the study period has been very similar across regions. The similarity in trends, combined with the assumption that areas within the regions with high case frequency will have environmental similarities, leads to the prediction that any changes in Lyme disease case timing will be similar across regions of Norway.

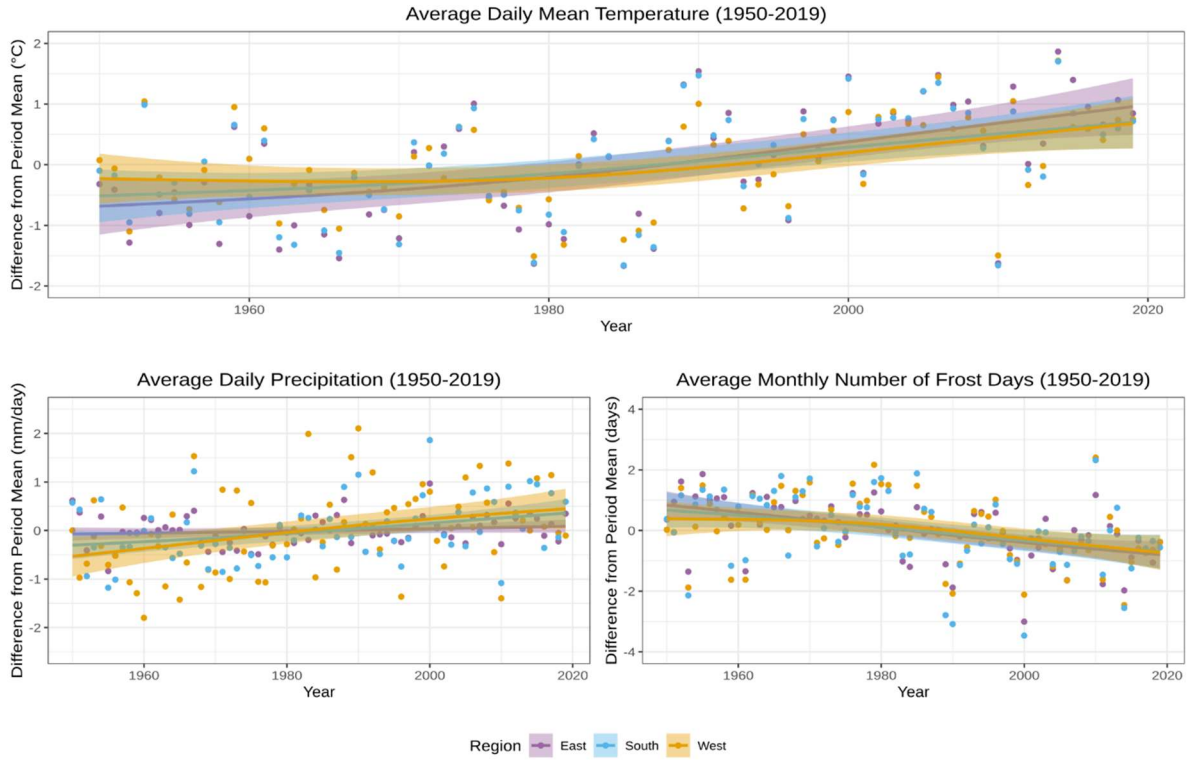

Figure 2. Long term, annual trends in daily mean temperature, daily precipitation, and average number of frost days per month over the time period 1950 to 2019 in the study regions in Norway. The y-axes show the difference from the period average of the value of the climate variable. Data for these graphs were extracted from the Copernicus Interactive Climate Atlas (Copernicus Climate Change Service, 2024) using the gridded land-only

observational dataset over Europe (Cornes et al., 2018). Trendlines were fit to the data using the default GAM model in ggplot2 (Wickham, 2016).

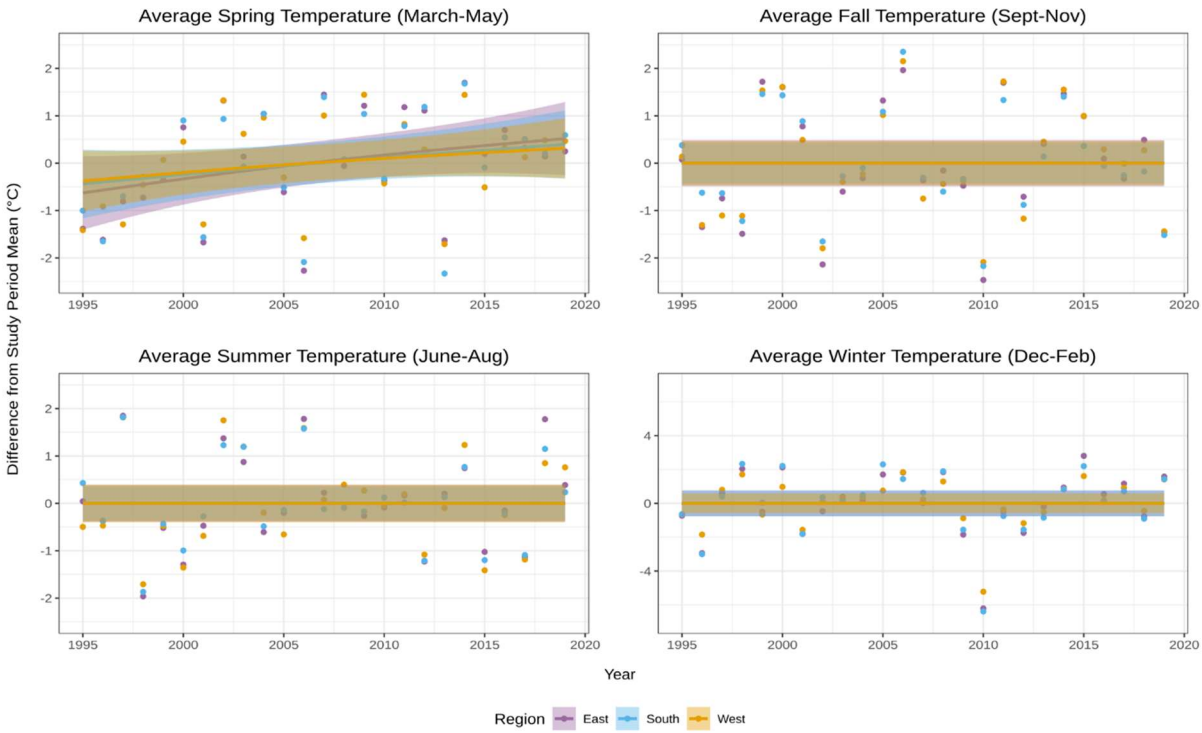

Figure 3. Seasonal temperature trends over the study period (1995 to 2019) and study regions in Norway. The graphs show, for each season, the difference between the average daily temperature and the seasonal average temperature across the study period. Positive values indicate years with a higher than average daily mean temperature for the season, and negative values indicate lower than average temperatures, compared to the average seasonal value for the study period. Data for these graphs were extracted from the Copernicus Interactive Climate Atlas (Copernicus Climate Change Service, 2024) using the gridded land-only observational dataset over Europe (Cornes et al., 2018). Trendlines were fit to the data using the default GAM model in ggplot2 (Wickham, 2016).

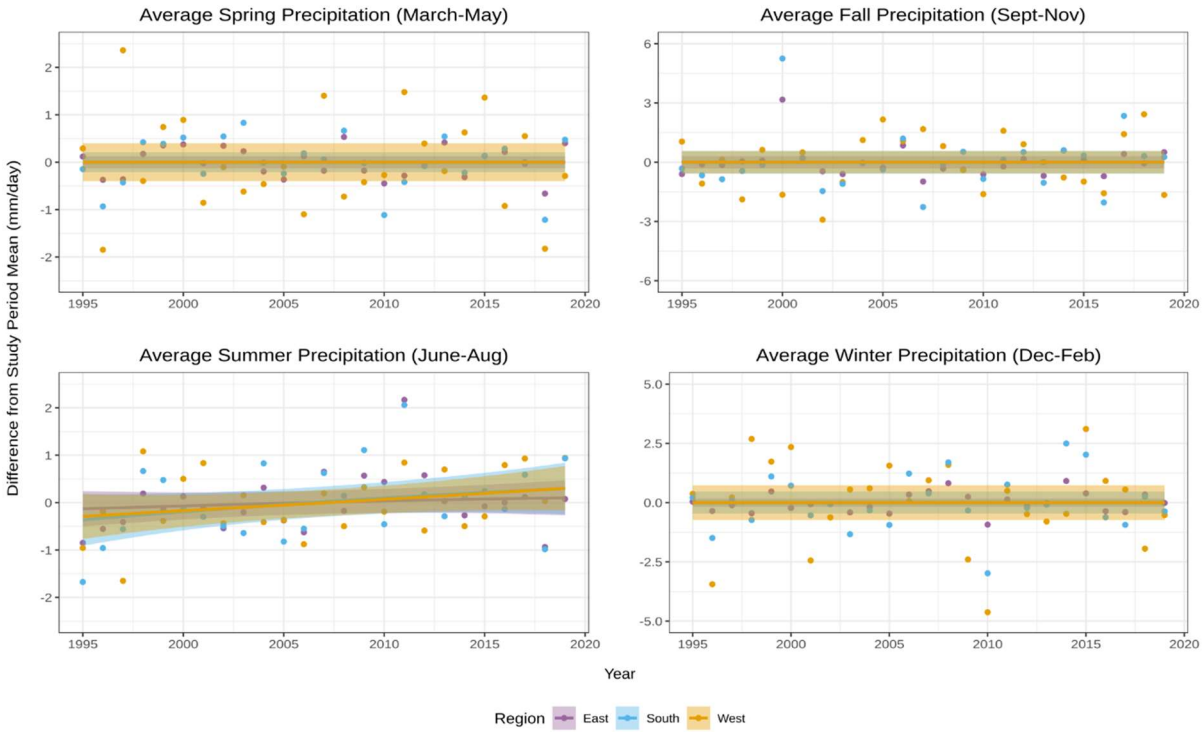

Figure 4. Seasonal precipitation trends over the study period (1995 to 2019) and study regions in Norway. The graphs show, for each season, the difference between the average daily precipitation and the seasonal average precipitation across the study period. Positive values indicate years with a higher than average amount of precipitation for the season, and negative values indicate lower than average precipitation, compared to the average seasonal value for the study period. Data for these graphs were extracted from the Copernicus Interactive Climate Atlas (Copernicus Climate Change Service, 2024) using the gridded land-only observational dataset over Europe (Cornes et al., 2018). Trendlines were fit to the data using the default GAM model in ggplot2 (Wickham, 2016).

Aims

In this thesis, I aim to use Lyme disease as a case study for exploring vector borne disease seasonality with a combination of statistical modeling of human case data, and mathematical modeling of the disease dynamics of hosts and vectors. The statistical analysis identifies seasonal and demographic trends from case data, and in the process generates questions that can be approached with theoretical modeling. The mathematical modelling aims to approach well described knowledge gaps regarding fundamental aspects of Lyme

disease that are barriers to effective control, specifically understanding how vector-host-pathogen interactions impact disease hazard (number of infected questing tick nymphs) across seasons (Kilpatrick et al., 2017).

The aim of **Paper 1** is to quantify changes in annual incidence and seasonal timing of Lyme disease cases across Norway over a 25-year study period (1995-2019). In **Paper 2**, the main goals were to investigate whether the incidence of different clinical manifestations of Lyme disease varied based on patient age and sex, and to determine whether patient demography or clinical manifestation impacted case timing. Based on the hypothesis that ecological responses to climate change could be driving both the emergence and shifting seasonality of Lyme disease, **Paper 3** used a mathematical model with the goal of identifying possible ecological mechanisms that could underlie the advanced case seasonality observed in **Paper 1**. The aim of the model is to create a simulation where tick and host phenology can be altered to generate hypotheses regarding how the timing of interactions between vector and host populations can modulate disease hazard.

Study System

Lyme Disease Emergence

Lyme disease was not clinically recognized until the late 1970s when geographic clustering of childhood arthritis cases in Connecticut, USA led to the description of Lyme arthritis, a condition of asymmetric joint swelling putatively linked to an arthropod vector (Steere et al., 1977). A few years later in 1981, the causative agent of Lyme disease was discovered to be a tick-borne spirochete bacterium, now known as *Borrelia burgdorferi* sensu lato (Burgdorfer, 1991). While the discovery of Lyme disease seems to have been motivated by an increase in case frequency, it was likely facilitated by social development and improved

laboratory methods, such as the discovery of the microimmunofluorescence test in 1968 (Burgdorfer, 1984; Wang, 2000), spurred by the rapidly growing science and technology sector (Bohrer, 2008). While there exist earlier descriptions of Lyme disease symptoms (Anderson & Magnarelli, 1994) and genomic evidence that *B. burgdorferi* has been endemic in Europe and North America since the last glacial maximum (Vollmer et al., 2013; Walter et al., 2017), there is significant public health evidence of Lyme disease emergence beginning in the late 1970s and continuing to present day in both Europe and North America (Eddens et al., 2019; Steere et al., 2004; Vandekerckhove et al., 2021).

Clinical Manifestations

Lyme disease pathogenesis is very heterogeneous among individuals, and many of the symptoms can be difficult to distinguish from other conditions (Cochat Costa Rodrigues et al., 2017; Cruz et al., 2017; Trevisan et al., 2020). The most typical initial manifestation of Lyme disease is a "bullseye" shaped dermal lesion expanding from the site of the tick bite, known as erythema migrans, that typically occurs 2 to 30 days after infection and can be accompanied by flu-like symptoms (Johnson et al., 2018; Steinbrink et al., 2022). If the infection is left untreated in the early stages of infection that are localized in the skin near the tick bite, the pathogen can disseminate in the body creating a systemic infection (Hyde, 2017; Steere et al., 2016). It is estimated that dissemination occurs in 15-20% of untreated cases (Koedel et al., 2015; Ornstein et al., 2001; Strnad & Rego, 2020). Early-stage dissemination often involves neurological manifestations, termed neuroborreliosis, that can involve the central and/or peripheral nervous systems (Garkowski et al., 2017; Steinbrink et al., 2022). Late-stage dissemination encompasses diverse sequelae including arthritis, acrodermatitis chronica atrophicans, and carditis (Cadavid et al., 2016; Coburn et al., 2021; Lochhead et al., 2021).

Lyme disease is typically diagnosed with an antibody test, though PCR methods for pathogen detection are also used (Borchers et al., 2015; Eldin et al., 2019; Marques et al., 2021). Lyme disease is treated with antibiotics, with similar guidelines across Europe and North America (Marques et al., 2021). Recovery time after treatment can be very variable between individuals, with some patients experiencing symptoms for a prolonged period of time (Koedel et al., 2015; Monaghan et al., 2023).

Pathogenesis and seroconversion are known to vary based on patient age and sex, but the epidemiological significance of patient demography is not yet well understood (Carlsson et al., 2018; Krawczuk et al., 2020; Steere et al., 2003; Woudenberg et al., 2020). North American and European patients exhibit differences in clinical manifestations, with Lyme arthritis being more common in North America and neuroborreliosis more common in Europe (Arvikar & Steere, 2022; Marques et al., 2021). Children and adults exhibit some differences in clinical manifestations of Lyme disease, including that children are more likely to develop neuroborreliosis and borrelial lymphocytoma than adults (Stanek & Strle, 2018). Within neuroborreliosis cases, children are more likely to exhibit cranial meningoradiculitis while adults are more likely to exhibit spinal meningoradiculitis (Oschmann et al., 1998). These age-based differences in clinical manifestations lead to the prediction that case timing could be different between adults and children.

It has been shown that females more often report localized Lyme disease infections while males present more disseminated infections (Nygård et al., 2005; Skufca et al., 2022; Tulloch et al., 2020). This trend has generally been attributed to gender-related differences in healthcare-seeking behavior (Bennet et al., 2007; Doyal, 2001; Eliassen et al., 2017), but may also have physiological underpinnings (Dias et al., 2022). While the analyses presented in Paper 1 and Paper 2 only include cases of disseminated disease, it would be reasonable to

predict that differences in healthcare-seeking behavior could result in delayed case timing in males compared to females.

Tick Vectors

In North America, the most common vectors are *I. scapularis* in eastern US and Canada, followed by *I. pacificus* in the west (Steere et al., 2016). The most common vector in Europe is *I. ricinus,* and *I. persulcatus* is the most common vector in Asia, though it is also found in parts of Europe, including Baltic countries and parts of Scandinavia (Steere et al., 2016). These four vector species are closely related and occupy similar ecological niches (Gray et al., 2016). There are many articles describing what is currently known of the biology and ecology of Lyme disease vectoring ticks (Gray et al., 2021; Kahl & Gray, 2023; Korenberg et al., 2021; Padgett & Lane, 2001; Sonenshine & Simo, 2021). I will here summarize key life history traits, which are generally conserved across the four main Lyme disease vectors, with emphasis on *I. ricinus*, and mention a few differences between these species.

There are four instars, or main life stages, of ixodid ticks: egg, larva, nymph, and adult, also known as imago (Figure 5). All feeding instars of the Lyme disease vectoring ticks can bite humans, except in *I. persulcatus*, where adult females are the main vectors (Gray et al., 2016). The total duration of the life cycle is around 3-6 years in most regions, but can be faster or slower based on environmental conditions (Grigoryeva & Shatrov, 2022; Kahl & Gray, 2023; Korenberg et al., 2021; Sirotkin & Korenberg, 2022). Plasticity in the timing and duration of the life cycle is enhanced by two types of diapause, behavioral and developmental (also known as morphogenetic), which enable ticks to prolong the duration of life stages and match time periods of questing activity and development with favorable environmental

conditions. Behavioral diapause controls the activity levels of fully developed unfed ticks, while developmental diapause delays interstadial development (Gray et al., 2016). The plasticity of the tick life cycle and differences in diapause patterns lends complexity to the population structure because individuals in the same life stage can have very different calendar ages (Balashov, 2012).

Photoperiod is a primary cue for inducing diapause, although other environmental factors, such as temperature, and endogenous factors, such as tick age, appear to have modifying effects (Gray et al., 2016; Korenberg et al., 2021). The extent to which ticks undergo true behavioral diapause, rather than a period of quiescence that can be readily interrupted given suitable environmental conditions, remains unclear (Gray et al., 2016). There is evidence for both ticks that quest during warm winter months as well as photoperiod driven diapause in fully developed unfed nymphs (Gray et al., 2016). A key difference between species and populations of Lyme disease vectoring ticks is the timing and duration of their life cycle events and activity levels, which appear to be environmental adaptations (Gilbert et al., 2014; Gray et al., 2016; Korenberg et al., 2021; Kurtenbach et al., 2006; Padgett & Lane, 2001). For example, there is evidence for differences between Lyme disease vectoring species regarding whether diapause happens in the embryo or in the adult instar before oviposition (Gray et al., 2016; Korenberg et al., 2021). Populations of *I. ricinus* collected from different regions have differential activity levels in response to temperature, which has interesting implications for climate adaptivity (Gilbert et al., 2014). There are also findings of population-level differences in questing behaviors in *I. scapularis* (Arsnoe et al., 2015).

Interstadial development necessitates only a single meal of blood, and adult females require a blood meal for egg development, resulting in a maximum of three complete feedings

during the tick's life cycle (Kahl & Gray, 2023). Adult males may take small amounts of blood while on a host's body seeking a female for mating, but these feedings are small and therefore generally not considered important for pathogen transmission (Kahl & Gray, 2023). Lyme disease vectoring ticks spend the majority of their lives free-living, either resting in the upper layers of soil and leaf litter or questing on vegetation, and are not associated with host nests and burrows (Gray et al., 2016; Korenberg et al., 2021). The duration of feeding events, while representing only a tiny fraction of the tick life span, is long relative to other blood-feeding arthropods (Kahl & Gray, 2023). Typically, larvae will feed on a host for 2-4 days, nymphs for 3-5 days, and adult females for 7-10 days (Kahl & Gray, 2023). Ticks are sensitive to desiccation when questing, and will retreat from higher levels of vegetation to the more humid microclimate of leaf litter and hydrate using water vapor in the air (Kahl & Gray, 2023).

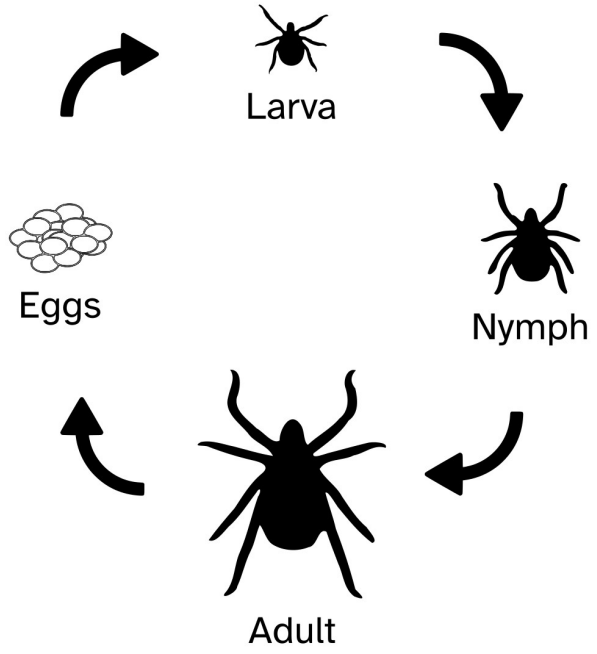

Figure 5. An illustration of the life cycle of Lyme disease vectoring ticks. A single successful bloodmeal is required for interstadial development and oviposition.

Hosts

Generally, tick larvae preferentially feed on small mammals and ground-feeding birds, nymphs feed broadly across vertebrates, and adults will feed primarily on large mammals, including deer and domesticated animals such as sheep (Korenberg et al., 2021; Stewart & Bloom, 2020). Ticks in different regions feed on different host species based on host availability, but it is unclear to what extent species and populations have physiologically adapted to the regionally available host complement.

Non-reservoir hosts are also important for disease dynamics because they can control the size and structure of the tick population by altering stage-specific survival rates and reproductive success (Mysterud et al., 2016). Thus, host community structure is important for determining both tick population sizes and infection prevalence (Gage et al., 2008). The role of deer in driving Lyme disease risk has been debated because deer are not reservoir competent but serve as a common reproduction host for adult female ticks in both North America and Eurasia (Gandy et al., 2021; Gilbert et al., 2012; Kugeler et al., 2015; Mysterud et al., 2016). The role of host biodiversity in driving Lyme disease risk, as well as zoonotic disease risk in general, has also been discussed (Civitello et al., 2015; Köhler et al., 2023; Levy, 2013; Ostfeld & Keesing, 2000; Randolph & Dobson, 2012; Rohr et al., 2019). The general idea behind the link between biodiversity and disease risk is that a biodiverse host community will include non-reservoir hosts which serve as dead-ends for disease transmission, thereby diluting disease risk (Keesing & Ostfeld, 2021).

Pathogens

In North America, *B. burgdorferi* sensu stricto is the most common genospecies infecting humans (Cerar et al., 2016). In Europe, there is much higher diversity of

genospecies with geographic variability; overall *B. garinii* and *B. afzelii* are most common (Rauter & Hartung, 2005). The different genospecies vary in host associations (Wolcott et al., 2021). A recent review of host associations notes major gaps in the empirical data, but notes that almost all genospecies that are pathogenic to humans have at least two types of host reservoirs (Wolcott et al., 2021). Generally, *B. afzelii* is associated with rodents (Hanincová et al., 2003), and *B. garinii* is associated with birds (Comstedt et al., 2011), though this is, in part, an oversimplification as *B. garinii* has been identified in mice in Switzerland (Hügli et al., 2002) and *B. afzelii* has been found in ticks feeding on birds (Franke et al., 2010; Lommano et al., 2014). Within the many genospecies of *B. burgdorferi* sl there are also several recognized strains with geographic associations, which have demonstrated variance in clinical manifestations and inflammatory potential (Cerar et al., 2016). Based on within genospecies comparison of strains, ecological niche appears more relevant for some clinical and immune characteristics than phylogeny (Cerar et al., 2016).

In addition to having different host associations, *B. burgdorferi* sl genospecies exhibit differences in associated clinical manifestations in humans (Jahfari et al., 2017). In Norway, it was found that *B. garinii* was the main genospecies found in cerebrospinal fluid of children with neuroborreliosis (Barstad et al., 2018), despite being only the second most common genospecies in ticks, representing around 20-30% of tick infections (Mysterud, Heylen, et al., 2019). This is consistent with findings throughout Europe, where neuroborreliosis is the most common form of disseminated infection (Barstad et al., 2018). The most commonly found genospecies in ticks in Europe, *B. afzelii*, is associated with late-stage dermatological manifestations, which are much less frequent than neuroborreliosis (Coipan et al., 2016; Rupprecht et al., 2008). However, *B. afzelii* and hedgehog-associated *B. bavariensis* have also

been indicated as causative agents of neuroborreliosis (Mysterud, Heylen, et al., 2019; Strle et al., 2006). It remains unclear if clinical associations to genospecies are caused by differences in pathogeneicity, sensitivity and specificity of diagnostic tests, or likelihood of presenting easily recognizable early symptoms such as erythema migrans that result in timely treatment (Carlsson et al., 2003; Logar et al., 2004; McManus & Cincotta, 2015; Mysterud, Heylen, et al., 2019). All genospecies appear to respond equally to antibiotic therapy (Steere et al., 2016).

Methods

Analysis of Lyme Disease Surveillance Data

The Lyme disease surveillance data used in this thesis has been collected by the Norwegian Surveillance System for Communicable Diseases (MSIS), administrated by the Norwegian Institute of Public Health. Lyme disease surveillance has been ongoing in Norway since 1991, when case reporting became mandatory for care providers, including laboratories and clinicians (MacDonald et al., 2016). Consistent case reporting criteria has been maintained since 1995, whereby only cases of disseminated infection are notifiable and must have laboratory confirmation by one of the following: antibody test, nucleic acid test, or pathogen isolation (MacDonald et al., 2016; Mysterud, Heylen, et al., 2019; Norwegian Public Health Institute, 2023). Case reports include a wide variety of clinical and demographic information, although not every case report includes all possible fields. For example, about half of case reports contain the municipality in which the tick bite occurred.

The study period in **Paper 1** and **Paper 2** was 1995-2019 because over this time there has been little change in diagnostics in Norway, with the exception of the standardization of spinal fluid testing protocols for children since 2011 (Mysterud, Heylen, et al., 2019). The

date of diagnostic testing was available for every patient and used in **Paper 1** and **Paper 2** as a uniform metric for exploring the timing of cases within the year. **Paper 1** focused on national and regional trends in case seasonality, and included only cases in adults (20+ years), pooled across sex. The regional analysis grouped counties into four biogeographical regions, following designations from prior studies (Mysterud et al., 2016; Mysterud, Heylen, et al., 2019). **Paper 2** expanded the analysis of surveillance data from **Paper 1** to explore the seasonality of cases grouped by age, sex, and clinical manifestation.

A Bayesian modeling framework was used to quantify annual and seasonal trends in the timing of case data. By fitting a flexible seasonal trend to case timing across the entire time series, we were able to measure shifts in the timing of the week in which case numbers peaked. The statistical package INLA (http://www.r-inla.org) was used to fit the Bayesian models. INLA uses a method of Integrated Nested Laplace Approximation to fit Bayesian models rapidly, such that the analysis could be conducted on an average personal computer (Rue et al., 2009).

Matrix Population Models

In **Paper 3** we use an SI (Susceptible-Infected) framework to simulate disease dynamics in structured populations of ticks and hosts. The mathematical model presented in **Paper 3** is based on a matrix population model, a structured, discrete time framework for describing dynamics in a population stratified according to states such as age, stage, or infection status (Caswell, 2001). The use of periodic matrix models on a discrete monthly timescale follows established matrix modeling theory that has been in use since the 1960s (Bacaër, 2009; Caswell & Trevisan, 1994; Skellam, 1967). The extension of such stage-

structured matrix models to describe infectious disease dynamics is also well established (Klepac & Caswell, 2011; Klepac et al., 2009).

In **Paper 3**, an existing tick matrix population model (Vindenes & Mysterud, 2024) is extended to include a pathogen transmission function during feeding events, infection status of ticks and small mammal hosts (susceptible or infected), and monthly vital rates in the small mammal host affecting the demographic turnover. The tick model employed in this framework is based on a matrix population model with 17 life stages, which account for instar, feeding status (fed or unfed), season of feeding (spring or fall), and overwintering (Vindenes & Mysterud, 2024). Tick abundance depends on the availability of two types of hosts, a small host with seasonal variation in availability and a large host that remains constant throughout the year (Vindenes & Mysterud, 2024). For the exploratory purpose of the study, the monthly timescale was considered optimal for exploring seasonal fluctuations while minimizing the number of parameters explicitly defined in the model. Only seasonal and not annual cycles were simulated in this model, as the size of the small host population was reset every January.

The baseline parameter values were based on generalizations of *I. ricinus,* for the tick vector, and *Myodes glareolus* (bank vole), for the small mammal host, in northern ecosystems. The bank vole was used because it is an important host for the transmission cycle of *B. burgdorferi* sl in Europe (Aminikhah et al., 2021), and the generalization of its life cycle captures the main seasonal aspects of many other small mammal hosts (Tanton, 1969). The model primarily represents the transmission of *B. afzelii*, the genospecies of *B. burgdorferi* sl that is most commonly found in bank voles (Mysterud, Stigum, et al., 2019). As *B. afzelii* is typically associated with localized infections, the disease hazard represented in the model is

mainly for more common presentations of Lyme disease than the cases included in the surveillance data used in **Papers 1** and **Paper 2**. The model was used to explore alternative scenarios that simulated shifts in tick questing phenology and changes in monthly vital rates for the small host. Seasonal population sizes were extracted from the equilibrium state of the model, obtained by population projection.

Main Results

In **Paper 1**, the statistical analysis of surveillance data revealed a six-week advancement in the seasonal timing of disseminated Lyme disease cases in southern Norway over the 25-year study period. The seasonal shift predominantly occurred in the first 10 years of the study period, preceding the period with the most rapid increase in annual incidence. Annual incidence increased across geographic regions in Norway. Changes in plant phenology, measured by peak spring greening observed by Normalized Difference Vegetation Index (NDVI), over the same study period and area were used as a yardstick for interpreting the observed shift in case timing. The shift in case seasonality outpaced a concurrent shift in peak spring greening, which advanced by around three weeks over the study period in the same study area. The shift in peak spring greening also predominantly occurred during the first 10 years and then stabilized for the remainder of the study period. The advancement of case timing and similarity between study regions were consistent with the climate-based predictions outlined in the Introduction.

The analysis in **Paper 2** identified that the seasonal case timing in youth (0-19 years, both sexes) was consistently around 4.4 weeks earlier than adults, regardless of clinical manifestation. Both adults and youth had a similar advancement in case timing over the study period, indicating that the advancement trend is unrelated to patient demography. Other

demographic features of the surveillance data include a bimodal distribution of incidence over patient age, with children (0-9 years) having the highest incidence, seconded by seniors (70-79 years). Males had a higher incidence than females in all age groups except for children (0-9 years). Adult males had higher proportion of arthritis cases compared to adult females. While all demographic groups predominantly had neuroborreliosis manifestations, youth (0-19 years) presented with a higher proportion of neuroborreliosis cases and a lower proportion of arthritic manifestations compared to adults. These findings partially aligned with the predictions outlined earlier, as while a difference in case timing between children and adults was identified, no clear difference in case timing between males and females was quantified.

In the mathematical model presented in **Paper 3,** tick questing phenology had an important effect on disease hazard. Earlier questing exposed ticks, particularly larvae, to higher infection prevalence in the small host population due to the seasonality of host demography leading to a high number of infected adults in the beginning of the year. In spring, the small mammal population was comprised of a larger proportion of older individuals which were infected by ticks the prior year. This was in contrast with the summer and fall population, dominated by susceptible juveniles. Thus, host demographic turnover, driven by reproduction, rapidly diluted infection prevalence in the host population and thereby reduced the infection probability for feeding ticks. Synchrony in questing between tick stages was important for pathogen transmission cycles because the demographic turnover in hosts diluted infection levels very rapidly in summer.

Discussion

Shifting Seasons as a Driver of Disease Emergence

Over recent decades, climate change, in addition to other factors, has already altered the prevalence and distribution of infectious diseases (Altizer et al., 2013; Campbell-Lendrum et al., 2015), and specifically tick borne diseases (Gilbert, 2021). It is often difficult to disentangle the role of shifting climate seasonality from other climate trends in driving changes in disease dynamics. One possible link between shifting seasonality and disease emergence could be a longer duration of tick activity resulting in more disease cases. In **Paper 1**, we find that the timing of Lyme disease cases advanced by six weeks over the study period, but the duration of the season of Lyme cases did not change. It is interesting that there is no observed lengthening of the season given that models predict climate change can cause increased tick activity in autumn (Li et al., 2016; Ogden et al., 2008). This could occur because the activity potential of a longer duration of suitable climate for tick questing may not be fully realized by a tick population, for example because of low autumn host availability (Eisen, Eisen, Ogden, et al., 2016). Even if tick questing activity is prolonged, human exposure levels may be reduced in autumn (Eisen, Eisen, Ogden, et al., 2016).

In **Paper 3**, we found that advanced tick questing could increase disease hazard, but it remains unclear, and likely highly regionally variable, whether climate change will result in delayed or advanced tick questing, and/or an extension or reduction of questing duration, with several models showing different, but overlapping, predictions (Li et al., 2016; MacDonald et al., 2020; Ogden et al., 2020). Generally, tick activity is predicted to start earlier in the spring and have a longer duration (Levi et al., 2015; MacDonald et al., 2020; Monaghan et al., 2015). While tick activity appears to be primarily driven by climate, specifically humidity (Berger et al., 2014; Hauser et al., 2018; Requena-García et al., 2017; Schulz et al., 2014) and

temperature (Alonso-Carné et al., 2015; Eisen, Eisen, Ogden, et al., 2016; Wongnak et al., 2022), and cumulative growing degree days is a strong predictor of activity levels (Diuk-Wasser et al., 2006; Moore et al., 2014), photoperiod-induced diapause (Gray et al., 2016) makes tick responses to climate warming difficult to predict. Climate based predictions of tick dynamics based on seasonal environmental suitability for tick questing may not adequately account for ticks entering diapause, which could inhibit fall questing (Belozerov et al., 2002; Gray et al., 2016). Responses to photoperiod and climate drivers vary between tick populations from different regions (Eisen, Eisen, Ogden, et al., 2016; Gilbert et al., 2014; Ogden et al., 2020), which makes such effects difficult to generalize. Limited data is available on how temperature effects *B. burgdorferi* survival and replication inside the tick vector (Gray et al., 2009), in contrast to the malaria disease system where such effects are well studied (Mordecai et al., 2019).

Seasonal effects that impact Lyme disease hazard indirectly via host phenology, abundance, and movement could explain linkages between case seasonality and emergence as well as the divergence between the observed magnitude of case advancement in **Paper 1** and model-based predictions of shifts in case timing (Li et al., 2016; Monaghan et al., 2015). Following the model proposed in Moore et al. 2014, that links cumulative growing degree days to case seasonality, the observed six-week case advancement in **Paper 1** would require an increase of 450 cumulative growing degree days by mid-May. This value exceeds expectations for climate change projections to year 2050 for most of Norway (Skaugen & Tveito, 2004). While climate based projections of case seasonality are undoubtedly useful, the divergence between model predictions and empirical findings in **Paper 1** highlights the importance of combining such approaches with mechanistic models that include host and vector population dynamics and interactions.

A limitation of the mathematical model presented in **Paper 3** is that it only incorporates one small host, representing a small mammal life history. This is a large simplification of the complexity of hosts used by ticks. Avian hosts, such as the European Blackbird (*Turdus merula*), impact Lyme disease dynamics as an important reservoir of *B. garinii* (Brinkerhoff et al., 2009; Gryczyńska & Kowalec, 2019; Mysterud, Heylen, et al., 2019). Climate change has resulted not only in advanced migration phenology in many bird species (Barrett, 2002; Cotton, 2003; Jenni & Kéry, 2003; Lehikoinen et al., 2004), but also a reduction in migratory strategy in partial migrants, including the European Blackbird (Møller et al., 2014; Van Vliet et al., 2009). It is plausible that climate driven changes in bird migratory behavior increase the availability of birds as hosts for spring-feeding ticks, thus increasing *B. garinii* infection levels in the tick population. Extending the model framework presented in **Paper 3** to include an avian host would be an interesting future direction for research.

Case Seasonality Analysis

Many jurisdictions have instated Lyme disease surveillance since the 1990s, when Lyme disease became nationally notifiable in many European countries and the United States (Blanchard et al., 2022; Cartter et al., 2018; Nagarajan et al., 2023). Surveillance systems differ between countries in case definition and reporting policies (Blanchard et al., 2022; Vandekerckhove et al., 2021), particularly as to whether patients with erythema migrans are included in the case definition or only cases of disseminated infection are included (Nagarajan et al., 2023). Heterogeneity between surveillance systems creates difficulty in understanding Lyme disease epidemiology, comparing data between jurisdictions, and developing wide-scale interventions (Blanchard et al., 2022; Nagarajan et al., 2023). Under-reporting of Lyme

disease cases is a broadly recognized problem (Burn et al., 2023; Ogden et al., 2019; Rutz et al., 2018).

One of the challenges of working with Lyme disease surveillance data is that typically only positive results of tests are recorded. The surveillance data reports the number of cases in a given week, but not the proportion of tests that were positive, making health system effects much more difficult to control for. Health system effects can be very important in an emerging disease where awareness of the disease can play an important role in detection. In general, interpretation of the quality and completeness of surveillance data requires additional data collection processes (Lescano et al., 2008), which was outside of the scope of this thesis but has been discussed elsewhere (MacDonald et al., 2016). Many Lyme disease surveillance systems, including the Norwegian data, only include cases of disseminated disease, which represent only a small fraction of total cases. Thus, even in places with relatively high incidence, the number of cases per week is quite small and heavily zero inflated.

Estimation of changes in case seasonality requires the ability to pick out a weak signal from the data with a high level of confidence. In **Paper 1**, the challenge of small case totals, although partially mitigated by the long duration of the study period (25 years), had to be met by pooling county-level data into larger regions. Similarly, in **Paper 2**, sexes had to be grouped in youth because of low case totals. Although these groupings were necessary for statistical model fitting, it would have been ideal to be able to work on more demographic groups and a finer spatial scale. Spatial scale is particularly important because Lyme disease exhibits a high degree of local variability (Waller et al., 2007). Additionally, because Lyme disease has been emerging in Norway throughout the entire study period, particularly in the

context of coarse spatial scales, it is challenging to identify a baseline time period for comparison.

Given the many challenges of working with surveillance data, Bayesian methods are an attractive approach for model fitting (Robertson et al., 2010). Historically, Bayesian modeling has been hindered by the computational intensity of sampling parameters from the posterior distribution via Monte Carlo Markov Chain methods (Robertson et al., 2010; Rue et al., 2009). The package INLA simplified the implementation of flexible and complex components in the generalized linear mixed model structure that could separate annual and seasonal trends in the data. The modelling approach for the seasonal component was inspired by a previous analysis of mumps cases in New York City, that also included a flexible annual trend and a time-variant harmonic seasonal component, but did not use a Bayesian framework (Ruiz-Cárdenas et al., 2012). In **Paper 1** we were able to use INLA to fit a flexible seasonal trend that varied across years to data from the entire study period. This differentiated our method from a prior approach to analyzing Lyme disease case seasonality in the USA, which involved year by year analysis of seasonal peaks by fitting a polynomial regression function (Moore et al., 2014). An advantage of our method is an improved ability to quantify uncertainty in the estimated seasonal peaks by repeated sampling from the posterior distribution.

Demography and Sociological Features

Human demography is known to be important for vector borne diseases through a variety of pathways including vulnerability, mobility, and awareness (Athni et al., 2021; Ryan, 2020; Sahoo et al., 2017; Soriano-Paños et al., 2020), but has been given considerably little attention in the context of predicting vector borne disease outcomes. Demographic changes in

Thailand have resulted in an increase in the mean age of dengue hemorrhagic fever cases, which has important implications for clinical complications and health burden (Huang et al., 2022). For Lyme disease, surveillance data has been used to explore the demography of patients in several regions, which generally shows a bimodal distribution with elevated incidence in youth and older adults (Kugeler et al., 2022; Schwartz et al., 2017; Seukep et al., 2015; Tulloch et al., 2019). While behavioral factors modulating exposure are often assumed to drive the bimodal demographic pattern (Kugeler et al., 2022), little research has been conducted into possible physiological and immunological factors that could also be involved. Continued demographic transition to an older population age structure from reduced birth and death rates (Bongaarts, 2009) may have important implications for Lyme disease epidemiology but is typically not included in predictions of Lyme disease emergence.

Economic improvements reduce the incidence of many vector borne diseases (Campbell-Lendrum et al., 2015), but the relationship between economic development and incidence is less clear for Lyme disease. Vector control efforts and infrastructure changes have had a very significant impact on many vector borne diseases (Altizer et al., 2013), but are not very relevant for Lyme disease where sanitation and water storage do not impact disease hazard and limited vector control options are available (Ostfeld et al., 2006). Socioeconomic change influences land use and conversion between land cover types, which can influence both disease hazard and human exposure (Li et al., 2019). Projections of Lyme disease risk based on a combination of climate and socioeconomic forecasts suggest that Lyme disease hazard is expected to increase under scenarios with increased social, economic, and political disparities (Li et al., 2019). However, Lyme disease risk has also been linked with higher socioeconomic status in several contexts (Slatculescu et al., 2022; Springer & Johnson, 2018;

Tulloch et al., 2019), which is congruent with known risk factors that can be associated with higher socioeconomic status, such as residing in suburban areas (Kaup, 2018; Smith et al., 2001) and participation in outdoor leisure activities, such as hiking and gardening (Aenishaenslin et al., 2022; Mead et al., 2018).

A confounding factor in drawing linkages between socioeconomic status and Lyme disease risk stems from the case definition used for Lyme disease surveillance, as it appears that lower socioeconomic status and reduced health care access is associated with disseminated cases of Lyme disease, while higher socioeconomic status is associated with localized infections (Moon et al., 2021). Gender-based social inequality has been mentioned in **Paper 2** as it has been found that there is a female bias in studies on localized Lyme disease infections and a male bias in studies on disseminated infections (Eliassen et al., 2017; Nygård et al., 2005; Skufca et al., 2022; Tulloch et al., 2020; Tulloch et al., 2019). Further investigation into Lyme disease demography and the social and physiological risk factors for disease dissemination would be a very valuable direction for future research that is currently beyond the scope of the data recorded in surveillance systems.

Insights from Mathematical Models

Tick population models, including the one used in **Paper 3** and those described elsewhere (Dobson et al., 2011; Estrada-Peña & Estrada-Sánchez, 2013), are inherently limited by knowledge gaps resulting from a lack of empirical data on tick biology and ecology (Gray et al., 2021; Kahl & Gray, 2023; Sirotkin & Korenberg, 2022), particularly for non-questing stages that are more difficult to observe. For this reason, the model-based predictions discussed in **Paper 3** are intended to describe qualitative changes in outcomes between scenarios, rather than accurate quantitative predictions. Additionally, the model is flexible and

adaptable such that empirical data can be incorporated into the framework as they become available. Despite inherent limitations, population models are useful for exploring underlying linkages between tick and host phenology and disease dynamics, which may be very difficult and costly to observe in an empirical system.

A theoretical basis for understanding links between disease hazard and vector and host phenology is needed for untangling complex relationships in a vector borne disease system. This is exemplified in the literature on frogs infected by the trematode parasite *Ribeiroia ondatrae* that uses snails as an intermediate between terrestrial reservoirs and tadpoles. This is one of the only disease systems where it has been empirically demonstrated that changes in temperature alters phenological synchrony between hosts and parasites, yielding important changes to disease dynamics. Warmer temperatures cause parasites to be released from snails into the aquatic environment earlier in the year, yielding bidirectional impacts on frog disease outcomes (Paull & Johnson, 2011). Earlier parasite release coincides with higher snail mortality and reduced overlap between tadpoles and parasites, but also a higher risk of infection as the tadpoles are more susceptible earlier in their development (McDevitt-Galles et al., 2020; Paull & Johnson, 2014; Paull & Johnson, 2011). Similar effects could be occurring in the Lyme disease system, but the role of host immunity in driving pathogen loads has not been well explored. Observed heterogeneity in tick infestation and infection levels in rodents (Lindsø et al., 2023) could be related to host immunology. Migratory birds have been shown to have seasonal fluctuations in pathogen load, linked to immune modulation from migratory stress (Gylfe et al., 2000). It would be interesting to extend the model presented in **Paper 3** to include more within-host heterogeneity to gain insight into how factors such as body condition, stress, and immunity could impact seasonal pathogen loads and host infection susceptibility.

It is well recognized that climate and local adaptations drive the seasonal synchrony of activity levels of tick instars, and that questing synchrony is relevant for pathogen transmission cycles (Estrada-Peña & Estrada-Sánchez, 2013; Gatewood et al., 2009; Gilbert, 2021; Ogden et al., 2020; Randolph et al., 2000). It remains unclear and regionally diverse whether climate change is likely to increase or decrease the synchrony of nymphal and larval feeding (Altizer et al., 2013; Ogden et al., 2020; Ogden et al., 2008; Ostfeld & Brunner, 2015). This is another topic that lends itself to exploration with models because of the difficulty in observing tick phenology across instars for a long time period and at a large spatial scale, while controlling for inter-annual climate variability.

It has been postulated that a time lag between host inoculation by nymphs in spring and pathogen acquisition by larvae in summer favors pathogen genotypes that are able to persist in hosts for several months (Gatewood et al., 2009; Ostfeld & Brunner, 2015), while greater synchrony in larval and nymphal feeding, could select for pathogen strains with higher virulence (Altizer et al., 2013). However, even with a prolonged lag between nymphs and larvae questing, in cases where hosts have high demographic turnover and infected hosts have low survival, a virulence strategy could be more favorable than a persistence strategy. This is because it could be more beneficial for the pathogen to target high transmission rates between infected nymphs and susceptible larvae questing at the near edges of their activity periods than to attempt to bridge the gap between activity peaks during which high infected host mortality could occur. In a scenario where such an adaptation has occurred, phenological shifts that increase synchrony between nymphs and larvae could be more relevant because the virulent genotype that was dominant has more to gain from the phenological shift than a genotype with a persistent strategy. Similar hypotheses regarding the relationship between tick stage synchrony, host longevity, and disease transmission have been proposed elsewhere

(Eisen, Eisen, Ogden, et al., 2016; Ogden et al., 2020). An extension of the mathematical model presented in **Paper 3** that includes multiple pathogen genotypes with different evolutionary strategies could be used to explore such theories.

The pathway proposed in **Paper 3** that links tick questing phenology and host demographic turnover with disease hazard is a novel perspective on Lyme disease ecology, that could be relevant in other disease systems. Further empirical research is needed to demonstrate whether this pathway is actually occurring in nature. With more population data for hosts and vectors, the model could be extended to include spatial specificity and a finer temporal scale. Clinical and social research that explores human exposure and disease pathogenesis would be valuable for linking disease hazard model outputs with human case surveillance data. While the demographic analysis in **Paper 2** and the mathematical modeling exercise presented in **Paper 3** make an initial foray into exploring potential causes of the seasonal shift observed in **Paper 1**, we remain far from demonstrating why Lyme disease cases are occurring earlier in the year and whether this is linked with an increase in incidence and/or the spatial distribution of Lyme disease. I hope this work inspires further investigation into the seasonality of Lyme disease and other vector borne diseases.

Bibliography

Abrieux, A., Xue, Y., Cai, Y., Lewald, K. M., Nguyen, H. N., Zhang, Y., & Chiu, J. C. (2020). EYES ABSENT and TIMELESS integrate photoperiodic and temperature cues to regulate seasonal physiology in *Drosophila*. *Proceedings of the National Academy of Sciences*, *117*(26), 15293-15304. https://doi.org/10.1073/pnas.2004262117

Aenishaenslin, C., Charland, K., Bowser, N., Perez-Trejo, E., Baron, G., Milord, F., & Bouchard, C. (2022). Behavioral risk factors associated with reported tick exposure in a Lyme disease high incidence region in Canada. *BMC Public Health*, *22*(1), 807. https://doi.org/10.1186/s12889-022-13222-9

Alonso-Carné, J., García-Martín, A., & Estrada-Peña, A. (2015). Modelling the phenological relationships of questing immature *Ixodes ricinus* (Ixodidae) using temperature and NDVI data. *Zoonoses and Public Health*, *63*(1), 40-52. https://doi.org/10.1111/zph.12203

Altizer, S., Dobson, A., Hosseini, P., Hudson, P., Pascual, M., & Rohani, P. (2006). Seasonality and the dynamics of infectious diseases. *Ecology Letters*, *9*(4), 467-484. https://doi.org/10.1111/j.1461-0248.2005.00879.x

Altizer, S., Ostfeld, R. S., Johnson, P. T., Kutz, S., & Harvell, C. D. (2013). Climate change and infectious diseases: from evidence to a predictive framework. *Science*, *341*(6145), 514-519. https://doi.org/10.1126/science.1239401

Aminikhah, M., Forsman, J. T., Koskela, E., Mappes, T., Sane, J., Ollgren, J., Kivelä, S. M., & Kallio, E. R. (2021). Rodent host population dynamics drive zoonotic Lyme borreliosis and orthohantavirus infections in humans in Northern Europe. *Scientific Reports*, *11*(1), 16128. https://doi.org/10.1038/s41598-021-95000-y

Anderson, J. F., & Magnarelli, L. A. (1994). Lyme disease: A tick-associated disease originally described in Europe, but named after a town in Connecticut. *American Entomologist*, *40*(4), 217-228. https://doi.org/10.1093/ae/40.4.217

Arsnoe, I. M., Hickling, G. J., Ginsberg, H. S., McElreath, R., & Tsao, J. I. (2015). Different populations of blacklegged tick nymphs exhibit differences in questing behavior that have implications for human Lyme disease risk. *PLoS One*, *10*(5), e0127450. https://doi.org/10.1371/journal.pone.0127450

Arvikar, S. L., & Steere, A. C. (2022). Lyme arthritis. *Infectious Disease Clinics of North America*, *36*(3), 563-577. https://doi.org/10.1016/j.idc.2022.03.006

Athni, T. S., Shocket, M. S., Couper, L. I., Nova, N., Caldwell, I. R., Caldwell, J. M., Childress, J. N., Childs, M. L., De Leo, G. A., Kirk, D. G., MacDonald, A. J., Olivarius, K., Pickel, D. G., Roberts, S. O., Winokur, O. C., Young, H. S., Cheng, J., Grant, E. A., Kurzner, P. M., Kyaw, S., Lin, B. J., Lopez, R. C., Massihpour, D. S., Olsen, E. C., Roache, M., Ruiz, A., Schultz, E. A., Shafat, M., Spencer, R. L., Bharti, N., & Mordecai, E. A. (2021). The influence of vector-borne disease on human history: Socio-ecological mechanisms. *Ecology Letters*, *24*(4), 829-846. https://doi.org/10.1111/ele.13675

Bacaër, N. (2009). Periodic matrix population models: Growth rate, basic reproduction number, and entropy. *Bulletin of Mathematical Biology*, *71*(7), 1781-1792. https://doi.org/10.1007/s11538-009-9426-6

Balashov, Y. S. (2012). Demography and population models of ticks of the genus *Ixodes* with long-term life cycles. *Entomological Review*, *92*(9), 1006-1011. https://doi.org/10.1134/s0013873812090072

Barrett, R. T. (2002). The phenology of spring bird migration to north Norway. *Bird Study*, *49*(3), 270-277. https://doi.org/10.1080/00063650209461275

Barstad, B., Quarsten, H., Tveitnes, D., Noraas, S., Ask, I. S., Saeed, M., Bosse, F., Vigemyr, G., Huber, I., & Øymar, K. (2018). Direct molecular detection and genotyping of *Borrelia burgdorferi* sensu lato in cerebrospinal fluid of children with Lyme neuroborreliosis. *Journal of Clinical Microbiology*, *56*(5), 10.1128/jcm. 01868-01817. https://doi.org/10.1128/jcm.01868-17

Becker, A. D., Birger, R. B., Teillant, A., Gastanaduy, P. A., Wallace, G. S., & Grenfell, B. T. (2016). Estimating enhanced prevaccination measles transmission hotspots in the context of cross-scale dynamics. *Proceedings of the National Academy of Sciences*, *113*(51), 14595-14600. https://doi.org/10.1073/pnas.1604976113

Belozerov, V. N., Fourie, L. J., & Kok, D. J. (2002). Photoperiodic control of developmental diapause in nymphs of prostriate ixodid ticks (Acari: Ixodidae). *Experimental and Applied Acarology*, *28*(1–4), 163-168. https://doi.org/10.1023/a:1025377829119

Bennet, L., Stjernberg, L., & Berglund, J. (2007). Effect of gender on clinical and epidemiologic features of Lyme borreliosis. *Vector-Borne and Zoonotic Diseases*, *7*(1), 34-41. https://doi.org/10.1089/vbz.2006.0533

Berger, K. A., Ginsberg, H. S., Gonzalez, L., & Mather, T. N. (2014). Relative humidity and activity patterns of *Ixodes scapularis* (Acari: Ixodidae). *Journal of Medical Entomology*, *51*(4), 769-776. https://doi.org/10.1603/me13186

Blanchard, L., Jones-Diette, J., Lorenc, T., Sutcliffe, K., Sowden, A., & Thomas, J. (2022). Comparison of national surveillance systems for Lyme disease in humans in Europe and North America: a policy review. *BMC Public Health*, *22*(1), 1307. https://doi.org/10.1186/s12889-022-13669-w

Bohrer, R. A. (2008). Challenges for biotechnology law. *Biotechnology Law Report*, *27*(5), 421-424. https://doi.org/10.1089/blr.2008.9920

Bongaarts, J. (2009). Human population growth and the demographic transition. *Philosophical Transactions of the Royal Society B: Biological Sciences*, *364*(1532), 2985-2990. https://doi.org/10.1098/rstb.2009.0137

Borchers, A. T., Keen, C. L., Huntley, A. C., & Gershwin, M. E. (2015). Lyme disease: A rigorous review of diagnostic criteria and treatment. *Journal of Autoimmunity*, *57*, 82-115. https://doi.org/10.1016/j.jaut.2014.09.004

Brinkerhoff, R. J., Folsom-O'Keefe, C. M., Tsao, K., & Diuk-Wasser, M. A. (2009). Do birds affect Lyme disease risk? Range expansion of the vector-borne pathogen *Borrelia burgdorferi*. *Frontiers in Ecology and the Environment*, *9*(2), 103-110. https://doi.org/10.1890/090062

Bronson, F. H. (2009). Climate change and seasonal reproduction in mammals. *Philosophical Transactions of the Royal Society B: Biological Sciences*, *364*(1534), 3331-3340. https://doi.org/10.1098/rstb.2009.0140

Brunner, J. L., LoGiudice, K., & Ostfeld, R. S. (2008). Estimating reservoir competence of *Borrelia burgdorferi* hosts: Prevalence and infectivity, sensitivity, and specificity. *Journal of Medical Entomology*, *45*(1), 139-147. https://doi.org/10.1093/jmedent/45.1.139

Burgdorfer, W. (1984). Discovery of the Lyme disease spirochete and its relation to tick vectors. *The Yale journal of Biology and Medicine*, *57*, 515-520.

Burgdorfer, W. (1991). Lyme borreliosis: Ten years after discovery of the etiologic agent, *Borrelia burgdorferi*. *Infection*, *19*(4), 257-262. https://doi.org/10.1007/bf01644963

Burn, L., Tran, T. M. P., Pilz, A., Vyse, A., Fletcher, M. A., Angulo, F. J., Gessner, B. D., Moisi, J. C., Jodar, L., & Stark, J. H. (2023). Incidence of Lyme borreliosis in Europe from national surveillance systems (2005-2020). *Vector-Borne and Zoonotic Diseases*, *23*(4), 156-171. https://doi.org/10.1089/vbz.2022.0071

Burtis, J. C., Foster, E., Schwartz, A. M., Kugeler, K. J., Maes, S. E., Fleshman, A. C., & Eisen, R. J. (2022). Predicting distributions of blacklegged ticks (*Ixodes scapularis*), Lyme disease spirochetes (*Borrelia burgdorferi* sensu stricto) and human Lyme disease cases in the Eastern United States. *Ticks and Tick-borne Diseases*, *13*(5), 102000. https://doi.org/10.1016/j.ttbdis.2022.102000

Cadavid, D., Auwaerter, P. G., Rumbaugh, J., & Gelderblom, H. (2016). Antibiotics for the neurological complications of Lyme disease. *Cochrane Database of Systematic Reviews*, *12*(12), CD006978. https://doi.org/10.1002/14651858.CD006978.pub2

Caminade, C., McIntyre, K. M., & Jones, A. E. (2019). Impact of recent and future climate change on vector-borne diseases. *Annals of the New York Academy of Sciences*, *1436*(1), 157-173. https://doi.org/10.1111/nyas.13950

Campbell-Lendrum, D., Manga, L., Bagayoko, M., & Sommerfeld, J. (2015). Climate change and vector-borne diseases: What are the implications for public health research and policy? *Philosophical Transactions of the Royal Society B: Biological Sciences*, *370*(1665), 20130552. https://doi.org/10.1098/rstb.2013.0552

Carlsson, H., Ekerfelt, C., Henningsson, A. J., Brudin, L., & Tjernberg, I. (2018). Subclinical Lyme borreliosis is common in South-Eastern Sweden and may be distinguished from Lyme neuroborreliosis by sex, age and specific immune marker patterns. *Ticks and Tick-borne Diseases*, *9*(3), 742-748. https://doi.org/10.1016/j.ttbdis.2018.02.011

Carlsson, S.-a., Granlund, H., Jansson, C., Nyman, D., & Wahlberg, P. (2003). Characteristics of erythema migrans in *Borrelia afzelii* and *Borrelia garinii* infections. *Scandinavian journal of infectious diseases*, *35*(1), 31-33. https://doi.org/10.1080/0036554021000026978

Cartter, M. L., Lynfield, R., Feldman, K. A., Hook, S. A., & Hinckley, A. F. (2018). Lyme disease surveillance in the United States: Looking for ways to cut the Gordian knot. *Zoonoses and Public Health*, *65*(2), 227-229. https://doi.org/10.1111/zph.12448

Caswell, H. (2001). *Matrix population models* (Vol. 1). Sinauer Sunderland, MA.

Caswell, H., & Trevisan, M. C. (1994). Sensitivity analysis of periodic matrix models. *Ecology*, *75*(5), 1299-1303. https://doi.org/10.2307/1937455

Cerar, T., Strle, F., Stupica, D., Ruzic-Sabljic, E., McHugh, G., Steere, A. C., & Strle, K. (2016). Differences in genotype, clinical features, and inflammatory potential of *Borrelia burgdorferi* sensu stricto strains from Europe and the United States. *Emerging Infectious Diseases*, *22*(5), 818-827. https://doi.org/10.3201/eid2205.151806

Civitello, D. J., Cohen, J., Fatima, H., Halstead, N. T., Liriano, J., McMahon, T. A., Ortega, C. N., Sauer, E. L., Sehgal, T., Young, S., & Rohr, J. R. (2015). Biodiversity inhibits parasites: Broad evidence for the dilution effect. *Proceedings of the National Academy of Sciences*, *112*(28), 8667-8671. https://doi.org/10.1073/pnas.1506279112

Coburn, J., Garcia, B., Hu, L. T., Jewett, M. W., Kraiczy, P., Norris, S. J., & Skare, J. (2021). Lyme disease pathogenesis. *Current issues in molecular biology*, *42*, 473-518. https://doi.org/10.21775/cimb.042.473

Cochat Costa Rodrigues, M. C., Moreira, I., Peixoto, M. J., & Silveira, C. (2017). The new great imitator – Neuropsychiatric symptoms of Lyme disease. *European Psychiatry*, *41*(S1), S232-S232. https://doi.org/10.1016/j.eurpsy.2017.01.2242

Coipan, E. C., Jahfari, S., Fonville, M., Oei, G. A., Spanjaard, L., Takumi, K., Hovius, J. W., & Sprong, H. (2016). Imbalanced presence of *Borrelia burgdorferi* sl multilocus sequence types in clinical manifestations of Lyme borreliosis. *Infection, Genetics and Evolution*, *42*, 66-76. https://doi.org/10.1016/j.meegid.2016.04.019

Comstedt, P., Jakobsson, T., & Bergström, S. (2011). Global ecology and epidemiology of *Borrelia garinii* spirochetes. *Infection Ecology & Epidemiology*, *1*(1), 9545. https://doi.org/10.3402/iee.v1i0.9545

Copernicus Climate Change Service. (2024). *Copernicus Interactive Climate Atlas (C3S Atlas)* https://atlas.climate.copernicus.eu/atlas

Coppack, T., Pulido, F., Czisch, M., Auer, D. P., & Berthold, P. (2003). Photoperiodic response may facilitate adaptation to climatic change in long-distance migratory birds. *Proceedings of the Royal Society of London. Series B: Biological Sciences*, *270*(suppl_1), s43-s46. https://doi.org/10.1098/rsbl.2003.0005

Cornes, R. C., van der Schrier, G., van den Besselaar, E. J., & Jones, P. D. (2018). An ensemble version of the E-OBS temperature and precipitation data sets. *Journal of Geophysical Research: Atmospheres*, *123*(17), 9391-9409. https://doi.org/10.1029/2017JD028200

Cotton, P. A. (2003). Avian migration phenology and global climate change. *Proceedings of the National Academy of Sciences*, *100*(21), 12219-12222. https://doi.org/10.1073/pnas.1930548100

Cruz, A. I., Aversano, F. J., Seeley, M. A., Sankar, W. N., & Baldwin, K. D. (2017). Pediatric Lyme arthritis of the hip: The great imitator? *Journal of Pediatric Orthopaedics*, *37*(5), 355-361. https://doi.org/10.1097/bpo.0000000000000664

Dias, S. P., Brouwer, M. C., & van de Beek, D. (2022). Sex and gender differences in bacterial infections. *Infection and Immunity*, *90*(10), e00283-00222. https://doi.org/10.1128/iai.00283-22

Diuk-Wasser, M. A., Gatewood, A. G., Cortinas, M. R., Yaremych-Hamer, S., Tsao, J., Kitron, U., Hickling, G., Brownstein, J. S., Walker, E., Piesman, J., & Fish, D. (2006). Spatiotemporal patterns of host-Seeking *Ixodes scapularis* nymphs (Acari: Ixodidae) in the United States. *Journal of Medical Entomology*, *43*(2), 166-176. https://doi.org/10.1093/jmedent/43.2.166

Dobson, A. D., Finnie, T. J., & Randolph, S. E. (2011). A modified matrix model to describe the seasonal population ecology of the European tick *Ixodes ricinus*. *Journal of Applied Ecology*, *48*(4), 1017-1028. https://doi.org/10.1111/j.1365-2664.2011.02003.x

Doyal, L. (2001). Sex, gender, and health: the need for a new approach. *Bmj*, *323*(7320), 1061-1063. https://doi.org/10.1136/bmj.323.7320.1061

Ebi, K. L., Ogden, N. H., Semenza, J. C., & Woodward, A. (2017). Detecting and attributing health burdens to climate change. *Environmental Health Perspectives*, *125*(8), 085004. https://doi.org/10.1289/EHP1509

Eddens, T., Kaplan, D. J., Anderson, A. J., Nowalk, A. J., & Campfield, B. T. (2019). Insights from the geographic spread of the Lyme disease epidemic. *Clinical Infectious Diseases*, *68*(3), 426-434. https://doi.org/10.1093/cid/ciy510

Eisen, R. J., Eisen, L., & Beard, C. B. (2016). County-scale distribution of *Ixodes scapularis* and *Ixodes pacificus* (Acari: Ixodidae) in the continental United States. *Journal of Medical Entomology*, *53*(2), 349-386. https://doi.org/10.1093/jme/tjv237

Eisen, R. J., Eisen, L., Ogden, N. H., & Beard, C. B. (2016). Linkages of weather and climate with *Ixodes scapularis* and *Ixodes pacificus* (Acari: Ixodidae), enzootic transmission of *Borrelia burgdorferi*, and Lyme disease in North America. *Journal of Medical Entomology*, *53*(2), 250-261. https://doi.org/10.1093/jme/tjv199

Eldin, C., Raffetin, A., Bouiller, K., Hansmann, Y., Roblot, F., Raoult, D., & Parola, P. (2019). Review of European and American guidelines for the diagnosis of Lyme borreliosis. *Medecine et Maladies Infectieuses*, *49*(2), 121-132. https://doi.org/10.1016/j.medmal.2018.11.011

Eliassen, K. E., Berild, D., Reiso, H., Grude, N., Christophersen, K. S., Finckenhagen, C., & Lindbaek, M. (2017). Incidence and antibiotic treatment of erythema migrans in Norway 2005-2009. *Ticks and Tick-borne Diseases*, *8*(1), 1-8. https://doi.org/10.1016/j.ttbdis.2016.06.006

Environmental Protection Agency. (2021). Seasonality and climate change: A review of observed evidence in the United States. (EPA 430-R-21-002.). https://www.epa.gov/climate-indicators/seasonality-and-climate-change

Epstein, P. R. (2001). West Nile virus and the climate. *Journal of Urban Health: Bulletin of the New York Academy of Medicine*, *78*(2), 367-371. https://doi.org/10.1093/jurban/78.2.367

Ernakovich, J. G., Hopping, K. A., Berdanier, A. B., Simpson, R. T., Kachergis, E. J., Steltzer, H., & Wallenstein, M. D. (2014). Predicted responses of arctic and alpine ecosystems to altered seasonality under climate change. *Global Change Biology*, *20*(10), 3256-3269. https://doi.org/10.1111/gcb.12568

Estrada-Peña, A., & Estrada-Sánchez, D. (2013). Deconstructing Ixodes ricinus: A partial matrix model allowing mapping of tick development, mortality and activity rates. *Medical and Veterinary Entomology*, *28*(1), 35-49. https://doi.org/10.1111/mve.12009

Feng, X., Porporato, A., & Rodriguez-Iturbe, I. (2013). Changes in rainfall seasonality in the tropics. *Nature Climate Change*, *3*(9), 811-815. https://doi.org/10.1038/nclimate1907

Flynn, D. F. B., & Wolkovich, E. M. (2018). Temperature and photoperiod drive spring phenology across all species in a temperate forest community. *New Phytologist*, *219*(4), 1353-1362. https://doi.org/10.1111/nph.15232

Franke, J., Moldenhauer, A., Hildebrandt, A., & Dorn, W. (2010). Are birds reservoir hosts for *Borrelia afzelii*? *Ticks and Tick-borne Diseases*, *1*(2), 109-112. https://doi.org/10.1016/j.ttbdis.2010.03.001

Gage, K. L., Burkot, T. R., Eisen, R. J., & Hayes, E. B. (2008). Climate and vectorborne diseases. *American Journal of Preventive Medicine*, *35*(5), 436-450. https://doi.org/10.1016/j.amepre.2008.08.030

Gandy, S., Kilbride, E., Biek, R., Millins, C., & Gilbert, L. (2021). Experimental evidence for opposing effects of high deer density on tick-borne pathogen prevalence and hazard. *Parasites & Vectors*, *14*(1), 509. https://doi.org/10.1186/s13071-021-05000-0

Garkowski, A., Zajkowska, J., Zajkowska, A., Kułakowska, A., Zajkowska, O., Kubas, B., Jurgilewicz, D., Hładuński, M., & Łebkowska, U. (2017). Cerebrovascular manifestations of Lyme neuroborreliosis—A systematic review of published cases. *Frontiers in Neurology*, *8*, 146. https://doi.org/10.3389/fneur.2017.00146

Gatewood, A. G., Liebman, K. A., Vourc'h, G., Bunikis, J., Hamer, S. A., Cortinas, R., Melton, F., Cislo, P., Kitron, U., Tsao, J., Barbour, A. G., Fish, D., & Diuk-Wasser, M. A. (2009). Climate and tick seasonality are predictors of *Borrelia burgdorferi* genotype distribution. *Applied and Environmental Microbiology*, *75*(8), 2476-2483. https://doi.org/10.1128/AEM.02633-08

Gilbert, L. (2021). The impacts of climate change on ticks and tick-borne disease risk. *Annual Review of Entomology*, *66*(1), 373-388. https://doi.org/10.1146/annurev-ento-052720-094533

Gilbert, L., Aungier, J., & Tomkins, J. L. (2014). Climate of origin affects tick (*Ixodes ricinus*) host-seeking behavior in response to temperature: Implications for resilience to climate change? *Ecology and Evolution*, *4*(7), 1186-1198. https://doi.org/10.1002/ece3.1014

Gilbert, L., Maffey, G. L., Ramsay, S. L., & Hester, A. J. (2012). The effect of deer management on the abundance of *Ixodes ricinus* in Scotland. *Ecological Applications*, *22*(2), 658-667. https://doi.org/10.1890/11-0458.1

Gray, J., Kahl, O., & Zintl, A. (2021). What do we still need to know about *Ixodes ricinus*? *Ticks and Tick-borne Diseases*, *12*(3), 101682. https://doi.org/10.1016/j.ttbdis.2021.101682

Gray, J. S., Dautel, H., Estrada-Peña, A., Kahl, O., & Lindgren, E. (2009). Effects of climate change on ticks and tick-borne diseases in Europe. *Interdisciplinary Perspectives on Infectious Diseases*, *2009*, 593232. https://doi.org/10.1155/2009/593232

Gray, J. S., Kahl, O., Lane, R. S., Levin, M. L., & Tsao, J. I. (2016). Diapause in ticks of the medically important *Ixodes ricinus* species complex. *Ticks and Tick-borne Diseases*, *7*(5), 992-1003. https://doi.org/10.1016/j.ttbdis.2016.05.006

Grigoryeva, L. A., & Shatrov, A. B. (2022). Life cycle of the tick *Ixodes ricinus* (L.) (Acari: Ixodidae) in the north-west of Russia. *Systematic and Applied Acarology*, *27*(3), 538-550. https://doi.org/10.11158/saa.27.3.11

Gryczyńska, A., & Kowalec, M. (2019). Different competence as a Lyme borreliosis causative agent reservoir found in two thrush species: The blackbird (*Turdus merula*) and the song thrush (*Turdus philomelos*). *Vector-Borne and Zoonotic Diseases*, *19*(6), 450-452. https://doi.org/10.1089/vbz.2018.2351

Gylfe, Å., Bergström, S., Lundström, J., & Olsen, B. (2000). Reactivation of *Borrelia* infection in birds. *Nature*, *403*(6771), 724-725. https://doi.org/10.1038/35001663

Hanincová, K., Schäfer, S. M., Etti, S., Sewell, H. S., Taragelová, V., Ziak, D., Labuda, M., & Kurtenbach, K. (2003). Association of *Borrelia afzelii* with rodents in Europe. *Parasitology*, *126*(1), 11-20. https://doi.org/10.1017/s0031182002002548

Hanssen-Bauer, I., Drange, H., Førland, E., Roald, L., Børsheim, K., Hisdal, H., Lawrence, D., Nesje, A., Sandven, S., & Sorteberg, A. (2009). Climate in Norway 2100. *Background information to NOU Climate adaptation (In Norwegian: Klima i Norge 2100. Bakgrunnsmateriale til NOU Klimatilplassing), Oslo: Norsk klimasenter*.

Harvell, D., Altizer, S., Cattadori, I. M., Harrington, L., & Weil, E. (2009). Climate change and wildlife diseases: When does the host matter the most? *Ecology*, *90*(4), 912-920. https://doi.org/10.1890/08-0616.1

Hauser, G., Rais, O., Morán Cadenas, F., Gonseth, Y., Bouzelboudjen, M., & Gern, L. (2018). Influence of climatic factors on *Ixodes ricinus* nymph abundance and phenology over a long-term monthly observation in Switzerland (2000–2014). *Parasites & Vectors*, *11*(1), 1-12. https://doi.org/10.1186/s13071-018-2876-7

Huang, A. T., Takahashi, S., Salje, H., Wang, L., Garcia-Carreras, B., Anderson, K., Endy, T., Thomas, S., Rothman, A. L., & Klungthong, C. (2022). Assessing the role of multiple mechanisms increasing the age of dengue cases in Thailand. *Proceedings of the National Academy of Sciences*, *119*(20), e2115790119. https://doi.org/10.1073/pnas.2115790119

Hyde, J. A. (2017). *Borrelia burgdorferi* keeps moving and carries on: A review of borrelial dissemination and invasion. *Frontiers in Immunology*, *8*, 114. https://doi.org/10.3389/fimmu.2017.00114

Hügli, D., Hu, C. M., Humair, P.-F., Wilske, B., & Gern, L. (2002). Apodemus species mice are reservoir hosts of *Borrelia garinii* OspA serotype 4 in Switzerland. *Journal of Clinical Microbiology*, *40*(12), 4735-4737. https://doi.org/10.1016/j.ijmm.2008.06.001

Jahfari, S., Krawczyk, A., Coipan, E. C., Fonville, M., Hovius, J. W., Sprong, H., & Takumi, K. (2017). Enzootic origins for clinical manifestations of Lyme borreliosis. *Infection, Genetics and Evolution*, *49*, 48-54. https://doi.org/10.1016/j.meegid.2016.12.030

Jenni, L., & Kéry, M. (2003). Timing of autumn bird migration under climate change: Advances in long–distance migrants, delays in short–distance migrants. *Proceedings of the Royal Society of London. Series B: Biological Sciences*, *270*(1523), 1467-1471. https://doi.org/10.1098/rspb.2003.2394

Johnson, K. O., Nelder, M. P., Russell, C., Li, Y., Badiani, T., Sander, B., Sider, D., & Patel, S. N. (2018). Clinical manifestations of reported Lyme disease cases in Ontario, Canada: 2005-2014. *PLoS One*, *13*(6), e0198509. https://doi.org/10.1371/journal.pone.0198509

Kahl, O., & Gray, J. S. (2023). The biology of *Ixodes ricinus* with emphasis on its ecology. *Ticks and Tick-borne Diseases*, *14*(2), 102114. https://doi.org/10.1016/j.ttbdis.2022.102114

Kaup, B. Z. (2018). The making of Lyme disease: A political ecology of ticks and tick-borne illness in Virginia. *Environmental Sociology*, *4*(3), 381-391. https://doi.org/10.1080/23251042.2018.1436892

Keesing, F., & Ostfeld, R. S. (2021). Dilution effects in disease ecology. *Ecology Letters*, *24*(11), 2490-2505. https://doi.org/10.1111/ele.13875

Ketzler, G., Römer, W., & Beylich, A. A. (2021). The climate of Norway. *Landscapes and landforms of norway*, 7-29. https://doi.org/10.1007/978-3-030-52563-7_2

Khong, V. H., Carmona, P., & Gandon, S. (2023). Seasonality and the persistence of vector-borne pathogens. *Journal of The Royal Society Interface*, *20*(209), 20230470. https://doi.org/10.1098/rsif.2023.0470

Kilpatrick, A. M., Dobson, A. D. M., Levi, T., Salkeld, D. J., Swei, A., Ginsberg, H. S., Kjemtrup, A., Padgett, K. A., Jensen, P. M., Fish, D., Ogden, N. H., & Diuk-Wasser, M. A. (2017). Lyme disease ecology in a changing world: Consensus, uncertainty and critical gaps for improving control. *Philosophical Transactions of the Royal Society B: Biological Sciences*, *372*(1722), 20160117. https://doi.org/10.1098/rstb.2016.0117

Klepac, P., & Caswell, H. (2011). The stage-structured epidemic: linking disease and demography with a multi-state matrix approach model. *Theoretical Ecology*, *4*(3), 301-319. https://doi.org/10.1007/s12080-010-0079-8

Klepac, P., Pomeroy, L. W., Bjørnstad, O. N., Kuiken, T., Osterhaus, A. D., & Rijks, J. M. (2009). Stage-structured transmission of phocine distemper virus in the Dutch 2002 outbreak. *Proceedings of the Royal Society B: Biological Sciences*, *276*(1666), 2469-2476. https://doi.org/10.1098/rspb.2009.0175

Koedel, U., Fingerle, V., & Pfister, H. W. (2015). Lyme neuroborreliosis - Epidemiology, diagnosis and management. *Nature Reviews Neurology*, *11*(8), 446-456. https://doi.org/10.1038/nrneurol.2015.121

Korenberg, E. I., Sirotkin, M. B., & Kovalevskii, Y. V. (2021). Adaptive features of the biology of closely related species of Ixodid ticks that determine their distribution (Illustrated on the example of the taiga tick *Ixodes persulcatus* Sch. 1930 and the castor bean tick *Ixodes ricinus* L. 1758). *Biology Bulletin Reviews*, *11*(6), 602-615. https://doi.org/10.1134/s2079086421060050

Kovats, R. S., Woolhouse, M. E. J., Dye, C., Campbell-Lendrum, D. H., McMichel, A. J., Woodward, A., & Cox, J. S. H. (2001). Early effects of climate change: Do they include changes in vector-borne disease? *Philosophical Transactions of the Royal Society of London. Series B: Biological Sciences*, *356*(1411), 1057-1068. https://doi.org/10.1098/rstb.2001.0894

Krawczuk, K., Czupryna, P., Pancewicz, S., Ołdak, E., Król, M., & Moniuszko-Malinowska, A. (2020). Comparison of neuroborreliosis between children and adults. *Pediatric Infectious Disease Journal*, *39*(1), 7-11. https://doi.org/10.1097/inf.0000000000002493

Kugeler, K. J., Jordan, R. A., Schulze, T. L., Griffith, K. S., & Mead, P. S. (2015). Will culling white-tailed deer prevent Lyme disease? *Zoonoses and Public Health*, *63*(5), 337-345. https://doi.org/10.1111/zph.12245

Kugeler, K. J., Mead, P. S., Schwartz, A. M., & Hinckley, A. F. (2022). Changing trends in age and sex distributions of Lyme disease—United States, 1992-2016. *Public Health Reports*, *137*(4), 655-659. https://doi.org/10.1177/00333549211026777

Kurtenbach, K., Hanincova, K., Tsao, J. I., Margos, G., Fish, D., & Ogden, N. H. (2006). Fundamental processes in the evolutionary ecology of Lyme borreliosis. *Nature Reviews Microbiology*, *4*(9), 660-669. https://doi.org/10.1038/nrmicro1475

Köhler, C. F., Holding, M. L., Sprong, H., Jansen, P. A., & Esser, H. J. (2023). Biodiversity in the Lyme-light: Ecological restoration and tick-borne diseases in Europe. *Trends in Parasitology*, *39*(5), 373-385. https://doi.org/10.1016/j.pt.2023.02.005

Lawrence, A. J., & Soame, J. M. (2004). The effects of climate change on the reproduction of coastal invertebrates. *Ibis*, *146*(s1), 29-39. https://doi.org/10.1111/j.1474-919x.2004.00325.x

Lehikoinen, E., Sparks, T. H., & Zalakevicius, M. (2004). Arrival and departure dates. *Birds and Climate Change*, *35*, 1-31. https://doi.org/10.1016/S0065-2504(04)35001-4

Lescano, A. G., Larasati, R. P., Sedyaningsih, E. R., Bounlu, K., Araujo-Castillo, R. V., Munayco-Escate, C. V., Soto, G., Mundaca, C. C., & Blazes, D. L. (2008). Statistical analyses in disease surveillance systems. *BMC Proceedings*, *2*(S3), 1-6. https://doi.org/10.1186/1753-6561-2-s3-s7

Levi, T., Keesing, F., Oggenfuss, K., & Ostfeld, R. S. (2015). Accelerated phenology of blacklegged ticks under climate warming. *Philosophical Transactions of the Royal Society B: Biological Sciences*, *370*(1665), 20130556. https://doi.org/10.1098/rstb.2013.0556

Levy, S. (2013). The Lyme disease debate host biodiversity and human disease risk. *Environmental Health Perspectives*, *121*(4), A120-A125. https://doi.org/10.1289/ehp.121-a120

Li, S., Gilbert, L., Harrison, P. A., & Rounsevell, M. D. (2016). Modelling the seasonality of Lyme disease risk and the potential impacts of a warming climate within the

heterogeneous landscapes of Scotland. *Journal of The Royal Society Interface*, *13*(116), 20160140. https://doi.org/10.1098/rsif.2016.0140

Li, S., Gilbert, L., Vanwambeke, S. O., Yu, J., Purse, B. V., & Harrison, P. A. (2019). Lyme disease risks in Europe under multiple uncertain drivers of change. *Environmental Health Perspectives*, *127*(6), 67010. https://doi.org/10.1289/EHP4615

Lindsø, L. K., Anders, J. L., Viljugrein, H., Herland, A., Stigum, V. M., Easterday, W. R., & Mysterud, A. (2023). Individual heterogeneity in ixodid tick infestation and prevalence of *Borrelia burgdorferi* sensu lato in a northern community of small mammalian hosts. *Oecologia*, 1-13. https://doi.org/10.1007/s00442-023-05476-w

Lochhead, R. B., Strle, K., Arvikar, S. L., Weis, J. J., & Steere, A. C. (2021). Lyme arthritis: Linking infection, inflammation and autoimmunity. *Nature Reviews Rheumatology*, *17*(8), 449-461. https://doi.org/10.1038/s41584-021-00648-5

Logar, M., Ružić-Sabljić, E., Maraspin, V., Lotrič-Furlan, S., Cimperman, J., Jurca, T., & Strle, F. (2004). Comparison of erythema migrans caused by *Borrelia afzelii* and *Borrelia garinii*. *Infection*, *32*, 15-19. https://doi.org/10.1007/s15010-004-3042-z

Lommano, E., Dvořák, C., Vallotton, L., Jenni, L., & Gern, L. (2014). Tick-borne pathogens in ticks collected from breeding and migratory birds in Switzerland. *Ticks and Tick-borne Diseases*, *5*(6), 871-882. https://doi.org/10.1016/j.ttbdis.2014.07.001

MacDonald, A. J., McComb, S., O'Neill, C., Padgett, K. A., & Larsen, A. E. (2020). Projected climate and land use change alter western blacklegged tick phenology, seasonal host-seeking suitability and human encounter risk in California. *Global Change Biology*, *26*(10), 5459-5474. https://doi.org/10.1111/gcb.15269

MacDonald, E., Vestrheim, D. F., White, R. A., Konsmo, K., Lange, H., Aase, A., Nygard, K., Stefanoff, P., Aaberge, I., & Vold, L. (2016). Are the current notification criteria for Lyme borreliosis in Norway suitable? Results of an evaluation of Lyme borreliosis surveillance in Norway, 1995-2013. *BMC Public Health*, *16*(1), 729. https://doi.org/10.1186/s12889-016-3346-9

Marques, A. R., Strle, F., & Wormser, G. P. (2021). Comparison of Lyme disease in the United States and Europe. *Emerging Infectious Diseases*, *27*(8), 2017-2024. https://doi.org/10.3201/eid2708.204763

McDevitt-Galles, T., Moss, W. E., Calhoun, D. M., & Johnson, P. T. J. (2020). Phenological synchrony shapes pathology in host–parasite systems. *Proceedings of the Royal Society B*, *287*(1919), 20192597. https://doi.org/10.1098/rspb.2019.2597

McManus, M., & Cincotta, A. (2015). Effects of *Borrelia* on host immune system: possible consequences for diagnostics. *Advances in Integrative Medicine*, *2*(2), 81-89. https://doi.org/10.1016/j.aimed.2014.11.002

Mead, P., Hook, S., Niesobecki, S., Ray, J., Meek, J., Delorey, M., Prue, C., & Hinckley, A. (2018). Risk factors for tick exposure in suburban settings in the Northeastern United States. *Ticks and Tick-borne Diseases*, *9*(2), 319-324. https://doi.org/10.1016/j.ttbdis.2017.11.006

Medeiros, M. C. I., Ricklefs, R. E., Goldberg, T. L., Ruiz, M. O., Hamer, G. L., & Brawn, J. D. (2016). Overlap in the seasonal infection patterns of avian malaria parasites and West Nile virus in vectors and hosts. *The American Journal of Tropical Medicine and Hygiene*, *95*(5), 1121-1129. https://doi.org/10.4269/ajtmh.16-0236

Medlock, J. M., Hansford, K. M., Bormane, A., Derdakova, M., Estrada-Peña, A., George, J. C., Golovljova, I., Jaenson, T. G., Jensen, J. K., Jensen, P. M., Kazimirova, M., Oteo, J. A., Papa, A., Pfister, K., Plantard, O., Randolph, S. E., Rizzoli, A., Santos-Silva, M.

M., Sprong, H., Vial, L., Hendrickx, G., Zeller, H., & Van Bortel, W. (2013). Driving forces for changes in geographical distribution of *Ixodes ricinus* ticks in Europe. *Parasites & Vectors*, *6*(1), 1-11. https://doi.org/10.1186/1756-3305-6-1

Mellard, J. P., Audoye, P., & Loreau, M. (2019). Seasonal patterns in species diversity across biomes. *Ecology*, *100*(4), e02627. https://doi.org/10.1002/ecy.2627

Monaghan, A. J., Moore, S. M., Sampson, K. M., Beard, C. B., & Eisen, R. J. (2015). Climate change influences on the annual onset of Lyme disease in the United States. *Ticks and Tick-borne Diseases*, *6*(5), 615-622. https://doi.org/10.1016/j.ttbdis.2015.05.005

Monaghan, M., Norman, S., Gierdalski, M., Marques, A., Bost, J. E., & DeBiasi, R. L. (2023). Pediatric Lyme disease: Systematic assessment of post-treatment symptoms and quality of life. *Pediatric Research*, 1-8. https://doi.org/10.1038/s41390-023-02577-3

Moon, K. A., Pollak, J. S., Poulsen, M. N., Heaney, C. D., Hirsch, A. G., & Schwartz, B. S. (2021). Risk factors for Lyme disease stage and manifestation using electronic health records. *BMC Infectious Diseases*, *21*(1), 1-13. https://doi.org/10.1186/s12879-021-06959-y

Moore, S. M., Eisen, R. J., Monaghan, A., & Mead, P. (2014). Meteorological influences on the seasonality of Lyme disease in the United States. *The American Journal of Tropical Medicine and Hygiene*, *90*(3), 486-496. https://doi.org/10.4269/ajtmh.13-0180

Mora, C., McKenzie, T., Gaw, I. M., Dean, J. M., von Hammerstein, H., Knudson, T. A., Setter, R. O., Smith, C. Z., Webster, K. M., Patz, J. A., & Franklin, E. C. (2022). Over half of known human pathogenic diseases can be aggravated by climate change. *Nature Climate Change*, *12*(9), 869-875. https://doi.org/10.1038/s41558-022-01426-1

Mordecai, E. A., Caldwell, J. M., Grossman, M. K., Lippi, C. A., Johnson, L. R., Neira, M., Rohr, J. R., Ryan, S. J., Savage, V., & Shocket, M. S. (2019). Thermal biology of mosquito-borne disease. *Ecology Letters*, *22*(10), 1690-1708. https://doi.org/10.1111/ele.13335

Mysterud, A., Easterday, W. R., Stigum, V. M., Aas, A. B., Meisingset, E. L., & Viljugrein, H. (2016). Contrasting emergence of Lyme disease across ecosystems. *Nature Communications*, *7*(1), 11882. https://doi.org/10.1038/ncomms11882

Mysterud, A., Heylen, D. J. A., Matthysen, E., Garcia, A. L., Jore, S., & Viljugrein, H. (2019). Lyme neuroborreliosis and bird populations in Northern Europe. *Proceedings of the Royal Society B*, *286*(1903), 20190759. https://doi.org/10.1098/rspb.2019.0759

Mysterud, A., Jore, S., Østerås, O., & Viljugrein, H. (2017). Emergence of tick-borne diseases at northern latitudes in Europe: A comparative approach. *Scientific Reports*, *7*(1), 16316. https://doi.org/10.1038/s41598-017-15742-6

Mysterud, A., Stigum, V. M., Jaarsma, R. I., & Sprong, H. (2019). Genospecies of *Borrelia burgdorferi* sensu lato detected in 16 mammal species and questing ticks from northern Europe. *Scientific Reports*, *9*(1), 5088. https://doi.org/10.1038/s41598-019-41686-0

Mysterud, A., Stigum, V. M., Seland, I. V., Herland, A., Easterday, W. R., Jore, S., Osteras, O., & Viljugrein, H. (2018). Tick abundance, pathogen prevalence, and disease incidence in two contrasting regions at the northern distribution range of Europe. *Parasites & Vectors*, *11*(1), 309. https://doi.org/10.1186/s13071-018-2890-9

Møller, A. P., Jokimäki, J., Skorka, P., & Tryjanowski, P. (2014). Loss of migration and urbanization in birds: A case study of the blackbird (*Turdus merula*). *Oecologia*, *175*(3), 1019-1027. https://doi.org/10.1007/s00442-014-2953-3

Nagarajan, A., Skufca, J., Vyse, A., Pilz, A., Begier, E., Riera-Montes, M., Gessner, B. D., & Stark, J. H. (2023). The landscape of Lyme borreliosis surveillance in Europe. *Vector-Borne and Zoonotic Diseases*, *23*(4), 142-155. https://doi.org/10.1089/vbz.2022.0067

Norwegian Public Health Institute. (2023). Meldingskriterier for sykdommer i MSIS. https://www.fhi.no/publ/informasjonsark/meldingskriterier-for-sykdommer-i-msis/

Nygård, K., Brantsæter, A. B., & Mehl, R. (2005). Disseminated and chronic Lyme borreliosis in Norway, 1995–2004. *Eurosurveillance*, *10*(10), 1-2. https://doi.org/10.2807/esm.10.10.00568-en

Ogden, N. H., Ben Beard, C., Ginsberg, H. S., & Tsao, J. I. (2020). Possible effects of climate change on ixodid ticks and the pathogens they transmit: Predictions and observations. *Journal of Medical Entomology*, *58*(4), 1536-1545. https://doi.org/10.1093/jme/tjaa220

Ogden, N. H., Bigras-Poulin, M., Hanincová, K., Maarouf, A., O'Callaghan, C. J., & Kurtenbach, K. (2008). Projected effects of climate change on tick phenology and fitness of pathogens transmitted by the North American tick *Ixodes scapularis*. *Journal of Theoretical Biology*, *254*(3), 621-632. https://doi.org/10.1016/j.jtbi.2008.06.020

Ogden, N. H., Bouchard, C., Badcock, J., Drebot, M. A., Elias, S. P., Hatchette, T. F., Koffi, J. K., Leighton, P. A., Lindsay, L. R., Lubelczyk, C. B., Peregrine, A. S., Smith, R. P., & Webster, D. (2019). What is the real number of Lyme disease cases in Canada? *BMC Public Health*, *19*(1), 1-12. https://doi.org/10.1186/s12889-019-7219-x

Ogden, N. H., & Lindsay, L. R. (2016). Effects of climate and climate change on vectors and vector-borne diseases: Ticks are different. *Trends in Parasitology*, *32*(8), 646-656. https://doi.org/10.1016/j.pt.2016.04.015

Oita, S., Ibáñez, A., Lutzoni, F., Miadlikowska, J., Geml, J., Lewis, L. A., Hom, E. F. Y., Carbone, I., U'Ren, J. M., & Arnold, A. E. (2021). Climate and seasonality drive the richness and composition of tropical fungal endophytes at a landscape scale. *Communications Biology*, *4*(1), 313. https://doi.org/10.1038/s42003-021-01826-7

Ornstein, K., Berglund, J., Nilsson, I., Norrby, R., & Bergstrom, S. (2001). Characterization of Lyme borreliosis isolates from patients with erythema migrans and neuroborreliosis in Southern Sweden. *Journal of Clinical Microbiology*, *39*(4), 1294-1298. https://doi.org/10.1128/JCM.39.4.1294-1298.2001

Oschmann, P., Dorndorf, W., Hornig, C., Schäfer, C., Wellensiek, H., & Pflughaupt, K. (1998). Stages and syndromes of neuroborreliosis. *Journal of neurology*, *245*, 262-272. https://doi.org/10.1007/s004150050216

Ostfeld, R. S., & Brunner, J. L. (2015). Climate change and *Ixodes* tick-borne diseases of humans. *Philosophical Transactions of the Royal Society B: Biological Sciences*, *370*(1665), 20140051. https://doi.org/10.1098/rstb.2014.0051

Ostfeld, R. S., & Keesing, F. (2000). Biodiversity and disease risk: The case of Lyme disease. *Conservation Biology*, *14*(3), 722-728. https://doi.org/10.1046/j.1523-1739.2000.99014.x

Ostfeld, R. S., Levi, T., Jolles, A. E., Martin, L. B., Hosseini, P. R., & Keesing, F. (2014). Life history and demographic drivers of reservoir competence for three tick-borne zoonotic pathogens. *PLoS One*, *9*(9), e107387. https://doi.org/10.1371/journal.pone.0107387

Ostfeld, R. S., Price, A., Hornbostel, V. L., Benjamin, M. A., & Keesing, F. (2006). Controlling ticks and tick-borne zoonoses with biological and chemical agents.

BioScience, *56*(5), 383. https://doi.org/10.1641/0006-3568(2006)056[0383:ctatzw]2.0.co;2
Padgett, K. A., & Lane, R. S. (2001). Life cycle of *Ixodes pacificus* (Acari: Ixodidae): Timing of developmental processes under field and laboratory conditions. *Journal of Medical Entomology*, *38*(5), 684-693. https://doi.org/10.1603/0022-2585-38.5.684
Paul, M. J., Zucker, I., & Schwartz, W. J. (2007). Tracking the seasons: The internal calendars of vertebrates. *Philosophical Transactions of the Royal Society B: Biological Sciences*, *363*(1490), 341-361. https://doi.org/10.1098/rstb.2007.2143
Paull, S. H., & Johnson, P. T. (2014). Experimental warming drives a seasonal shift in the timing of host-parasite dynamics with consequences for disease risk. *Ecology Letters*, *17*(4), 445-453. https://doi.org/10.1111/ele.12244
Paull, S. H., & Johnson, P. T. J. (2011). High temperature enhances host pathology in a snail–trematode system: Possible consequences of climate change for the emergence of disease. *Freshwater Biology*, *56*(4), 767-778. https://doi.org/10.1111/j.1365-2427.2010.02547.x
Ramachandran, N. (2011). Climate change, seasonality and hunger: The South Asian experience. In *Global Food Insecurity* (pp. 201-215). Springer Netherlands. https://doi.org/10.1007/978-94-007-0890-7_14
Randolph, S. E., & Dobson, A. D. M. (2012). Pangloss revisited: A critique of the dilution effect and the biodiversity-buffers-disease paradigm. *Parasitology*, *139*(7), 847-863. https://doi.org/10.1017/s0031182012000200
Randolph, S. E., Green, R. M., Peacey, M. F., & Rogers, D. J. (2000). Seasonal synchrony: The key to tick-borne encephalitis foci identified by satellite data. *Parasitology*, *121*(1), 15-23. https://doi.org/10.1017/s0031182099006083
Rauter, C., & Hartung, T. (2005). Prevalence of *Borrelia burgdorferi* sensu lato genospecies in *Ixodes ricinus* ticks in Europe: A metaanalysis. *Applied and Environmental Microbiology*, *71*(11), 7203-7216. https://doi.org/10.1128/aem.71.11.7203-7216.2005
Requena-García, F., Cabrero-Sañudo, F., Olmeda-García, S., González, J., & Valcárcel, F. (2017). Influence of environmental temperature and humidity on questing ticks in Central Spain. *Experimental and Applied Acarology*, *71*(3), 277-290. https://doi.org/10.1007/s10493-017-0117-y
Rizzoli, A., Hauffe, H., Carpi, G., Vourc, H. G., Neteler, M., & Rosa, R. (2011). Lyme borreliosis in Europe. *Eurosurveillance*, *16*(27), 19906. https://doi.org/10.2807/ese.16.27.19906-en
Robertson, C., Nelson, T. A., MacNab, Y. C., & Lawson, A. B. (2010). Review of methods for space–time disease surveillance. *Spatial and Spatio-temporal Epidemiology*, *1*(2–3), 105-116. https://doi.org/10.1016/j.sste.2009.12.001
Rohr, J. R., Civitello, D. J., Halliday, F. W., Hudson, P. J., Lafferty, K. D., Wood, C. L., & Mordecai, E. A. (2019). Towards common ground in the biodiversity–disease debate. *Nature Ecology & Evolution*, *4*(1), 24-33. https://doi.org/10.1038/s41559-019-1060-6
Rue, H., Martino, S., & Chopin, N. (2009). Approximate Bayesian inference for latent Gaussian models by using integrated nested Laplace approximations. *Journal of the Royal Statistical Society Series B-Statistical Methodology*, *71*(2), 319-392. https://doi.org/10.1111/j.1467-9868.2008.00700.x
Ruiz-Cárdenas, R., Krainski, E. T., & Rue, H. (2012). Direct fitting of dynamic models using integrated nested Laplace approximations—INLA. *Computational Statistics & Data Analysis*, *56*(6), 1808-1828. https://doi.org/10.1016/j.csda.2011.10.024

Rupprecht, T. A., Koedel, U., Fingerle, V., & Pfister, H.-W. (2008). The pathogenesis of lyme neuroborreliosis: from infection to inflammation. *Molecular medicine*, *14*, 205-212. https://doi.org/10.2119/2007-00091.Rupprecht

Rutz, H., Hogan, B., Hook, S., Hinckley, A., & Feldman, K. (2018). Impacts of misclassification on Lyme disease surveillance. *Zoonoses and Public Health*, *66*(1), 174-178. https://doi.org/10.1111/zph.12525

Ryan, S. J. (2020). Mapping thermal physiology of vector-borne diseases in a changing climate: Shifts in geographic and demographic risk of suitability. *Current Environmental Health Reports*, *7*(4), 415-423. https://doi.org/10.1007/s40572-020-00290-5

Sahoo, S. K., Taraphdar, P., Mallick, A. K., Dasgupta, A., Preeti, P. S., & Biswas, D. (2017). How aware are we regarding vector borne diseases? A community based study in a slum of Kolkata, India. *International Journal of Research in Medical Sciences*, *5*(6), 2629. https://doi.org/10.18203/2320-6012.ijrms20172460

Saikkonen, K., Taulavuori, K., Hyvönen, T., Gundel, P. E., Hamilton, C. E., Vänninen, I., Nissinen, A., & Helander, M. (2012). Climate change-driven species' range shifts filtered by photoperiodism. *Nature Climate Change*, *2*(4), 239-242. https://doi.org/10.1038/nclimate1430

Schulz, M., Mahling, M., & Pfister, K. (2014). Abundance and seasonal activity of questing *Ixodes ricinus* ticks in their natural habitats in Southern Germany in 2011. *Journal of Vector Ecology*, *39*(1), 56-65. https://doi.org/10.1111/j.1948-7134.2014.12070.x

Schwartz, A. M., Hinckley, A. F., Mead, P. S., Hook, S. A., & Kugeler, K. J. (2017). Surveillance for Lyme disease - United States, 2008-2015. *MMWR Surveillance Summaries*, *66*(22), 1-12. https://doi.org/10.15585/mmwr.ss6622a1

Semenza, J. C., & Menne, B. (2009). Climate change and infectious diseases in Europe. *The Lancet infectious diseases*, *9*(6), 365-375. https://doi.org/10.1016/S1473-3099(09)70104-5

Semenza, J. C., & Paz, S. (2021). Climate change and infectious disease in Europe: Impact, projection and adaptation. *The Lancet Regional Health–Europe*, *9*. https://doi.org/10.1016/j.lanepe.2021.100230

Seukep, S. E., Kolivras, K. N., Hong, Y., Li, J., Prisley, S. P., Campbell, J. B., Gaines, D. N., & Dymond, R. L. (2015). An examination of the demographic and environmental variables correlated with Lyme disease emergence in Virginia. *EcoHealth*, *12*(4), 634-644. https://doi.org/10.1007/s10393-015-1034-3

Sirotkin, M. B., & Korenberg, E. I. (2022). Thermal constants of development of *Ixodes persulcatus* and *Ixodes ricinus* ticks, which determine the duration of their life cycle and their distribution. *Entomological Review*, *102*(2), 257-263. https://doi.org/10.1134/S0013873822020117

Skaugen, T. E., & Tveito, O. E. (2004). Growing-season and degree-day scenario in Norway for 2021-2050. *Climate Research*, *26*, 221-232. https://doi.org/10.3354/cr026221

Skellam, J. (1967). Seasonal periodicity in theoretical population ecology. Proceedings of the Fifth Berkeley Symposium on Mathematical Statistics and Probability,

Skufca, J., De Smedt, N., Pilz, A., Vyse, A., Begier, E., Blum, M., Riera-Montes, M., Gessner, B., Skovdal, M., & Stark, J. H. (2022). Incidence of Lyme neuroborreliosis in Denmark: Exploring observed trends using public surveillance data, 2015-2019. *Ticks and Tick-borne Diseases*, *13*(6), 102039. https://doi.org/10.1016/j.ttbdis.2022.102039

Slatculescu, A. M., Pugliese, M., Sander, B., Zinszer, K., Nelder, M. P., Russell, C. B., & Kulkarni, M. A. (2022). Rurality, socioeconomic status, and residence in environmental risk areas associated with increased Lyme disease incidence in Ontario, Canada: A case-control study. *Vector-Borne and Zoonotic Diseases*, *22*(12), 572-581. https://doi.org/10.1089/vbz.2022.0044

Smith, G., Wileyto, E. P., Hopkins, R. B., Cherry, B. R., & Maher, J. P. (2001). Risk factors for Lyme disease in Chester County, Pennsylvania. *Public Health Reports*, *116*(1_suppl), 146-156. https://doi.org/10.1093/phr/116.s1.146

Sonenshine, D. E., & Simo, L. (2021). Biology and molecular biology of *Ixodes scapularis*. In *Lyme Disease and Relapsing Fever Spirochetes: Genomics, Molecular Biology, Host Interactions and Disease Pathogenesis* (pp. 339-366). Caister Academic Press. https://doi.org/10.21775/9781913652616.12

Soriano-Paños, D., Arias-Castro, J. H., Reyna-Lara, A., Martínez, H. J., Meloni, S., & Gómez-Gardeñes, J. (2020). Vector-borne epidemics driven by human mobility. *Physical Review Research*, *2*(1), 013312. https://doi.org/10.1103/physrevresearch.2.013312

Springer, Y. P., & Johnson, P. T. J. (2018). Large-scale health disparities associated with Lyme disease and human monocytic ehrlichiosis in the United States, 2007–2013. *PLoS One*, *13*(9), e0204609. https://doi.org/10.1371/journal.pone.0204609

Stanek, G., & Reiter, M. (2011). The expanding Lyme *Borrelia* complex — Clinical significance of genomic species? *Clinical Microbiology and Infection*, *17*(4), 487-493. https://doi.org/10.1111/j.1469-0691.2011.03492.x

Stanek, G., & Strle, F. (2018). Lyme borreliosis–from tick bite to diagnosis and treatment. *FEMS microbiology reviews*, *42*(3), 233-258. https://doi.org/10.1093/femsre/fux047

Steere, A. C., Coburn, J., & Glickstein, L. (2004). The emergence of Lyme disease. *Journal of Clinical Investigation*, *113*(8), 1093-1101. https://doi.org/10.1172/jci21681

Steere, A. C., Malawista, S. E., Snydman, D. R., Shope, R. E., Andiman, W. A., Ross, M. R., & Steele, F. M. (1977). An epidemic of oligoarticular arthritis in children and adults in three Connecticut communities. *Arthritis & Rheumatism*, *20*(1), 7-17. https://doi.org/10.1002/art.1780200102

Steere, A. C., Sikand, V. K., Schoen, R. T., & Nowakowski, J. (2003). Asymptomatic infection with *Borrelia burgdorferi*. *Clinical Infectious Diseases*, *37*(4), 528-532. https://doi.org/10.1086/376914

Steere, A. C., Strle, F., Wormser, G. P., Hu, L. T., Branda, J. A., Hovius, J. W., Li, X., & Mead, P. S. (2016). Lyme borreliosis. *Nature Reviews Disease Primers*, *2*(1), 16090. https://doi.org/10.1038/nrdp.2016.90

Steinbrink, A., Brugger, K., Margos, G., Kraiczy, P., & Klimpel, S. (2022). The evolving story of *Borrelia burgdorferi* sensu lato transmission in Europe. *Parasitology Research*, *121*(3), 781-803. https://doi.org/10.1007/s00436-022-07445-3

Stewart, P. E., & Bloom, M. E. (2020). Sharing the ride: *Ixodes scapularis* symbionts and their interactions. *Frontiers in Cellular and Infection Microbiology*, *10*, 142. https://doi.org/10.3389/fcimb.2020.00142

Strle, F., Ružić-Sabljić, E., Cimperman, J., Lotrič-Furlan, S., & Maraspin, V. (2006). Comparison of findings for patients with *Borrelia garinii* and *Borrelia afzelii* isolated from cerebrospinal fluid. *Clinical Infectious Diseases*, *43*(6), 704-710. https://doi.org/10.1086/506936

Strnad, M., & Rego, R. O. M. (2020). The need to unravel the twisted nature of the *Borrelia burgdorferi* sensu lato complex across Europe. *Microbiology*, *166*(5), 428-435. https://doi.org/10.1099/mic.0.000899

Suepa, T., Qi, J., Lawawirojwong, S., & Messina, J. P. (2016). Understanding spatio-temporal variation of vegetation phenology and rainfall seasonality in the monsoon Southeast Asia. *Environmental Research*, *147*, 621-629. https://doi.org/10.1016/j.envres.2016.02.005

Tanton, M. (1969). The estimation and biology of populations of the bank vole (*Clethrionomys glareolus* (Schr.)) and wood mouse (*Apodemus sylvaticus* (L.)). *The Journal of Animal Ecology*, 511-529. https://doi.org/10.2307/3031

Tougeron, K., Brodeur, J., Le Lann, C., & van Baaren, J. (2020). How climate change affects the seasonal ecology of insect parasitoids. *Ecological Entomology*, *45*(2), 167-181. https://doi.org/10.1111/een.12792

Trevisan, G., Bonin, S., & Ruscio, M. (2020). A practical approach to the diagnosis of Lyme borreliosis: From clinical heterogeneity to laboratory methods. *Frontiers in Medicine*, *7*, 265. https://doi.org/10.3389/fmed.2020.00265

Tsai, H.-Y., Rubenstein, D. R., Fan, Y.-M., Yuan, T.-N., Chen, B.-F., Tang, Y., Chen, I.-C., & Shen, S.-F. (2020). Locally-adapted reproductive photoperiodism determines population vulnerability to climate change in burying beetles. *Nature Communications*, *11*(1), 1398. https://doi.org/10.1038/s41467-020-15208-w

Tulloch, J. S. P., Christley, R. M., Radford, A. D., Warner, J. C., Beadsworth, M. B. J., Beeching, N. J., & Vivancos, R. (2020). A descriptive epidemiological study of the incidence of newly diagnosed Lyme disease cases in a UK primary care cohort, 1998-2016. *BMC Infectious Diseases*, *20*(1), 285. https://doi.org/10.1186/s12879-020-05018-2

Tulloch, J. S. P., Semper, A. E., Brooks, T. J. G., Russell, K., Halsby, K. D., Christley, R. M., Radford, A. D., Vivancos, R., & Warner, J. C. (2019). The demographics and geographic distribution of laboratory-confirmed Lyme disease cases in England and Wales (2013-2016): An ecological study. *BMJ Open*, *9*(7), e028064. https://doi.org/10.1136/bmjopen-2018-028064

Van Vliet, J., Musters, C. J. M., & Ter Keurs, W. J. (2009). Changes in migration behaviour of Blackbirds *Turdus merula* from the Netherlands. *Bird Study*, *56*(2), 276-281. https://doi.org/10.1080/00063650902792148

Vandekerckhove, O., De Buck, E., & Van Wijngaerden, E. (2021). Lyme disease in Western Europe: An emerging problem? A systematic review. *Acta Clinica Belgica*, *76*(3), 244-252. https://doi.org/10.1080/17843286.2019.1694293

Varpe, Ø. (2017). Life history adaptations to seasonality. *Integrative and Comparative Biology*, *57*(5), 943-960. https://doi.org/10.1093/icb/icx123

Varpe, Ø., Jørgensen, C., Tarling, G. A., & Fiksen, Ø. (2009). The adaptive value of energy storage and capital breeding in seasonal environments. *Oikos*, *118*(3), 363-370. https://doi.org/10.1111/j.1600-0706.2008.17036.x

Vindenes, Y., & Mysterud, A. (2024). Unraveling the seasonal dynamics of ixodid ticks: A flexible matrix population model with delayed life history effects. *bioRxiv*, 2024.2001.2008.574636. https://doi.org/10.1101/2024.01.08.574636

Vollmer, S. A., Feil, E. J., Chu, C.-Y., Raper, S. L., Cao, W.-C., Kurtenbach, K., & Margos, G. (2013). Spatial spread and demographic expansion of Lyme borreliosis spirochaetes in

Eurasia. *Infection, Genetics and Evolution*, *14*, 147-155. https://doi.org/10.1016/j.meegid.2012.11.014

Walker, W. H., Meléndez-Fernández, O. H., Nelson, R. J., & Reiter, R. J. (2019). Global climate change and invariable photoperiods: A mismatch that jeopardizes animal fitness. *Ecology and Evolution*, *9*(17), 10044-10054. https://doi.org/10.1002/ece3.5537

Waller, L. A., Goodwin, B. J., Wilson, M. L., Ostfeld, R. S., Marshall, S. L., & Hayes, E. B. (2007). Spatio-temporal patterns in county-level incidence and reporting of Lyme disease in the Northeastern United States, 1990–2000. *Environmental and Ecological Statistics*, *14*(1), 83-100. https://doi.org/10.1007/s10651-006-0002-z

Walter, K. S., Carpi, G., Caccone, A., & Diuk-Wasser, M. A. (2017). Genomic insights into the ancient spread of Lyme disease across North America. *Nature Ecology & Evolution*, *1*(10), 1569-1576. https://doi.org/10.1038/s41559-017-0282-8

Wang, C., Henry, H. A. L., Miao, X., Shi, B., Song, Y., Liang, Q., & Sun, W. (2023). Seasonal variation modifies the spatial patterns of soil microbial community structure and enzyme activity in a meadow steppe. *Applied Soil Ecology*, *182*, 104686. https://doi.org/10.1016/j.apsoil.2022.104686

Wang, S. p. (2000). The microimmunofluorescence test for *Chlamydia pneumoniae* infection: Technique and interpretation. *The Journal of Infectious Diseases*, *181*(s3), S421-S425. https://doi.org/10.1086/315622

Wickham, H. (2016). *ggplot2: Elegant Graphics for Data Analysis*. In Springer-Verlag New York. https://ggplot2.tidyverse.org

Wolcott, K. A., Margos, G., Fingerle, V., & Becker, N. S. (2021). Host association of *Borrelia burgdorferi* sensu lato: A review. *Ticks and Tick-borne Diseases*, *12*(5), 101766. https://doi.org/10.1603/022.038.0404

Wongnak, P., Bord, S., Jacquot, M., Agoulon, A., Beugnet, F., Bournez, L., Cèbe, N., Chevalier, A., Cosson, J.-F., Dambrine, N., Hoch, T., Huard, F., Korboulewsky, N., Lebert, I., Madouasse, A., Mårell, A., Moutailler, S., Plantard, O., Pollet, T., Poux, V., René-Martellet, M., Vayssier-Taussat, M., Verheyden, H., Vourc'h, G., & Chalvet-Monfray, K. (2022). Meteorological and climatic variables predict the phenology of *Ixodes ricinus* nymph activity in France, accounting for habitat heterogeneity. *Scientific Reports*, *12*(1), 7833. https://doi.org/10.1038/s41598-022-11479-z

Wood, S. H., Hindle, M. M., Mizoro, Y., Cheng, Y., Saer, B. R. C., Miedzinska, K., Christian, H. C., Begley, N., McNeilly, J., McNeilly, A. S., Meddle, S. L., Burt, D. W., & Loudon, A. S. I. (2020). Circadian clock mechanism driving mammalian photoperiodism. *Nature Communications*, *11*(1), 4291. https://doi.org/10.1038/s41467-020-18061-z

Woudenberg, T., Böhm, S., Böhmer, M., Katz, K., Willrich, N., Stark, K., Kuhnert, R., Fingerle, V., & Wilking, H. (2020). Dynamics of *Borrelia burgdorferi*-Specific Antibodies: Seroconversion and Seroreversion between Two Population-Based, Cross-Sectional Surveys among Adults in Germany. *Microorganisms*, *8*(12), 1859-1859. https://doi.org/10.3390/microorganisms8121859

Zagatto, M. R. G., Niva, C. C., Thomazini, M. J., Baretta, D., Santos, A., Nadolny, H., Cardoso, G. B. X., & Brown, G. G. (2017). Soil invertebrates in different land use systems: How integrated production systems and seasonality affect soil mesofauna communities. *Journal of Agricultural Science and Technology B*, *7*(3), 150-161. https://doi.org/10.17265/2161-6264/2017.03.003

1

PROCEEDINGS B

royalsocietypublishing.org/journal/rspb

Research

Cite this article: Goren A, Viljugrein H, Rivrud IM, Jore S, Bakka H, Vindenes Y, Mysterud A. 2023 The emergence and shift in seasonality of Lyme borreliosis in Northern Europe. *Proc. R. Soc. B* **290**: 20222420. https://doi.org/10.1098/rspb.2022.2420

Received: 2 December 2022
Accepted: 27 January 2023

Subject Category:
Ecology

Subject Areas:
ecology, health and disease and epidemiology

Keywords:
seasonality, vector-borne zoonoses, disease ecology, Lyme borreliosis, Lyme disease, climate change

Author for correspondence:
Asena Goren
e-mail: asena.goren@ibv.uio.no

Electronic supplementary material is available online at https://doi.org/10.6084/m9.figshare.c.6414112.

THE ROYAL SOCIETY PUBLISHING

The emergence and shift in seasonality of Lyme borreliosis in Northern Europe

Asena Goren[1], Hildegunn Viljugrein[1,2], Inger Maren Rivrud[3], Solveig Jore[4], Haakon Bakka[2], Yngvild Vindenes[1] and Atle Mysterud[1,5]

[1]Centre for Ecological and Evolutionary Synthesis (CEES), Department of Biosciences, University of Oslo, PO Box 1066 Blindern, Oslo NO-0316, Norway
[2]Norwegian Veterinary Institute, PO Box 64, NO-1431 Ås, Norway
[3]Norwegian Institute for Nature Research (NINA), Sognsveien 68, NO-0855 Oslo, Norway
[4]Zoonotic, Food and Waterborne Infections, The Norwegian Public Health Institute, PO Box 4404 Nydalen, NO-0403 Oslo, Norway
[5]Norwegian Institute for Nature Research (NINA), PO Box 5685 Sluppen, NO-7485 Trondheim, Norway

AG, 0000-0003-1042-3413; HV, 0000-0002-3798-5267; IMR, 0000-0002-9778-7422; SJ, 0000-0001-8527-4892; HB, 0000-0001-8272-865X; YV, 0000-0003-1197-5818; AM, 0000-0001-8993-7382

Climate change has had a major impact on seasonal weather patterns, resulting in marked phenological changes in a wide range of taxa. However, empirical studies of how changes in seasonality impact the emergence and seasonal dynamics of vector-borne diseases have been limited. Lyme borreliosis, a bacterial infection spread by hard-bodied ticks, is the most common vector-borne disease in the northern hemisphere and has been rapidly increasing in both incidence and geographical distribution in many regions of Europe and North America. By analysis of long-term surveillance data (1995–2019) from across Norway (latitude 57°58′–71°08′ N), we demonstrate a marked change in the within-year timing of Lyme borreliosis cases accompanying an increase in the annual number of cases. The seasonal peak in cases is now six weeks earlier than 25 years ago, exceeding seasonal shifts in plant phenology and previous model predictions. The seasonal shift occurred predominantly in the first 10 years of the study period. The concurrent upsurgence in case number and shift in case timing indicate a major change in the Lyme borreliosis disease system over recent decades. This study highlights the potential for climate change to shape the seasonal dynamics of vector-borne disease systems.

1. Introduction

Emergence and range expansion of vector-borne and other infectious diseases are expected to accompany the many threats of the climate crisis [1,2]. Climate warming and environmental changes are suspected to have already led to both geographical range expansion of many vector-borne diseases and increased incidence in regions where diseases are already established [3–5]. Ecosystems at northern latitudes are experiencing above-average climate warming, which can create more favourable conditions for arthropod disease vectors and thus increase disease hazard [6,7]. In addition to warming, climate change has modified the seasonal structure in northern latitudes, introducing shorter winters, an earlier onset of spring and a longer growing season [8]. Phenological changes in the activity patterns of organisms have become one of the most notable effects of climate change in temperate regions and can be observed across taxa, from changes in the onset of plant growth, to reproductive timing in birds and mammals [9,10].

The speed at which different species respond to climate warming varies, and asynchronous responses by interacting species can create phenological

mismatches [11–14]. Vector-borne zoonoses are maintained by inherently complex ecological networks of hosts, vectors and pathogens [2]. Phenological overlaps between interacting components are key determinants of disease dynamics, and climate change-induced asynchronies are likely to alter disease trends. Empirical evidence demonstrating linkages between climate change, seasonality and disease outcomes has been limited [15,16]. Analysis of consistent, long-term surveillance data has been recognized as a critical step in developing an understanding of the ecological and climatic drivers of disease risk [3,4,15]. Explicit consideration of case seasonality in surveillance data can improve the detection of long-term changes in disease trends and is important for identifying potential effects of climate change on disease dynamics [17–21].

Lyme borreliosis, or Lyme disease, is a zoonotic infection caused by certain genospecies of the *Borrelia burgdorferi sensu lato* (sl) complex that are transmitted by tick vectors in the genus *Ixodes* [22]. The ixodid tick vectors are highly generalist hematophages that feed on a wide range of vertebrates including small and large mammals, birds and reptiles. A blood meal is required for the tick to develop between life stages, from larvae to nymphs and then adults, and for adult females to lay eggs [23]. *B. burgdorferi* sl is acquired by larval and nymphal ticks during feeding on infected hosts, and then transmitted during subsequent feedings [24]. The different pathogenic *B. burgdorferi* sl genospecies are associated with different vertebrate groups. In Europe, *Borrelia afzelii* is found in small mammals and *B. garinii* in birds [25]. In North America, *B. burgdorferi sensu stricto* is the main pathogenic genospecies and is found in both mammals and birds [26]. Hence, the circulation in the ecosystem of pathogens causing Lyme borreliosis differs markedly between the continents.

Lyme borreliosis is the most common vector-borne disease across temperate regions of the northern hemisphere [27–30]. Over recent decades, there has been an increase in both the number of Lyme borreliosis cases and the geographical distribution range, with emergence particularly impacting northern latitudes and high-elevation regions in North America and Europe [27,31–34]. Several studies have investigated spatial disease trends and the environmental factors that influence regional disease risk [33–37]. For temporal disease trends, empirical exploration of seasonality change is restricted to cases in the USA [38–40]. However, as the European and North American disease systems differ fundamentally due to contrasting hosts, pathogens and vectors, it is necessary to consider these systems independently [41]. For the European disease system, changes in Lyme borreliosis seasonality have only been predicted by a mechanistic model based on data from Scotland [42]. Our study is the first in Europe to use surveillance data to explore changes in the seasonality of Lyme borreliosis cases.

The goal of this study is to quantify changes in both the incidence and seasonal timing of Lyme borreliosis cases at the expanding northern distribution range in Europe. Lyme borreliosis surveillance data have been consistently reported in Norway under uniform criteria since 1995, presenting an excellent data source for this undertaking. Furthermore, Norway comprises distinct ecoregions with differences in climate and host composition, which allows for a unique opportunity to compare disease seasonality in ecologically distinct areas unified under a single-surveillance umbrella. Changes in plant phenology, described by spring greening measured from satellite data using the Normalized Difference Vegetation Index (NDVI), are used as a yardstick for interpreting the magnitude of phenological responses to climate change in the study area [9].

2. Methods

(a) Study area

Norway's Lyme borreliosis surveillance data include cases reported from the entire country, spanning a latitudinal range of 57°58′–71°08′ N [34,43]. For this analysis, cases reported at the municipality scale were grouped into four biogeographical regions, North, South, East and West (figure 1*a*), following designations from prior studies [25,34]. The four regions represent contrasting ecosystems with marked differences in topography and climate. The West region is separated from the East by a mountain range and experiences a temperate maritime climate, in contrast with the more continental climate of the East. The region South is mild and humid [44]. Forest and species composition also differ between regions [45]. Large mammal communities in particular are different between regions, which has especial importance for the vector life cycle [46]. The region West is dominated by red deer (*Cervus elaphus*), while roe deer (*Capreolus capreolus*) and moose (*Alces alces*) are most prominent in the regions East and South. Generally, the same small mammal and avian host species occur across the regions studied, though quantitative evidence of differences in abundances and host importance between regions remains limited [24,47].

Documented effects of climate change have been recorded across Norway over the study period [48]. For the reference period of 1979–2008, the annual mean temperature for mainland Norway has increased by 0.5–0.6°C, with winter temperatures increasing by about 1°C. The growing season, defined by the numbers of days with a mean temperature above 5°C, has increased by 1–2 weeks nationally, with the greatest increase in the Western coastal regions. Annual precipitation has increased in all regions, on average by 3% per decade, with the Western region most impacted by increased precipitation. The precipitation has primarily increased in the spring and decreased in the autumn [48]. The streamflow during the spring has also increased due to earlier snowmelt and earlier timing of snowmelt-driven flooding events [48,49]. The snow season has become shorter in most parts of mainland Norway, with reduced annual snow depth and fewer days of snow cover [48]. Advancement in spring plant phenology in response to climate change has been documented [50,51].

(b) Lyme borreliosis surveillance data

Lyme borreliosis surveillance data has been collected by the Norwegian Surveillance System for Communicable Diseases (MSIS) since 1991, when it became mandatory for care providers to report cases of positive diagnosis [52]. MSIS is curated and administrated by the Norwegian Institute of Public Health. The study period used for this analysis is from 1995 to 2019 because consistent criteria for reporting cases of disseminated Lyme borreliosis have been maintained over this time. A detailed account of reporting criteria has been reported elsewhere [25,52]. The only significant documented change in diagnostics over the study period is the standardization of spinal fluid testing protocols for children since 2011 [25]. Because of this change in testing protocol and to reduce bias from health system effects, case reports used for this study were restricted to patients over age 19. Cases were spatially localized to the region in which the tick bite occurred when these data were available (*ca* 50% of cases), otherwise the municipality in which the person resides was used. If the location of bite was reported as outside of

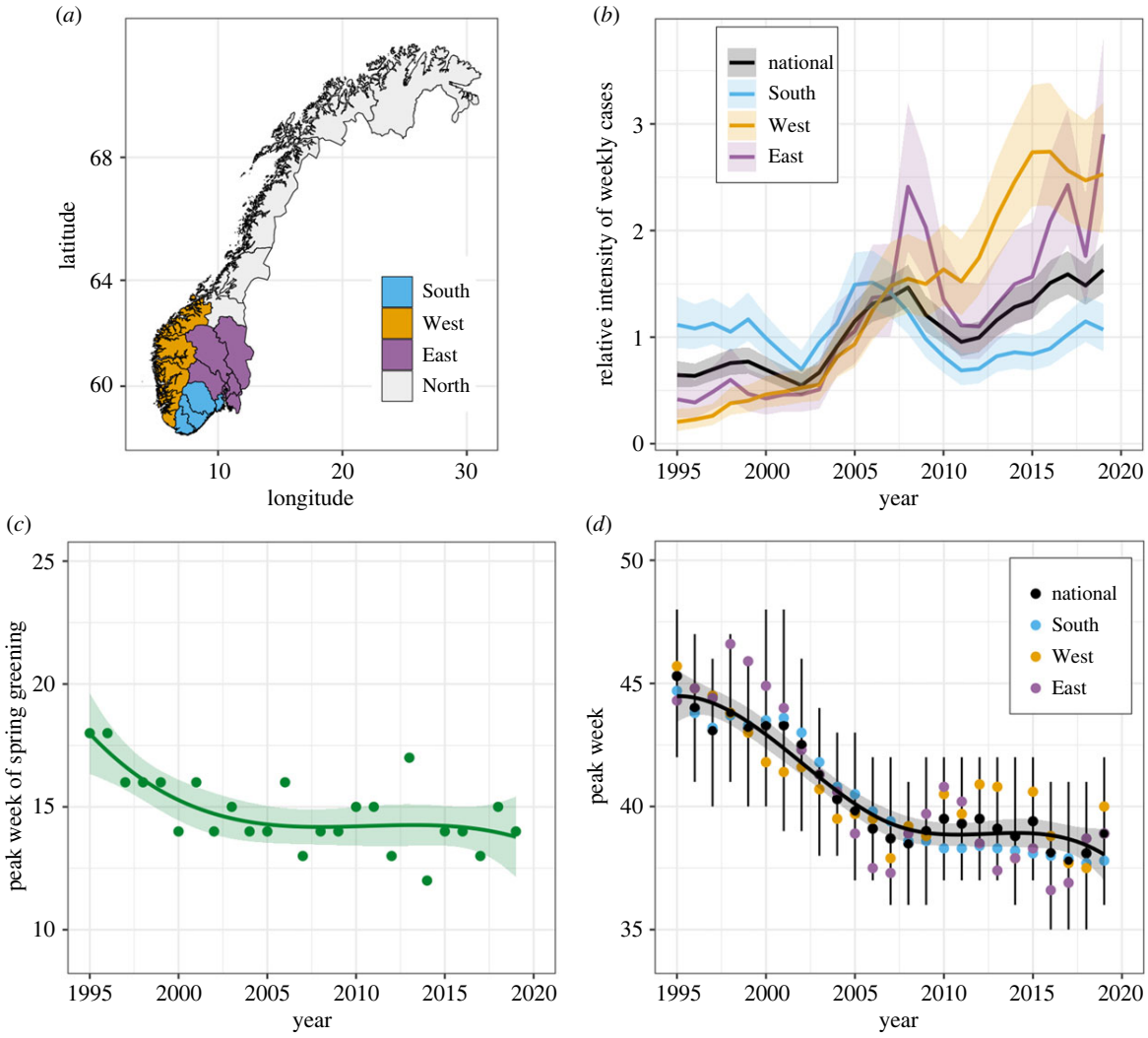

Figure 1. Key changes in the seasonal and long-term trends of Lyme borreliosis. (*a*) Map of Norway showing the regional aggregations used in this, and prior, studies [25,34]. The statistical models are fitted to national data, as well as to the South, West and East regions independently. (*b*) The annual component from the main model for Lyme borreliosis cases fitted to the national data (black) and to regional data for the South (blue), West (yellow) and East (purple). The trends show relative changes in average weekly case totals predicted for each year (relative case intensity). Because the intercept is not included, the trends are not comparable on an absolute scale. (*c*) The shift in the week of peak spring vegetation greening, measured by NDVI. The points represent the week in which peak greening was observed. The trendline is fitted from a linear model with a basis spline for year, with three degrees of freedom. (*d*) Predicted peak weeks for Lyme borreliosis cases from the main national model (black) and the regional models fitted to the South, West and East (blue, yellow and purple). Black points represent the annual peaks from the national model, and the corresponding black vertical lines show the 95% credible intervals, quantified by repeated sampling from the posterior distribution. The black curve with a shaded confidence interval is a basis spline with four degrees of freedom fitted to the predicted national peaks.

Norway these cases were not included in the study. Case timing is based on the date on which the patient went for diagnostic testing, which is available for every case. This date will typically occur several weeks after the tick bite, allowing time for disseminated disease symptoms to have manifested [53].

(c) Normalized difference vegetation index

Changes in the seasonality of plant development were used as a yardstick to contextualize the magnitude of temporal changes in the seasonality of Lyme borreliosis cases. Plant development was characterized using remote sensing NDVI satellite data to determine peak spring greening (when the rate of plant green-up is fastest) each year from 1995 to 2019. NDVI data are a widely used indicator of ecological responses to environmental change [54]. Changes in plant phenology are not expected to affect the timing of Lyme borreliosis cases directly, but are a useful point of reference for exploring downstream effects of climate change.

NDVI images are produced from satellite instrumentation that has been available from various sources since 1981 [55]. Moderate Resolution Imaging Spectroradiometer (MODIS) data at 250 m resolution have been available since 2000 and were downloaded from NASA Earthdata (https://urs.earthdata.nasa.gov/home) using the 'MODIStsp' package in R [56]. For the first 5 years of the study period (1995–2000), NDVI data from the Global Inventory Modelling and Mapping Studies (GIMMS) at the 8 km resolution scale were downloaded using the 'gimms' package in R [57]. MODIS and GIMMS data have been shown to be highly correlated and suitable for making continuous time series [55]. The high correlation ($r > 0.9$) was confirmed for this study by checking the years 2000–2005 in which data from both sources were available.

NDVI data were processed for areas below 200 m above sea level in the West, East and South regions combined, to estimate a yardstick that is on the national scale and relevant to areas in which Lyme borreliosis is most common. The MODIS NDVI images are collected once every 16 days, and the GIMMS NDVI images every 15/16 days. All images were processed following the procedures in Bischof *et al*. [58] and Rivrud *et al*. [59,60]. For each image pixel, the NDVI over the study period was scaled (0–1) and a double logistic regression curve was fitted annually

following Bischof *et al*. [58] and Rivrud *et al*. [59,60] to estimate a continuous time series from which derivatives, e.g. rate of change in green-up, start of spring, end of spring, and more, can be calculated [58,60]. Further details on the processing and modelling of NDVI data can be found elsewhere [58–60].

The day on which the rate of increase in greenness was at the maximum was used to determine the date of peak spring greening, and the corresponding week number was then extracted to make the data comparable to the Lyme borreliosis case data. A linear regression using a basis spline with three degrees of freedom was applied to visualize the change in peak spring greening over the study period. The basis spline with three degrees of freedom was selected for having the lowest Akaike information criterion (AIC) in comparison with a linear model and more flexible splines (see electronic supplementary material).

(d) Statistical analysis

The statistical software R v.4.2.2 was used for all statistical analyses [61]. The package INLA (http://www.r-inla.org) was used to fit all models. INLA uses a method of Integrated Nested Laplace Approximation to rapidly fit Bayesian models [62]. The R script (reproducing all the results and figures) and further details on the statistical analyses are available in the electronic supplementary material.

The number of Lyme borreliosis cases per week was modelled with a generalized linear mixed model (GLMM) including a flexible seasonal component that allows for the separation of a yearly trend and a seasonal trend. The number of cases y_{ij} in week i (from 1 to 52) and year j were assumed to follow a Poisson distribution,

$$y_{ij} \sim \text{Poisson}(\lambda_{ij}), \tag{2.1}$$

where λ_{ij} is the expected number of cases according to the model. As is standard for Poisson GLMMs, we used a logarithmic link function (i.e. $\ln(\lambda_{ij})$ is a linear predictor). The model formula was specified as follows:

$$\ln(\lambda_{ij}) = \beta_0 + \ln(N_j) + Y_j + W_{ij} + \varepsilon_{ij}, \tag{2.2}$$

where β_0 is the intercept, Y_j is the year effect (modelled as a first-order random walk), W_{ij} is the seasonal effect (specified below), $\ln(N_j)$ is the population offset and ε_{ij} is a Gaussian random effect used to account for overdispersion [63].

The population offset $\ln(N_j)$ is the logarithm of the total adult population N_j in the region. This was included to account for any changes in the number of observed cases due to changes in population size. Including a population offset makes the log-linear model equivalent to modelling the log of the expected number of cases relative to the population size (i.e. $\ln(\lambda_{ij}/N_j)$). Population size data were obtained on 25 January 2022 from Statistics Norway, Population Count (https://www.ssb.no/en/befolkning/folketall).

The main advantage of this model is its ability to separate the yearly (Y_j) and seasonal (W_{ij}) components, so that changes in seasonality can be isolated from long-term disease trends. The modelling approach for the seasonal component was inspired by an analysis of monthly registered cases of mumps in New York City by Ruiz-Cárdenas *et al*. in 2012 [64]. The long-term trend (Y_j) is modelled as a first-order random walk (prior specified in the electronic supplementary material). The seasonal component is based on a periodic function, where the effect of week number i in year j is given by

$$W_{ij} = \beta_{ij}\sin\left(\frac{2\pi}{52}\right) + \gamma_{ij}\cos\left(\frac{2\pi}{52}\right), \tag{2.3}$$

where β_{ij} and γ_{ij} are each modelled with a first-order random walk to make the seasonal effect of sequential weeks highly correlated, and the constant factor $2\pi/52$ defines the period in weeks within year. This seasonal effect is smooth across the study period because the parameters β_{ij} and γ_{ij} vary slowly.

Using trigonometric identities, equation (2.3) above can be rewritten as follows:

$$W_{ij} = A_{ij}\sin\left(\frac{2\pi}{52} + p_{ij}\right), \tag{2.4}$$

where A_{ij} represents the amplitude (determined by $A_{ij}^2 = \beta_{ij}^2 + \gamma_{ij}^2$), and p_{ij} represents the phase shift of the sinusoidal function (determined by $\tan(p_{ij}) = \beta_{ij}/\gamma_{ij}$). Importantly, the phase shift in equation (2.4) uniquely identifies a peak week of each year during which the number of Lyme borreliosis cases is at the maximum predicted by the model. Thus, changes in case seasonality over the study period can be quantified by extracting the peak week for each year from the model. In total, this results in a flexible seasonal component that can capture changes in seasonality over time. Credible intervals (95%) for the annual seasonal peaks were computed from 1000 samples from the posterior model. Long-term trends in annual seasonal peaks were visualized by fitting a basis spline with four degrees of freedom using the 'ggplot2' package in tidyverse [65].

(e) Regional analysis

To compare regional differences in seasonality, the model described above was fit to the South, West and East regions separately, as well as to national data that includes all regions. The North region contained only few cases (approx. 5% of total cases) and was not analysed separately. Fitting the models for each region separately can reveal any differences between the regions in the seasonality and long-term trends of cases and indicate if changes in the geographical distribution of cases could underlie national shifts in case timing. Regional models accounted for local adult population offsets, using data obtained from Statistics Norway.

(f) Model selection and alternative models

To determine whether case seasonality changed over the study period, the main model described above was compared with two alternative models with fixed seasonality across years. The alternative models only differed from the main model in the construction of the seasonal component. All models were fitted using the national dataset for this comparison.

The first alternative model removed the flexibility of the seasonal component by fixing the amplitude A_{ij} and the phase p_{ij} in the periodic function (equation (2.4)) so that they are the same each year. An additional alternative model with an improved description of a fixed seasonality was modelled using a cyclic random walk to fit a flexible spline with one knot per week [62,66]. This improved alternative model has a closely tailored seasonal component compared to the coarser sinusoidal seasonal model. Comparing these models allowed us to determine whether a closely fit but fixed seasonal trend describes the data better than a more coarsely fit but flexible seasonal trend that changes over time.

Comparison of the models was done through cross-validation (see electronic supplementary material). A randomly selected 10% of the data were removed before each model was refitted, and model performance was compared across 10 repetitions. Prediction quality was scored by root-mean-square error (RMSE), mean absolute error (MAE) and the negative log-likelihood (NLL) [67]. Additionally, the deviance information criterion (DIC) score, as given by INLA, was used as a metric for model comparison [68].

3. Results

The main model with a flexible seasonal trend that changes across years demonstrated good fit throughout the study

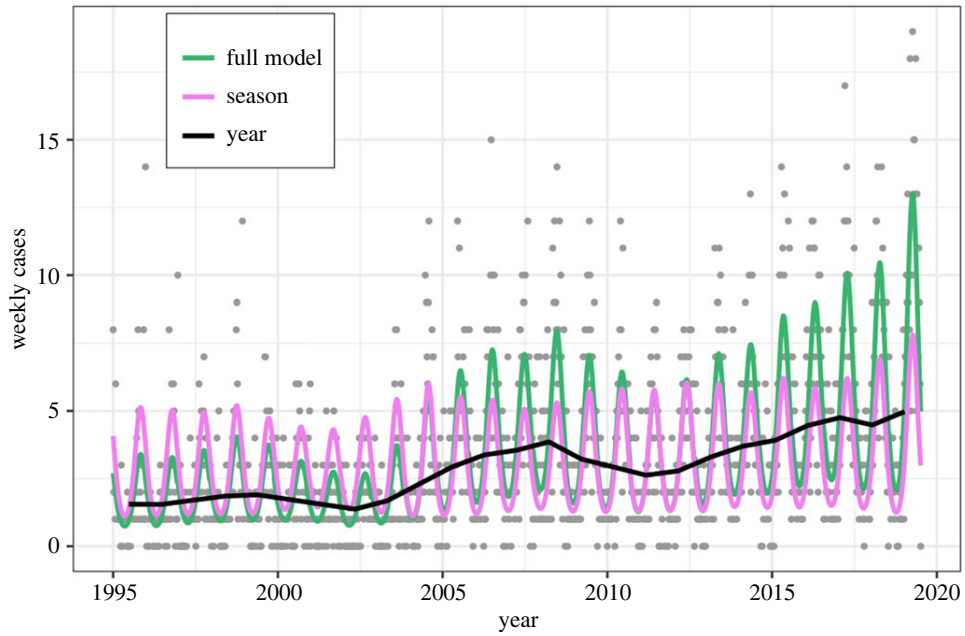

Figure 2. Weekly case numbers over the study period (grey points), together with model predictions (green) for the main national model. The yearly trend is shown in black (seasonal effect estimates set to zero), and the seasonal trend is shown in magenta (yearly effect estimates set to zero).

Table 1. Model performance metrics from cross-validation and DIC for comparing different candidate structures for the seasonality component. The main model includes a flexible seasonal component, while the two alternative models include a fixed seasonal component (see main text and electronic supplementary material). The metrics used were RMSE, MAE, NLL and DIC.

model	RMSE	MAE	NLL	DIC
main model	2.08	1.53	2560.5	5065.5
fixed cyclic random walk	2.12	1.56	2589.6	5096.0
fixed sinusoidal	2.13	1.57	2599.2	5104.2

period (figure 2; electronic supplementary material, figure S6) and performed well in cross-validation assessments (electronic supplementary material, figure S16). The main model outperformed both alternative models with fixed seasonality on all cross-validation metrics and using DIC (table 1), indicating that there has been a shift in Lyme borreliosis case seasonality over the study period (1995–2019). With the main model, we were able to separately quantify year-to-year changes in the number of cases and changes in within-year seasonality. The main model's parameters specifying the random effect distributions are reported in the electronic supplementary material, table S1. The seasonal component accounted for a larger amount of the total variance than the year component, highlighting the importance of including the seasonal trend (electronic supplementary material, table S2). There was no remaining temporal autocorrelation in the residuals (electronic supplementary material, figure S13). The unimodal seasonality employed by the main model is supported by the cross-validation and through analysis of the residuals, which show that the seasonality component of the main model is descriptive across weeks within the year (electronic supplementary material, figure S14). Thus, our findings support that the seasonality of Lyme borreliosis cases in Norway is characterized by a single main peak.

There was a clear national trend of increasing relative case intensity over time (reflecting the year component of the main model), with strong regional differences (figure 1*b*). While nationally the average weekly cases have more than tripled over the study period, there has only been a small increase in the region South (figure 1*b*). This is in contrast with the West, where in 2019 there were more than 10 times as many cases than at the start of the study period. The region South reported the majority of raw case counts in Norway every year until 2010, when the West surpassed it in the proportion of total cases reported annually. However, throughout the study period, the South maintained the highest annual incidence (number of cases per 100 000 adults) due to the much smaller population size relative to the other regions (electronic supplementary material, figure S9). Statistics describing trends in the raw data can be found in the electronic supplementary material.

There was a distinct change in the seasonal timing of Lyme borreliosis cases, characterized by an earlier shift in the week in which case numbers peaked (figure 1*d*). The extent of the seasonal shift was around six weeks over the 25-year study period, averaging to a rate of change of around 0.2 weeks per year. In the mid-1990s, the seasonal peak was typically in late October, while in 2018 it was in early September. Most of the seasonal shift occurred in the first 10 years of the study period, after which the peaks have been more stable. This is illustrated in figure 1*d*, where the trend line fitted to annual peaks is a basis spline with four degrees of freedom, which had a lower AIC than a linear model (difference of 7.8). No regional differences in the seasonal shift over the study period were observed. Each regional model exhibited the same overall pattern as the national model, and all regional peaks were within the credible intervals of the national model (electronic supplementary material, figures S11 and S12).

The shift in case seasonality outpaced the NDVI yardstick, which showed a shift towards an earlier peak spring greening of around three weeks over the study period (figure 1*c*). As with case timing, no regional differences in the NDVI trend were observed. Although the shift in NDVI was less pronounced than the shift in Lyme borreliosis cases, both had a similar overall trend with a rapid shift in the first 10 years and then a stabilization for the rest of the study period.

4. Discussion

Climate change is expected to impact the dynamics and geographical extent of vector-borne diseases, but simultaneous disease emergence and changing seasonality have rarely been quantified. Lyme borreliosis exhibits a highly seasonal incidence pattern and high sensitivity to environmental conditions, making it an interesting case study for exploring changes in seasonality. By applying a statistical model framework that explicitly accounts for seasonality in long-term surveillance data, we provide the first empirical evidence supporting a marked shift in Lyme borreliosis seasonality accompanying disease emergence and major climatic changes in northern latitudes of Europe.

Alteration of seasonality is a critical pathway by which climate change can affect ecosystem dynamics [69,70]. Changes in the seasonality of Lyme borreliosis cases were consistent between ecoregions of Norway (figure 1*d*), despite major regional differences in the species composition of large vertebrate hosts. All regions share the same tick vector, indicating that changes in vector phenology are likely an important driver of the observed patterns of Lyme borreliosis cases. Lyme borreliosis infections have been shown to peak in synchrony (with a lag) with high activity levels of nymphal ticks [38,39,42]. Ticks have the capacity for rapid modification of their questing activity and stage durations on the individual scale, yielding high plasticity in their life-history responses to environmental drivers [23,71–73]. The findings in this study support the intuitive effect of warmer springs shifting the Lyme borreliosis season earlier.

It has been hypothesized that warmer spring weather could potentially lead to increased nymphal tick activity in autumn due to a shortened development cycle leading to a second annual peak of the nymph stage [23,38,74,75]. A mechanistic model based on data from Scotland predicted increased incidence rates and a lengthening of the Lyme borreliosis season, but small changes in seasonality that varied between regions, with some regions having an earlier shift and other regions having a later shift in seasonality [42]. Our empirical analysis found only a consistent earlier shift in Lyme borreliosis cases in Norway, across all ecoregions. Both unimodal and bimodal distributions of tick questing activity levels have been observed in Europe, typically with a strong spring activity peak and, in some regions, a second, smaller autumn activity peak [76,77]. In Norway, tick activity data are limited to one study site in the Western region, where it was found that tick questing levels peaked in early summer (May–June), and only in some years, there was also a small activity peak in early autumn [64]. We found no evidence for a later secondary peak of Lyme borreliosis cases (electronic supplementary material, figures S1 and S13). This is consistent with findings in Denmark, where tick activity levels are reported to have a bimodal pattern while human Lyme borreliosis cases have a unimodal distribution [78–81]. These findings suggest that the seasonal pattern of Lyme borreliosis cases is driven by processes other than tick activity levels alone. In Norway, pathogen prevalence in small mammal hosts has been found to be consistently higher in spring than in fall, while pathogen prevalence in questing ticks is seasonally variable across years [24,34]. Human activity patterns may also lead to variable exposure across seasons.

The shift in Lyme borreliosis seasonality observed in this study far exceeds the magnitude of change observed in the USA [38,40]. An empirical study of Lyme borreliosis cases over a similar time period (1992–2007) across 12 U.S. states found that warmer southern states had an earlier seasonal onset than colder northern states [38]. However, there was high inter-annual variability in timing of cases and no consistent shift in seasonality [38]. The value of using a yardstick has been highlighted when comparing quantitative estimates of phenology [9]. For this study, NDVI was selected because it is a well-developed index for the onset of plant growth [54]. The seasonal shift in Lyme borreliosis cases documented here paralleled the shift in the onset of plant growth but with a larger magnitude of shift (figure 1*c*,*d*). The difference in magnitude of shift between peak spring greening and Lyme borreliosis case timing highlights that there are likely differences in the climatic drivers of these two manifestations of climate change. Empirical evidence suggests that several species of arthropods are highly sensitive to climate change and can show more rapid phenological shifts than plants and vertebrates [9,82]. It remains a gap in current understanding of tick biology to what extent tick stage durations are controlled by photoperiod or temperature [83,84]. The rapid seasonal shift observed in this study suggests that photoperiod has a limited effect on tick emergence from winter diapause, and that climatic drivers, such as increasingly warm spring temperatures and shifts in spring moisture levels and snow melt, primarily drive the tick life cycle.

Alternative or additional explanations for the rapid shift in seasonality of Lyme disease cases other than changes in tick vector phenology cannot be excluded. Phenological changes have also been documented in many host species linked to the Lyme borreliosis disease system, such as onset of the deer calving season [85,86] and the timing of migration and reproduction of birds [87]. Migratory birds play an important role in the Lyme borreliosis disease system [47,88], but whether changes to avian host phenology can drive the marked changes in Lyme borreliosis disease seasonality remains unclear. Changes to the healthcare system could underlie unexpected epidemiological patterns observed over long study periods. It is possible that improvements to health technologies and increased disease awareness among physicians and the public may have contributed to some of the seasonality shift observed over the study period by hastening the speed of diagnosis for patients with Lyme borreliosis. However, there is currently no documented evidence of any systemic and consistent social or health system change that would significantly impact speed of diagnostics over the study period.

Interestingly, the majority of the seasonal shift in cases in Norway took place preceding a period of rapid increase in case numbers and geographical range expansion (figure 1*b*, *d*). While we cannot document a causal relationship, the increased incidence may have been facilitated by the

preceding shift in seasonality. There are many potential mechanisms by which a shift in seasonality could increase disease incidence. For example, warmer spring weather could reduce critical mortality periods for immature ticks emerging from winter diapause [23,84,89,90]. Warmer springs also could increase synchrony between larval and nymphal stages, thereby changing pathogen transmission profiles and shifting the seasonality of Lyme borreliosis risk in accordance with changes in vector stage timing [20,26,91].

This study provides quantitative evidence demonstrating seasonality changes in a vector-borne disease. Further research is needed to isolate the ecological drivers of seasonality and how phenological changes in birds, mammals and arthropods combine to impact pathogen circulation and, in turn, human disease risks.

Ethics. The project was approved by the Regional Committee for Medical and Health Research Ethics (REK sør-øst B; Reference 115365).

Data accessibility. The data files and code are submitted with the manuscript as electronic supplementary material.

The data are provided in the electronic supplementary material [92].

Authors' contributions. A.G.: formal analysis, investigation, methodology, visualization, writing—original draft and writing—review and editing; H.V.: formal analysis, investigation, methodology, supervision, validation, visualization and writing—review and editing; I.M.R.: investigation, methodology, visualization and writing—review and editing; S.J.: conceptualization, resources, supervision and writing—review and editing; H.B.: methodology and writing—review and editing; Y.V.: conceptualization, funding acquisition, project administration, supervision, validation, visualization and writing—review and editing; A.M.: conceptualization, funding acquisition, project administration, supervision and writing—review and editing.

All authors gave final approval for publication and agreed to be held accountable for the work performed therein.

Conflict of interest declaration. The authors declare no competing interests.

Funding. The project is funded through the University of Oslo (PhD grant) and the Research Council of Norway (project TimeLyme, 313286).

References

1. Jones KE, Patel NG, Levy MA, Storeygard A, Balk D, Gittleman JL, Daszak P. 2008 Global trends in emerging infectious diseases. *Nature* **451**, 990–993. (doi:10.1038/nature06536)
2. Gallana M, Ryser-Degiorgis MP, Wahli T, Segner H. 2013 Climate change and infectious diseases of wildlife: altered interactions between pathogens, vectors and hosts. *Cur. Zool.* **59**, 427–437. (doi:10.1093/czoolo/59.3.427)
3. Ogden NH. 2017 Climate change and vector-borne diseases of public health significance. *FEMS Microbiol. Lett.* **364**, fnx186. (doi:10.1093/femsle/fnx186)
4. Rogers D, Randolph S. 2006 Climate change and vector-borne diseases. *Adv. Parasitol.* **62**, 345–381. (doi:10.1016/S0065-308X(05)62010-6)
5. Semenza JC, Suk JE. 2018 Vector-borne diseases and climate change: a European perspective. *FEMS Microbiol. Lett.* **365**, fnx244. (doi:10.1093/femsle/fnx244)
6. Shukla PR *et al.* (eds) 2022 Climate Change 2022: Mitigation of Climate Change. Working Group III Contribution to the IPCC Sixth Assessment Report. Cambridge, UK & New York, NY: Cambridge University Press. (doi:10.1017/9781009157926)
7. Medlock JM, Leach SA. 2015 Effect of climate change on vector-borne disease risk in the UK. *Lancet Infect. Dis.* **15**, 721–730. (doi:10.1016/S1473-3099(15)70091-5)
8. Menzel A *et al.* 2006 European phenological response to climate change matches the warming pattern. *Glob. Change Biol.* **12**, 1969–1976. (doi:10.1111/j.1365-2486.2006.01193.x)
9. Visser ME, Both C. 2005 Shifts in phenology due to global climate change: the need for a yardstick. *Proc. R. Soc. B* **272**, 2561–2569. (doi:10.1098/rspb.2005.3356)
10. Visser ME, Gienapp P. 2019 Evolutionary and demographic consequences of phenological mismatches. *Nat. Ecol. Evol.* **3**, 879–885. (doi:10.1038/s41559-019-0880-8)
11. Williams JW, Ordonez A, Svenning JC. 2020 A unifying framework for studying and managing climate-driven rates of ecological change. *Nat. Ecol. Evol.* **5**, 17–26. (doi:10.1038/s41559-020-01344-5)
12. Kharouba HM, Wolkovich EM. 2020 Disconnects between ecological theory and data in phenological mismatch research. *Nat. Clim. Change* **10**, 406–415. (doi:10.1038/s41558-020-0752-x)
13. Stenseth NChr, Mysterud A. 2002 Climate, changing phenology, and other life history traits: nonlinearity and match-mismatch to the environment. *Proc. Natl Acad. Sci. USA* **99**, 13 379–13 381. (doi:10.1073/pnas.212519399)
14. Tougeron K, Brodeur J, Lann CL, Baaren J. 2019 How climate change affects the seasonal ecology of insect parasitoids. *Ecol. Entomol.* **45**, 167–181. (doi:10.1111/een.12792)
15. Kovats RS, Campbell-Lendrum DH, McMichel AJ, Woodward A, Cox J. 2001 Early effects of climate change: do they include changes in vector-borne disease? *Phil. Trans. R. Soc. Lond. Ser. B* **356**, 1057–1068. (doi:10.1098/rstb.2001.0894)
16. Ogden NH, Lindsay LR. 2016 Effects of climate and climate change on vectors and vector-borne diseases: ticks are different. *Trends Parasitol.* **32**, 646–656. (doi:10.1016/j.pt.2016.04.015)
17. White ER, Hastings A. 2020 Seasonality in ecology: progress and prospects in theory. *Ecol. Complexity* **44**, 100867. (doi:10.1016/j.ecocom.2020.100867)
18. Altizer S, Dobson A, Hosseini P, Hudson P, Pascual M, Rohani P. 2006 Seasonality and the dynamics of infectious diseases. *Ecol. Lett.* **9**, 467–484. (doi:10.1111/j.1461-0248.2005.00879.x)
19. Fisman DN. 2007 Seasonality of infectious diseases. *Annu. Rev. Public Health* **28**, 127–143. (doi:10.1146/annurev.publhealth.28.021406.144128)
20. Altizer S, Ostfeld RS, Johnson PTJ, Kutz S, Harvell CD. 2013 Climate change and infectious diseases: from evidence to a predictive framework. *Science* **341**, 514–519. (doi:10.1126/science.1239401)
21. Johnson PTJ, de Roode JC, Fenton A. 2015 Why infectious disease research needs community ecology. *Science* **349**, 1259504. (doi:10.1126/science.1259504)
22. Gulia-Nuss M *et al.* 2016 Genomic insights into the *Ixodes scapularis* tick vector of Lyme disease. *Nat. Commun.* **7**, 10507. (doi:10.1038/ncomms10507)
23. Grigoryeva LA, Shatrov A. 2022 Life cycle of the tick *Ixodes ricinus* (L.) (Acari: Ixodidae) in the North-West of Russia. *Syst. Appl. Acarol.* **27**, 538–550. (doi:10.11158/saa.27.3.11)
24. Mysterud A, Stigum VM, Linløkken H, Herland A, Viljugrein H. 2019 How general are generalist parasites? The small mammal part of the Lyme disease transmission cycle in two ecosystems in northern Europe. *Oecologia* **190**, 115–126. (doi:10.1007/s00442-019-04411-2)
25. Mysterud A, Heylen DJA, Matthysen E, Garcia AL, Jore S, Viljugrein H. 2019 Lyme neuroborreliosis and bird populations in Northern Europe. *Proc. R. Soc. B* **286**, 20190759. (doi:10.1098/rspb.2019.0759)
26. Kurtenbach K, Hanincová K, Tsao JI, Margos G, Fish D, Ogden NH. 2006 Fundamental processes in the evolutionary ecology of Lyme borreliosis. *Nat. Rev. Microbiol.* **4**, 660–669. (doi:10.1038/nrmicro1475)
27. Rizzoli A, Hauffe HC, Carpi G, Vourc'h GI, Neteler M, Rosà R. 2011 Lyme borreliosis in Europe. *Eurosurveillance* **16**, 19906. (doi:10.2807/ese.16.27.19906-en)
28. Stone BL, Tourand Y, Brissette CA. 2017 Brave new worlds: the expanding universe of Lyme disease. *Vector-Borne Zoonotic Dis.* **17**, 619–629. (doi:10.1089/vbz.2017.2127)
29. Estrada-Peña A, Ayllón N, de la Fuente J. 2012 Impact of climate trends on tick-borne pathogen transmission. *Front. Physiol.* **3**, 64. (doi:10.3389/fphys.2012.00064)
30. Vandekerckhove O, Buck ED, Wijngaerden EV. 2019 Lyme disease in Western Europe: an emerging problem? A systematic review. *Acta Clin. Belg.* **76**, 244–252. (doi:10.1080/17843286.2019.1694293)

31. Kugeler KJ, Schwartz AM, Delorey MJ, Mead PS, Hinckley AF. 2021 Estimating the frequency of Lyme disease diagnoses, United States, 2010–2018. *Emerg. Infect. Dis.* **27**, 616–619. (doi:10.3201/eid2702.202731)
32. Jore S *et al.* 2011 Multi-source analysis reveals latitudinal and altitudinal shifts in range of *Ixodes ricinus* at its northern distribution limit. *Parasit. Vectors* **4**, 1–11. (doi:10.1186/1756-3305-4-84)
33. Ogden NH *et al.* 2008 Risk maps for range expansion of the Lyme disease vector, *Ixodes scapularis*, in Canada now and with climate change. *Int. J. Health Geogr.* **7**, 24. (doi:10.1186/1476-072X-7-24)
34. Mysterud A, Easterday WR, Stigum VM, Aas AB, Meisingset EL, Viljugrein H. 2016 Contrasting emergence of Lyme disease across ecosystems. *Nat. Commun.* **7**, 11882. (doi:10.1038/ncomms11882)
35. Kjær LJ *et al.* 2019 Predicting and mapping human risk of exposure to *Ixodes ricinus* nymphs using climatic and environmental data, Denmark, Norway and Sweden, 2016. *Eurosurveillance* **24**, 1800101. (doi:10.2807/1560-7917.ES.2019.24.9.1800101)
36. Ostfeld RS, Glass GE, Keesing F. 2005 Spatial epidemiology: an emerging (or re-emerging) discipline. *Trends Ecol. Evol.* **20**, 328–336. (doi:10.1016/j.tree.2005.03.009)
37. Mollalo A, Blackburn JK, Morris LR, Glass GE. 2017 A 24-year exploratory spatial data analysis of Lyme disease incidence rate in Connecticut, USA. *Geospatial Health* **12**, 588. (doi:10.4081/gh.2017.588)
38. Moore SM, Eisen RJ, Monaghan A, Mead P. 2014 Meteorological influences on the seasonality of lyme disease in the United States. *Am. J. Trop. Med. Hyg.* **90**, 486–496. (doi:10.4269/ajtmh.13-0180)
39. Sundheim KM, Levas MN, Balamuth F, Thompson AD, Neville DN, Garro AC, Kharbanda AB, Monuteaux MC, Nigrovic LE. 2021 Seasonality of acute Lyme disease in children. *Trop. Med. Infect. Dis.* **6**, 196. (doi:10.3390/tropicalmed6040196)
40. Monaghan AJ, Moore SM, Sampson KM, Beard CB, Eisen RJ. 2015 Climate change influences on the annual onset of Lyme disease in the United States. *Ticks Tick-Borne Dis.* **6**, 615–622. (doi:10.1016/j.ttbdis.2015.05.005)
41. Marques AR, Strle F, Wormser GP. 2021 Comparison of Lyme disease in the United States and Europe. *Emerg. Infect. Dis.* **27**, 2017–2024. (doi:10.3201/eid2708.204763)
42. Li S, Gilbert L, Harrison PA, Rounsevell MDA. 2016 Modelling the seasonality of Lyme disease risk and the potential impacts of a warming climate within the heterogeneous landscapes of Scotland. *J. R. Soc. Interface* **13**, 20160140. (doi:10.1098/rsif.2016.0140)
43. Mysterud A, Jore S, Østerås O, Viljugrein H. 2017 Emergence of tick-borne diseases at northern latitudes in Europe: a comparative approach. *Sci. Rep.* **7**, 1–12. (doi:10.1038/s41598-017-15742-6)
44. Qviller L, Grøva L, Viljugrein H, Klingen I, Mysterud A. 2014 Temporal pattern of questing tick *Ixodes ricinus* density at differing elevations in the coastal region of western Norway. *Parasit. Vectors* **7**, 1–12. (doi:10.1186/1756-3305-7-179)
45. Abrahamsen J, Jacobsen N, Kalliola R, Dahl E, Wilborg L, Påhlsson L. 1977 Naturgeografisk regioninndeling av Norden. *Nordiske Utredninger Series B* **34**, 1–135.
46. Mysterud A, Qviller L, Meisingset EL, Viljugrein H. 2016 Parasite load and seasonal migration in red deer. *Oecologia* **180**, 401–407. (doi:10.1007/s00442-015-3465-5)
47. Hasle G *et al.* 2009 Transport of ticks by migratory passerine birds to Norway. *J. Parasitol.* **95**, 1342–1351. (doi:10.1645/GE-2146.1)
48. Flæte O *et al.* 2010 Official Norwegian Reports NOU 2010: 10. Adapting to a Changing Climate. Oslo, Norway: Norwegian Ministry of The Environment. (https://www.regjeringen.no/en/dokumenter/nou-2010-10-2/id668985/)
49. Vormoor K, Lawrence D, Schlichting L, Wilson D, Wong WK. 2016 Evidence for changes in the magnitude and frequency of observed rainfall vs. snowmelt driven floods in Norway. *J. Hydrol.* **538**, 33–48. (doi:10.1016/j.jhydrol.2016.03.066)
50. Nordli Ø, Wielgolaski FE, Bakken AK, Hjeltnes SH, Måge F, Sivle A, Skre O. 2008 Regional trends for bud burst and flowering of woody plants in Norway as related to climate change. *Int. J. Biometeorol.* **52**, 625–639. (doi:10.1007/s00484-008-0156-5)
51. Karlsen SR, Høgda KA, Wielgolaski FE, Tolvanen A, Tømmervik H, Poikolainen J, Kubin E. 2009 Growing-season trends in Fennoscandia 1982–2006, determined from satellite and phenology data. *Clim. Res.* **39**, 275–286. (doi:10.3354/cr00828)
52. MacDonald E *et al.* 2016 Are the current notification criteria for Lyme borreliosis in Norway suitable? Results of an evaluation of Lyme borreliosis surveillance in Norway, 1995–2013. *BMC Public Health* **16**, 729. (doi:10.1186/s12889-016-3346-9)
53. Coburn J, Garcia B, Hu LT, Jewett MW, Kraiczy P, Norris SJ, Skare J. 2021 Lyme disease pathogenesis. *Curr. Issues Mol. Biol.* **42**, 473–518. (doi:10.21775/cimb.042.473)
54. Pettorelli N, Vik JO, Mysterud A, Gaillard JM, Tucker CJ, Stenseth NChr. 2005 Using the satellite-derived NDVI to assess ecological responses to environmental change. *Trends Ecol. Evol.* **20**, 503–510. (doi:10.1016/j.tree.2005.05.011)
55. Pinzon J, Tucker C. 2014 A non-stationary 1981–2012 AVHRR NDVI3g time series. *Remote Sensing* **6**, 6929–6960. (doi:10.3390/rs6086929)
56. Busetto L, Ranghetti L. 2016 MODIStsp: an R package for automatic preprocessing of MODIS Land Products time series. *Comput. Geosci.* **97**, 40–48. (doi:10.1016/j.cageo.2016.08.020)
57. Detsch F. 2021 gimms: Download and Process GIMMS NDVI3g Data. R package. Version 1.2.1. (See https://www.researchgate.net/publication/294891839_gimms_Download_and_Process_GIMMS_NDVI3g_Data↗Repl)
58. Bischof R, Loe LE, Meisingset EL, Zimmermann B, Moorter BV, Mysterud A. 2012 A migratory northern ungulate in the pursuit of spring: jumping or surfing the green wave? *Am. Nat.* **180**, 407–424. (doi:10.1086/667590)
59. Rivrud IM *et al.* 2019 Heritability of head size in a hunted large carnivore, the brown bear (*Ursus arctos*). *Evol. Appl.* **12**, 1124–1135. (doi:10.1111/eva.12786)
60. Rivrud IM, Sivertsen TR, Mysterud A, Åhman B, Støen OG, Skarin A. 2018 Reindeer green-wave surfing constrained by predators. *Ecosphere* **9**, e02210. (doi:10.1002/ecs2.2210)
61. R Core Team. 2022 *R: a language and environment for statistical computing*. Vienna, Austria: Foundation for Statistical Computing.
62. Rue H, Martino S, Chopin N. 2009 Approximate Bayesian inference for latent Gaussian models by using integrated nested Laplace approximations. *J. R. Stat. Soc. Ser. B (Statistical Methodology)* **71**, 319–392. (doi:10.1111/j.1467-9868.2008.00700.x)
63. Bakka H, Vanhatalo J, Illian JB, Simpson D, Rue H. 2019 Non-stationary Gaussian models with physical barriers. *Spatial Stat.* **29**, 268–288. (doi:10.1016/j.spasta.2019.01.002)
64. Ruiz-Cárdenas R, Krainski ET, Rue H. 2012 Direct fitting of dynamic models using integrated nested Laplace approximations—INLA. *Computat. Stat. Data Analysis* **56**, 1808–1828. (doi:10.1016/j.csda.2011.10.024)
65. Wickham H. 2016 *Ggplot2: elegant graphics for data analysis*. New York, NY: Springer-Verlag.
66. Lindgren F, Rue H. 2015 Bayesian spatial modelling with R-INLA. *J. Stat. Softw.* **63**, 1–25. (doi:10.18637/jss.v063.i19)
67. Jornsatian C, Bodhisuwan W. 2021 Zero-one inflated negative binomial - beta exponential distribution for count data with many zeros and ones. *Commun. Stat. Theory Methods* **51**, 8517–8531. (doi:10.1080/03610926.2021.1898642)
68. Sutanto HT, Pramoedyo H, Wardhani WS, Astutik S. 2021 The selection of Bayesian polynomial regression with INLA by using DIC, WAIC and CPO. *J. Phys Conf. Ser.* **1747**, 012029. (doi:10.1088/1742-6596/1747/1/012029)
69. Parmesan C. 2006 Ecological and evolutionary responses to recent climate change. *Ann. Rev. Ecol. Evol. Syst.* **37**, 637–669. (doi:10.1146/annurev.ecolsys.37.091305.110100)
70. Stenseth NC, Mysterud A, Ottersen G, Hurrell JW, Chan KS, Lima M. 2002 Ecological effects of climate fluctuations. *Science* **297**, 1292–1296. (doi:10.1126/science.1071281)
71. Gray J, Kahl O, Zintl A. 2021 What do we still need to know about *Ixodes ricinus*? *Ticks Tick-borne Dis.* **12**, 101682. (doi:10.1016/j.ttbdis.2021.101682)
72. Gray JS, Kahl O, Lane RS, Levin ML, Tsao JI. 2016 Diapause in ticks of the medically important *Ixodes ricinus* species complex. *Ticks Tick-borne Dis.* **7**, 992–1003. (doi:10.1016/j.ttbdis.2016.05.006)
73. Estrada-Peña A, Gray JS, Kahl O, Lane RS, Nijhof AM. 2013 Research on the ecology of ticks and tick-borne pathogens—methodological principles and caveats. *Front. Cell. Infect. Microbiol.* **3**, 29. (doi:10.3389/fcimb.2013.00029)

74. Ogden N, Lindsay L, Beauchamp G, Charron D, Maarouf A, O'callaghan C, Waltner-Toews D, Barker I. 2004 Investigation of relationships between temperature and developmental rates of tick *Ixodes scapularis* (Acari: Ixodidae) in the laboratory and field. *J. Med. Entomol.* **41**, 622–633. (doi:10.1603/0022-2585-41.4.622)
75. Kilpatrick AM *et al.* 2017 Lyme disease ecology in a changing world: consensus, uncertainty and critical gaps for improving control. *Phil. Trans. R. Soc. B* **372**, 20160117. (doi:10.1098/rstb.2016.0117)
76. Wongnak P *et al.* 2022 Meteorological and climatic variables predict the phenology of *Ixodes ricinus* nymph activity in France, accounting for habitat heterogeneity. *Sci. Rep.* **12**, 1–16. (doi:10.1038/s41598-022-11479-z)
77. Hauser G, Rais O, Morán Cadenas F, Gonseth Y, Bouzelboudjen M, Gern L. 2018 Influence of climatic factors on *Ixodes ricinus* nymph abundance and phenology over a long-term monthly observation in Switzerland (2000–2014). *Parasit. Vectors* **11**, 1–12. (doi:10.1186/s13071-018-2876-7)
78. Skufca J *et al.* 2022 Incidence of Lyme neuroborreliosis in Denmark: exploring observed trends using public surveillance data, 2015–2019. *Ticks Tick-borne Dis.* **13**, 102039. (doi:10.1016/j.ttbdis.2022.102039)
79. Jensen P. 2000 Host seeking activity of *Ixodes ricinus* ticks based on daily consecutive flagging samples. *Exp. Appl. Acarol* **24**, 695–708. (doi:10.1023/a:1010640219816)
80. Jensen PM, Frandsen F. 2000 Temporal risk assessment for Lyme borreliosis in Denmark. *Scand. J. Infect. Dis.* **32**, 539–544. (doi:10.1080/003655400458848)
81. Kantsø B, Svendsen CB, Jensen PM, Vennestrøm J, Krogfelt KA. 2010 Seasonal and habitat variation in the prevalence of *Rickettsia helvetica* in *Ixodes ricinus* ticks from Denmark. *Ticks Tick-Borne Dis.* **1**, 101–103. (doi:10.1016/j.ttbdis.2010.01.004)
82. Parmesan C. 2007 Influences of species, latitudes and methodologies on estimates of phenological response to global warming. *Glob. Change Biol.* **13**, 1860–1872. (doi:10.1111/j.1365-2486.2007.01404.x)
83. Ostfeld RS, Brunner JL. 2015 Climate change and *Ixodes* tick-borne diseases of humans. *Phil. Trans. R. Soc. B* **370**, 20140051. (doi:10.1098/rstb.2014.0051)
84. Dobson AD, Finnie TJ, Randolph SE. 2011 A modified matrix model to describe the seasonal population ecology of the European tick *Ixodes ricinus*. *J. Appl. Ecol.* **48**, 1017–1028. (doi:10.1111/j.1365-2664.2011.02003.x)
85. Coulson T, Kruuk L, Tavecchia G, Pemberton J, Clutton-Brock T. 2003 Estimating selection on neonatal traits in red deer using elasticity path analysis. *Evolution* **57**, 2879–2892. (doi:10.1111/j.0014-3820.2003.tb01528.x)
86. Plard F, Gaillard JM, Coulson T, Hewison AM, Delorme D, Warnant C, Bonenfant C. 2014 Mismatch between birth date and vegetation phenology slows the demography of roe deer. *PLoS Biol.* **12**, e1001828. (doi:10.1371/journal.pbio.1001828)
87. Visser ME, Noordwijk AV, Tinbergen J, Lessells C. 1998 Warmer springs lead to mistimed reproduction in great tits (*Parus major*). *Proc. R. Soc. Lond. B* **265**, 1867–1870. (doi:10.1098/rspb.1998.0514)
88. Hasle G, Bjune GA, Midthjell L, Red KH, Leinaas HP. 2011 Transport of *Ixodes ricinus* infected with *Borrelia* species to Norway by northward-migrating passerine birds. *Ticks Tick-borne Dis.* **2**, 37–43. (doi:10.1016/j.ttbdis.2010.10.004)
89. Van Gestel M, Matthysen E, Heylen D, Verheyen K. 2022 Survival in the understorey: testing direct and indirect effects of microclimatological changes on *Ixodes ricinus*. *Ticks Tick-borne Dis.* **13**, 102035. (doi:10.1016/j.ttbdis.2022.102035)
90. Herrmann C, Gern L. 2013 Survival of *Ixodes ricinus* (Acari: Ixodidae) nymphs under cold conditions is negatively influenced by frequent temperature variations. *Ticks Tick-Borne Dis.* **4**, 445–451. (doi:10.1016/j.ttbdis.2013.05.002)
91. Levi T, Keesing F, Oggenfuss K, Ostfeld RS. 2015 Accelerated phenology of blacklegged ticks under climate warming. *Phil. Trans. R. Soc. B* **370**, 20130556. (doi:10.1098/rstb.2013.0556)
92. Goren A, Viljugrein H, Rivrud IM, Jore S, Bakka H, Vindenes Y, Mysterud A. 2023 The emergence and shift in seasonality of Lyme borreliosis in Northern Europe. Figshare. (doi:10.6084/m9.figshare.c.6414112)

Supplementary materials

for ‘The emergence and shift in seasonality of Lyme borreliosis in northern Europe’

Asena Goren, Hildegunn Viljugrein, Inger Maren Rivrud, Solveig Jore, Haakon Bakka, Yngvild Vindenes, Atle Mysterud

This document includes R code for running the analysis and producing all the figures in the main text, as well as additional figures and tables. The INLA models are also described in more detail here.

1. Setup and data exploration

The models are fitted using the INLA-package. To install the package, run:

```
#install.packages("INLA",repos=c(getOption("repos"),INLA="https://inla.r-inla-do
wnload.org/R/stable"), dep=TRUE)
```

1.1 Datasets and libraries

The dataset (LymeData.csv) represents cases of Lyme borreliosis in Norway, aggregated to week, from 1995-2019. This data is gathered from surveillance data from the MSIS system. Each case is dated with the week number at which the patient went for diagnostic testing at the hospital. The dataframe has a running year-week index X, from the first week of 1995 to the last week of 2019.

```
# Lyme borreliosis data
dfa <- read.csv("LymeData.csv")
Y <- unique(dfa$year) #Years
wnr <- seq(1, 52, 1) #Week numbers within year

#NDVI data
peak.spring <- read.csv("NDVI_peakspring.csv")

#Dataset for plotting the map
load("Norway_df.RData")
```

Libraries and setup

Here, the libraries required to run the script are loaded into the R environment. This script was developed using R version 4.2.2, INLA version 22.05.07, and tidyverse version 1.3.1 (which is bundled with ggplot2 version 3.3.6).

```
library(INLA)
library(sn)
library(mgcv)
library(tidyverse)
library(patchwork)
library(sf)
library(raster)
library(ggiraph)
library(mapproj)
library(knitr)
library(cowplot)


#---------------------------------------
# Initialize random number generator
set.seed(123456)
```

1.2 Exploring the Data

Before modelling the data we can briefly explore the raw data.

Total number of cases nationally:

```
sum(dfa$cases)
```

```
## [1] 4426
```

Total number of cases in the South:

```
sum(dfa$casesSouth)
```

```
## [1] 1896
```

Total number of cases in the West:

```
sum(dfa$casesWest)
```

```
## [1] 1512
```

Total number of cases in the East:

```
sum(dfa$casesEast)
```

```
## [1] 795
```

The proportional increase in case totals from the start to the end of the study period can be estimated by comparing the averages of the case totals in the first three and last three years of the study period:

```
yrsums <- dfa %>% group_by(year) %>% summarize(n=sum(cases), nS=sum(casesSouth),
nW=sum(casesWest), nE=sum(casesEast))

changes <- data.frame(
  National_Change = mean(yrsums[23:25,]$n)/mean(yrsums[1:3,]$n),
  South_Change = mean(yrsums[23:25,]$nS)/mean(yrsums[1:3,]$nS),
  West_Change = mean(yrsums[23:25,]$nW)/mean(yrsums[1:3,]$nW),
  East_Change = mean(yrsums[23:25,]$nE)/mean(yrsums[1:3,]$nE))


changes
```

```
##   National_Change South_Change West_Change East_Change
## 1        3.116438     1.207792    12.48276    7.851852
```

From the above it can be estimated that, nationally, the number of cases approximately tripled over the 25 year study period. The region South had a small increase of around 20%, which is in stark contrast to the region West where there are more than 10 times the number of raw cases at the end of the study period compared to the start.

We can also calculate the proportion of national cases in the regions South and West to find the year in which the proportion of national cases in the West surpassed the South.

```
propSouth <- yrsums$nS / yrsums$n
propWest <- yrsums$nW / yrsums$n

propframe <- data.frame(
  Year = Y,
  Proportion_South = propSouth,
  Proportion_West = propWest
)

zoompf <- propframe[propframe$Year %in% 2007:2012,]

print(zoompf)
```

```
##    Year Proportion_South Proportion_West
## 13 2007        0.4832536       0.3301435
## 14 2008        0.3699187       0.2764228
## 15 2009        0.3622449       0.3112245
## 16 2010        0.3370166       0.4364641
## 17 2011        0.3092105       0.4013158
## 18 2012        0.3035714       0.4583333
```

From 2010 onwards the region West reports the highest proportion of cases nationally.

The national weekly incidence (per 100,000 adults) over the study period is visualized as raw data below. Additionally, the overall shape of the seasonal trend is visualized by the median weekly incidence over the whole study region and time period.

```
pRaw1 <- ggplot(dfa) +
  geom_line(aes(x=X, y=cases/pop*100000)) +
  ylab("Weekly Incidence") +
  xlab("Year") +
  scale_x_continuous(breaks=seq(1,1590,265), labels=c("1995","2000","2005","201
0","2015", "2020")) +
  theme_bw() + labs(tag = "(a)") + theme(plot.tag = element_text())

raw2 <- dfa
raw2$incidence <- raw2$cases/raw2$pop*100000
raw2 <- raw2 %>% group_by(week) %>% summarize(incidence = quantile(incidence, c
(0.25, 0.5, 0.75)), q = c("q0.25", "q0.5", "q0.75"))
raw2 <- pivot_wider(raw2, names_from = q, values_from = incidence)

pRaw2 <- ggplot(raw2) +
  geom_line(aes(x=week, y=q0.5)) +
  geom_ribbon(aes(x=week,ymax=q0.75, ymin=q0.25), fill="purple", alpha= 0.2) +
  stat_smooth(aes(x=week, y=q0.5), method="gam") +
  xlab("Week Number") +
  ylab("Median Incidence") +
  theme_bw() + labs(tag = "(b)") + theme(plot.tag = element_text())

figS1 <- plot_grid(pRaw1, pRaw2, nrow=2, align="hv", axis="l", rel_heights = c
(1,1, 1,1))

figS1
```

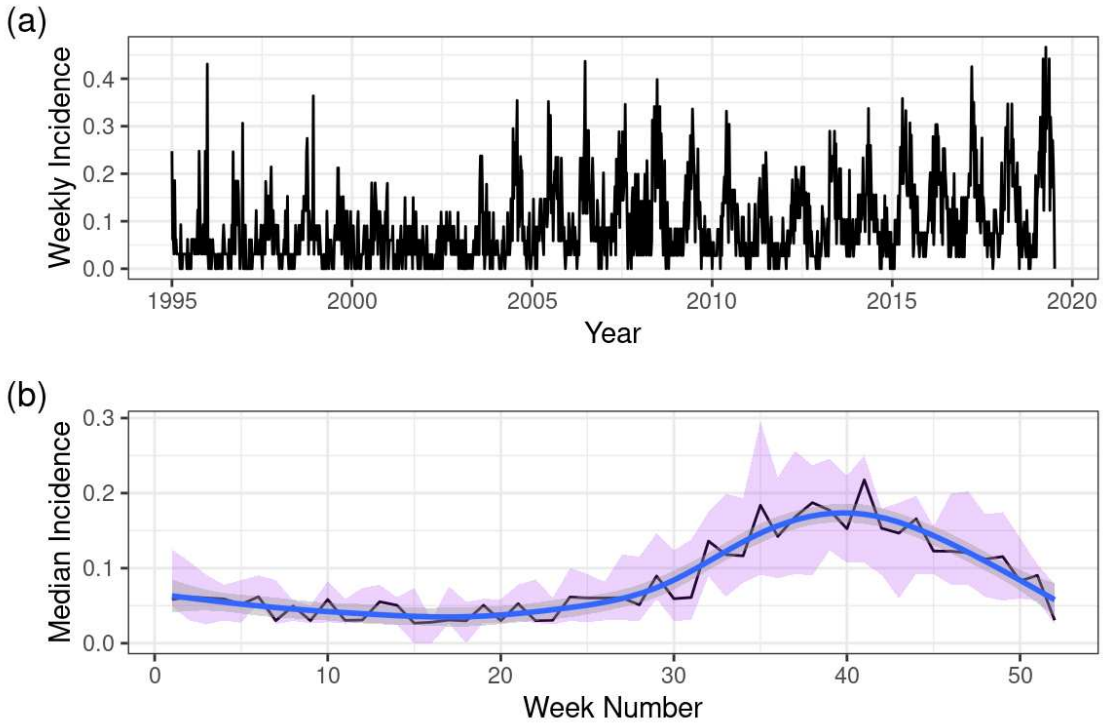

Figure S1: Exploration of temporal trends in unprocessed Lyme borreliosis surveillance data. (a) The national weekly incidence of Lyme borreliosis over the study period. (b) The median national weekly incidence pooled over the study period. The purple shaded area represents upper and lower quartiles. The blue trend line and shaded gray error region are a basic GAM spline highlighting the shape of the seasonal peak.

2. Map of regions

The data set of spatial coordinates used to plot the map of Norway was downloaded from https://gadm.org (https://gadm.org) (Sep 5, 2022). The data frame used for plotting is included as a separate ‘RData’ file. The statistical models are fitted to the national data as well as to the South, West and East regions independently. The regions are based on the 2017 county numbers, with the region East spanning county numbers 1-6, South 7-10, West 11-15, and North 16+.

```
regcols <- c("#56B4E9", "#E69F00", "#9b67a1", "#eeeeee")
names(regcols) <- c("South","West","East","North")

map_plot <- ggplot() +
  geom_polygon(data = Norway_df,
               aes(x = long, y = lat, group = group, fill=Region, color=Region),
               color="black",
               size = 0.2,
               alpha = 1) +
  coord_map() +
  theme_bw()+
  scale_fill_manual(values=regcols)+
  theme(legend.position = c(0.8, 0.27),
        legend.title = element_blank())

map_plot
```

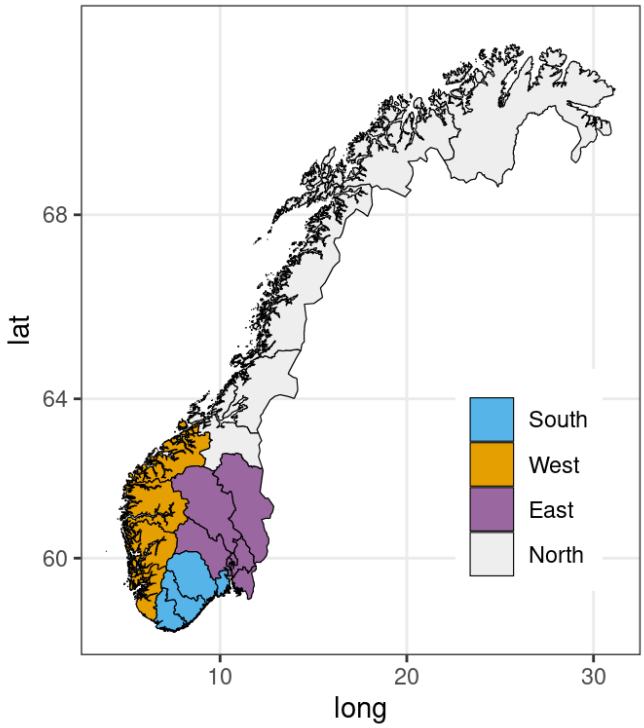

Figure S2: This is part of Figure 1. Map of Norway showing the regional aggregations used in this and prior studies. The statistical models are fitted to the national data as well as to the South, West and East regions independently.

3. Defining INLA-models

Here we describe the basic structure of the INLA-models used in the manuscript, including the R code for defining model structures and priors. Additional information can be found in the R-INLA documentation at https://www.r-inla.org/documentation (https://www.r-inla.org/documentation).

We start with a baseline model without a seasonal component specifically included, before expanding this below with three alternatives for adding the seasonal component (the models compared in the manuscript): 1) our main model with a flexible seasonal component, 2) an alternative model with fixed seasonality using a sinusoidal wave function, and 3) an alternative model with fixed seasonality using a second-order cyclic random walk.

3.1 Model without seasonality

We assume that the number of Lyme disease cases in week number i and year j is Poisson distributed with mean λ_{ij},

$$y_{ij} \sim \text{Poisson}(\lambda_{ij}).$$

The linear predictor for the mean number of cases in week i and year j is given by $\ln(\lambda_{ij})$, using the standard log-link function for Poisson models. Effects of covariates are thus assumed additive on this scale.

For this initial model without seasonality explicitly modeled, the linear predictor can be written as

$$\ln(\lambda_{ij}) = \beta_0 + W_{ij} + \ln(N_j),$$

where β_0 is the intercept, W_{ij} is a week effect (defined by a random walk, see below), and $\ln(N_j)$ is the population offset.

The week effect is modeled with a first order random walk process,

$$w(t+1) = w(t) + z_t,$$

where t represents running week number (through the entire data series), and z_t are iid (independently and identically distributed) Gaussian variables with mean 0 and standard deviation σ. The standard deviation is estimated in the INLA-model and depends on two constants defining a prior distribution as described below. More information about first order random walks is available in the INLA documentation:

```
inla.doc("rw1")
```

Setting priors

For the INLA model we set the prior for the precision $\tau = 1/\sigma^2$ of the random walk in the recommended 'standard' way, by using a 'penalized complexity prior' (PC prior) (Simpson et al. 2017; Gómez-Rubio 2020). More information about PC priors is available in the INLA documentation:

```
inla.doc("pc.prec")
```

The PC prior is defined by two constants σ_0 and α, defining the prior by the probability $P(\sigma > \sigma_0) = \alpha$. The prior is defined in R as follows:

```
hyper.rw1 = list(theta1=list(prior="pc.prec", param=c(0.3, 0.5)))
```

The value of σ_0 is set to 0.3 to limit the variance in z_t for the first order random walk. The value of α is set to 0.5, which makes $\sigma_0 = 0.3$ the median of the probability distribution.

Defining the model in R

The following code defines and fits the basic model without seasonality as described above. The population offset makes the log-linear model equivalent to the log of the expected number of cases per capita, i.e. incidence. The offset function fixes the coefficient of the $\ln N_j$ effect to 1.

```
#Define the linear predictor
formula00 <- cases ~ f(X, model = "rw1", hyper=hyper.rw1) + offset(log(pop))

#Fit the model
fit00 <- inla(formula00, data=dfa, family="poisson",
              control.predictor = list(compute=T, link=1),
              control.compute = list(config=T, dic=T, waic=T))


#Extract predicted cases on absolute scale
dfbasic <- data.frame(expPredictor = exp(fit00$summary.linear.predictor$mean), d
ata = dfa$cases, ids = dfa$X)

Basic <- ggplot(dfbasic) +
  geom_point(aes(x=ids, y=data), size=0.8, color="Gray60") +
  geom_line(aes(x=ids, y=expPredictor),  size=1, color="black") +
  ylab("Weekly Cases") +
  xlab("Year") +
  theme_bw() +
  scale_x_continuous(breaks=seq(1,1590,265), labels=c("1995","2000","2005","201
0","2015", "2020"))+
  theme(legend.position = c(.2, .8), legend.title.align = 0.5, legend.background
= element_rect(color="black", fill="white",linetype = "solid", size=.2, col="gre
y60"))

Basic
```

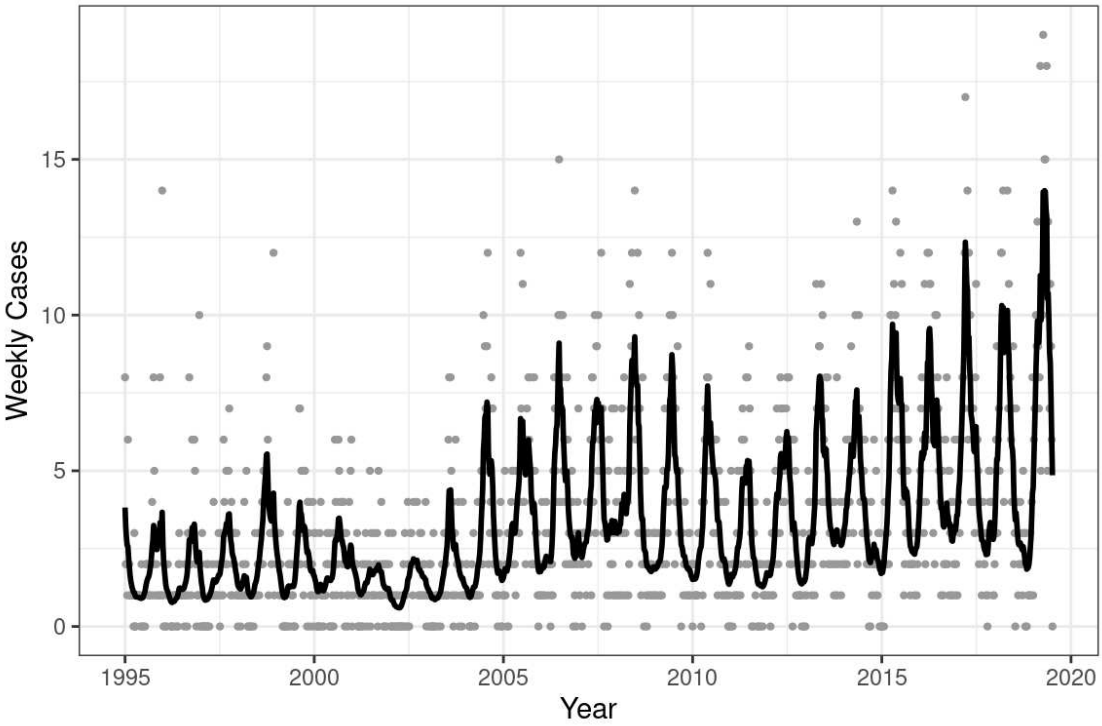

Figure S3: Predicted weekly case numbers from a basic model including only a running week effect and a population offset, fitted to the national data (grey points).

The cyclic fluctuations apparent in Figure S3 above highlight the need for a seasonal model to describe the within-year changes.

3.2 Main model with flexible seasonality

The baseline model was extended to separate the seasonal effect from annual (year-to-year) effect,

$$\log(\lambda_{ij}) = \beta_0 + W_{ij} + Y_j + \ln(N_j),$$

where Y_j is the year effect modeled with a first order random walk (with priors as described above). The seasonal effect W_{ij} was modeled using sine and cosine functions:

$$W_{ij} = \beta_{ij} \sin\left(\frac{2\pi i}{52}\right) + \gamma_{ij} \cos\left(\frac{2\pi i}{52}\right).$$

This expression is a “weighted random effect”, whereβ_{ij} and γ_{ij} are random effects fluctuating over time, and modeled as first order random walks with priors as defined above.

The terms $\sin\left(\frac{2\pi i}{52}\right)$ and $\cos\left(\frac{2\pi i}{52}\right)$ are constant vectors that were added to the dataframe as follows (the factor $\frac{2\pi}{52}$ defines the annual periodicity in weeks):

```
dfa$cos_i=cos( 2*pi / 52*dfa$X)
dfa$sin_i=sin( 2*pi / 52*dfa$X)
```

Phase shift defining peak week

Using trigonometric identities, the above definition of W_{ij} can be rewritten as

$$W_{ij} = A_{ij} \sin\left(\frac{2\pi i}{52} + p_{ij}\right),$$

defining a sine wave with amplitude A_{ij} (where $A_{ij}^2 = \beta_{ij}^2 + \gamma_{ij}^2$), period $\frac{2\pi}{52}$, and a phase shift p_{ij} defined by $\tan(p_{ij}) = \frac{\beta_{ij}}{\gamma_{ij}}$. This phase shift determines the peak week of annual cases in the model.

Accounting for overdispersion

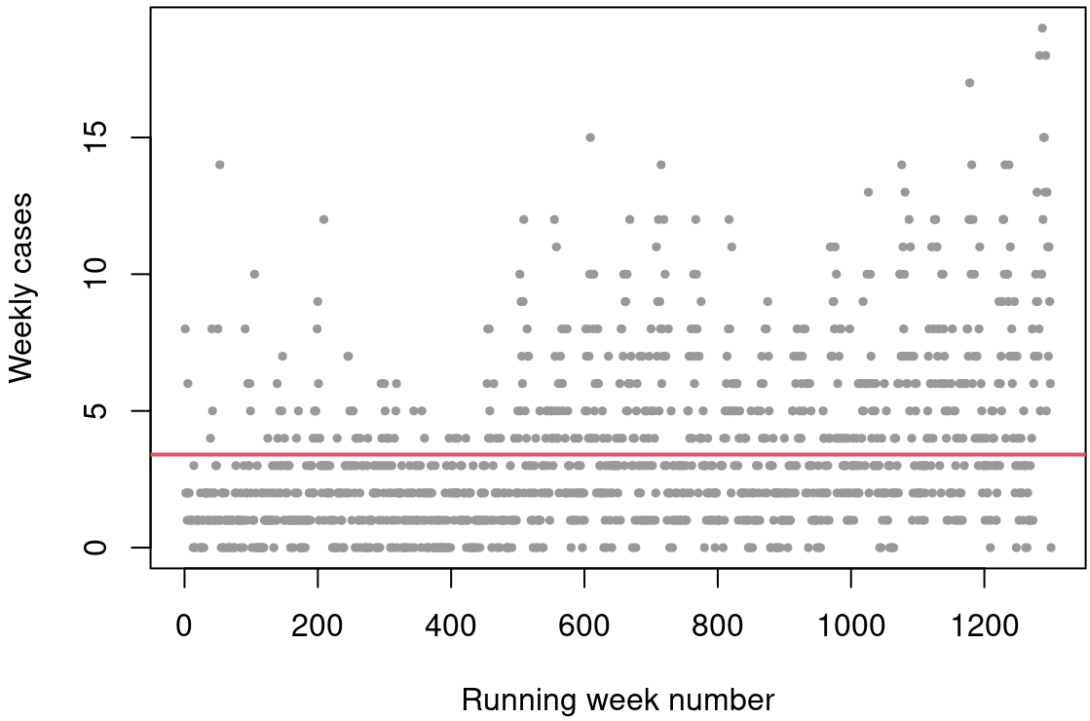

Figure S4: Plot of the cases per week in the national dataset. The mean weekly case number shown as red line.

Preliminary exploration of the case data (fig. S3) indicated that the variance of weekly case numbers will often be higher than the mean, and we therefore added a random effect ε_{ij} to account for overdispersion,

$$\log(\lambda_{ij}) = \beta_0 + W_{ij} + \ln(N_j) + \varepsilon_{ij}.$$

The random effect ε_{ij} was modeled as an iid random variable with the following priors (same as for the random walks defining the year effect Y_j, and the effects β_{ij} and γ_{ij}):

```
hyper.iid = list(theta1=list(prior="pc.prec", param=c(0.3, 0.5)))
```

On the absolute scale, the overdispersion is the exponential of the Gaussian residual, which is multiplied to the rest of the model, i.e.

$$\lambda_{ij} = e^{\text{effects}+\varepsilon_{ij}} = e^{\text{effects}} e^{\varepsilon_{ij}}.$$

When the overdispersion for an observation is small, this means that ϵ_{ij} is small. We ran the model with and without this overdispersion parameter included, and found that the model with overdispersion outperformed the model without overdispersion (based on DIC).

To create the random effects for β_{ij}, γ_{ij}, and ε_{ij} in INLA, there has to be a separate time column in the dataframe for each random effect used. Therefore, duplicate time columns representing running week number were added to the dataframe and named “t” and “t2” for the two seasonal components, and “iid” for the overdispersion component ε_{ij}:

```
dfa$t = dfa$X
dfa$t2 = dfa$X
dfa$iid = dfa$X
```

3.3 Alternative models with fixed seasonality

To investigate whether case seasonality changes over the study period we compared the main model with flexible seasonality (denoted ‘MAIN’ in the code) to two alternative models with fixed seasonality. The first alternative model with fixed seasonality assumes that the parameters β_{ij} and γ_{ij} defining the sinusoidal seasonal effect W_{ij} are constant for each week and not varying between years ($\beta_{ij} = \beta_i$ and $\gamma_{ij} = \gamma_i$). This model is denoted with ‘CSFIX’ in the code below, and yielded a poor fit to the data. For this reason we also constructed an alternative model for fixed seasonality which has more flexibility in the intra-annual trend than the sinusoidal function, using a second order random walk to fit a seasonality curve. The covariate for this expression is simply week number, because the value should be the same each year at the corresponding week number. To smooth this curve between years we specify that the curve should be cyclic. This second alternative model is denoted “RWFIX” in the code below. More information about second order cyclic random walks is available in the INLA documentation:

```
inla.doc("rw2")
```

Define and fit the models in R

The following code specifies the model forms and then uses INLA to fit the main model (flexible seasonality) and the two alternative models with fixed seasonality to the data. The models are first fitted to the national data, and then the main model is also fitted to the data sets from the regions South, West and East independently, in order to compare results between regions.

Specify the form of each model:

```
#Main model with flexible seasonal effect
formMAIN = cases ~ f(year, model = "rw1", hyper=hyper.rw1) +
  f(t, cos_i, model="rw1", constr=F, hyper=hyper.rw1) +
  f(t2, sin_i, model="rw1", constr=F, hyper=hyper.rw1) +
  f(iid, model="iid", hyper=hyper.iid) + offset(log(pop))

#Alternative model #1 with fixed seasonal effect (sine-cosine)
formCSFIX = cases ~ f(year, model = "rw1", hyper=hyper.rw1) +
  cos_i + sin_i +
  f(iid, model="iid", hyper=hyper.iid) + offset(log(pop))

#Alternative model #2 with fixed seasonal effect (cyclic random walk)
formRWFIX = cases ~ f(year, model = "rw1", hyper=hyper.rw1) +
  f(week, model="rw2", constr=T, scale.model=T, cyclic=T) +
  f(iid, model="iid", hyper=hyper.iid) + offset(log(pop))

#Main model for the region South only
formSOUTH = casesSouth ~ f(year, model = "rw1", hyper=hyper.rw1) +
  f(t, cos_i, model="rw1", constr=F, hyper=hyper.rw1) +
  f(t2, sin_i, model="rw1", constr=F, hyper=hyper.rw1) +
  f(iid, model="iid", hyper=hyper.iid) + offset(log(popSouth))

#Main model for the region West only
formWEST = casesWest ~ f(year, model = "rw1", hyper=hyper.rw1) +
  f(t, cos_i, model="rw1", constr=F, hyper=hyper.rw1) +
  f(t2, sin_i, model="rw1", constr=F, hyper=hyper.rw1) +
  f(iid, model="iid", hyper=hyper.iid) + offset(log(popWest))

#Main model for the region East only
formEAST = casesEast ~ f(year, model = "rw1", hyper=hyper.rw1) +
  f(t, cos_i, model="rw1", constr=F, hyper=hyper.rw1) +
  f(t2, sin_i, model="rw1", constr=F, hyper=hyper.rw1) +
  f(iid, model="iid", hyper=hyper.iid) + offset(log(popEast))
```

Fit each model with INLA:

```
fitMAIN = inla(formMAIN, data=dfa, family="poisson", control.predictor = list(co
mpute=T, link=1), control.compute = list(config=T,dic=T,waic=T))

fitCSFIX = inla(formCSFIX, data=dfa, family="poisson", control.predictor = list
(compute=T, link=1), control.compute = list(config=T,dic=T,waic=T))

fitRWFIX = inla(formRWFIX, data=dfa, family="poisson", control.predictor = list
(compute=T, link=1), control.compute = list(config=T,dic=T,waic=T))

fitSOUTH = inla(formSOUTH, data=dfa, family="poisson", control.predictor = list
(compute=T, link=1), control.compute = list(config=T,dic=T,waic=T))

fitWEST = inla(formWEST, data=dfa, family="poisson", control.predictor = list(co
mpute=T, link=1), control.compute = list(config=T,dic=T,waic=T))

fitEAST = inla(formEAST, data=dfa, family="poisson", control.predictor = list(co
mpute=T, link=1), control.compute = list(config=T,dic=T,waic=T))
```

4. Model outputs

In this section we go through the various outputs from the models fitted in the previous section.

4.1 Model predictions

The following code extracts the following components and predictions using different components:

- The weekly mean predictor on absolute scale ($E[\lambda_{ij}]$)
- the mean of the two components of the seasonal effect
- the intercept including population offset
- the predicted weekly case numbers using only the seasonal effect
- the predicted weekly case numbers using only the year effect

These are stored in a data frame along with the case data points and time series.

Main model

```
mfDFYR <- data.frame(expPredictor = exp(fitMAIN$summary.linear.predictor$mean -
fitMAIN$summary.random$iid$mean),
                     cyc2 = fitMAIN$summary.random$t$mean * dfa$cos_i,
                     cyc3 = fitMAIN$summary.random$t2$mean * dfa$sin_i,
                     inter = fitMAIN$summary.fixed$mean[1] + log(dfa$pop),
                     data = dfa$cases,
                     ids = dfa$X)
mfDFYR$seasonal <- exp(mfDFYR$cyc2+mfDFYR$cyc3+mfDFYR$inter)
mfDFYR$LT <- exp(rep(fitMAIN$summary.random$year$mean, each=52) + mfDFYR$inter)
idlt <- seq(from=26,to=1324,by=52)
mfDFYR$idlt <- seq(from=26,to=1324,by=52)
```

The following code plots the model predictions using different components of the main national model (other component estimates set to zero), plotted with the data on weekly cases of Lyme disease over the study period.

```
pMFyr <- ggplot(mfDFYR) +
  geom_point(aes(x=ids, y=data), size=0.8, color="grey60") +
  geom_line(aes(x=ids, y=expPredictor, color="Full model"),  size=1) +
  geom_line(aes(x=ids, y=seasonal, color="Season"), size=1) +
  geom_line(aes(x=idlt, y=LT[idlt], color="Year"), size=1) +
  xlab("Year") +
  ylab("Weekly Cases") +
  scale_color_manual(values=c("#3cb371","#ee82ee", 1))+
  theme_bw() +
  scale_x_continuous(breaks=seq(1,1590,265), labels=c("1995","2000","2005","201
0","2015", "2020"))+
  theme(legend.position = c(.2, .85), legend.title=element_blank(), legend.backg
round = element_rect(color="black", fill="white",linetype = "solid", size=.2, co
l="grey60"))

pMFyr
```

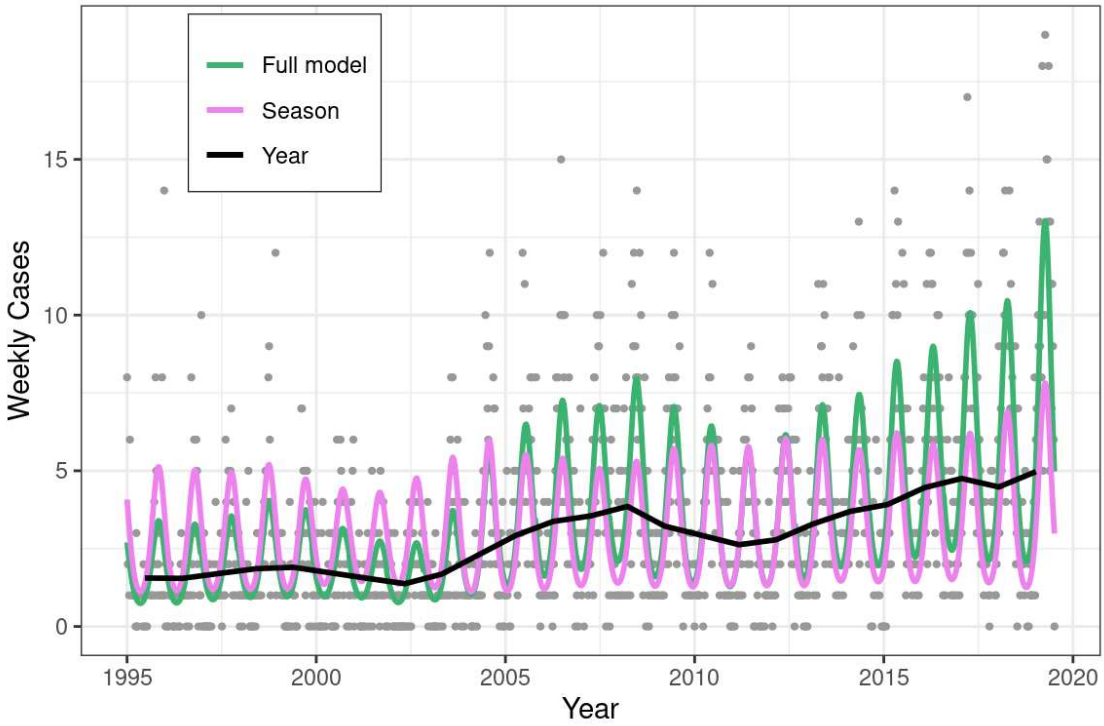

Figure S5: Same as Figure 2 from the main text. Predicted weekly cases over the study period, using the full national model (green), the seasonal component (magenta), or the year component (black). Case data are shown as grey points.

We can also make a zoomed in version of Figure 2, to see better how the main model fits the data each year. The green prediction curve goes through the center of the datapoints.

```
pMFyr + coord_cartesian(xlim = c(dfa[dfa$yrwk==201401,]$X, dfa[dfa$yrwk==20175
2,]$X)) +
  scale_x_continuous(breaks=seq(dfa[dfa$yrwk==201401,]$X, dfa[dfa$yrwk==20175
2,]$X+52,52), labels=c("2014","2015","2016","2017","2018"))
```

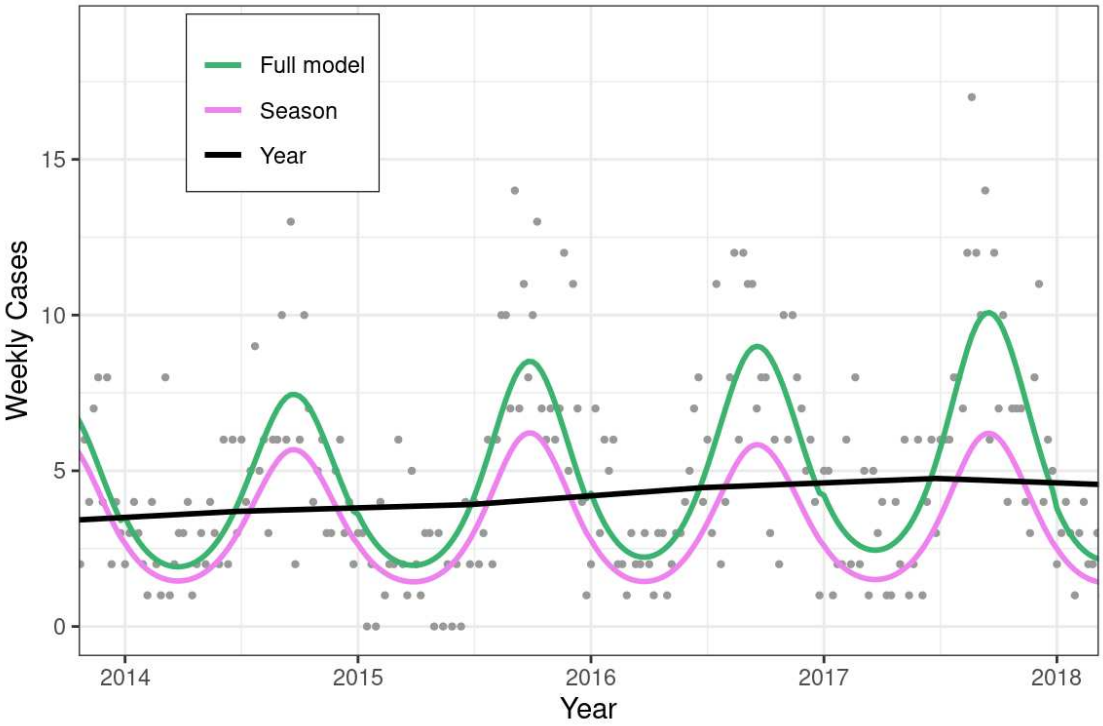

Figure S6: Same as Figure 2 above, but zoomed in on the years 2014-2018. Predicted weekly cases over the study period using the full national model (green), only the seasonal component (magenta), or only the year component (black). Case data are shown as grey points.

Alternative model 2

```
interFIX = fitRWFIX$summary.fixed$mean[1] + log(dfa$pop)
mfDFYRix <- data.frame(expPredictor=exp(fitRWFIX$summary.linear.predictor$mean -
fitRWFIX$summary.random$iid$mean),
                       data = dfa$cases,
                       ids = dfa$X,
                       LT= exp(rep(fitRWFIX$summary.random$year$mean, each=52) + i
nterFIX),
                       seasonal = exp(fitRWFIX$summary.random$week$mean[dfa$week]
+ interFIX))
mfDFYRix$idlt <- seq(from=26,to=1324,by=52)
```

Here we show the difference between the main model with a flexible seasonal trend and the second alternative model (rw2 cyclic) with fixed seasonality across years (compare the magenta part of the figures).

```
pMFix <- ggplot(mfDFYRix) +
  geom_point(aes(x=ids, y=data), size=0.8,color="grey60") +
  geom_line(aes(x=ids, y=expPredictor, color="Full model"),  size=1) +
  geom_line(aes(x=ids, y=seasonal, color="Season"), size=1) +
  geom_line(aes(x=idlt, y=LT[idlt], color="Year"), size=1) +
  xlab("Year") +
  ylab("Weekly Cases") +
  scale_color_manual(values=c("#3cb371","#ee82ee", 1)) +
  theme_bw() +
  scale_x_continuous(breaks=seq(1,1590,265), labels=c("1995","2000","2005","201
0","2015", "2020")) +
  theme(legend.position = c(.2, .8), legend.title=element_blank(), legend.backgr
ound = element_rect(color="black", fill="white",linetype = "solid", size=.2, col
="grey60"))
plot(pMFix)
```

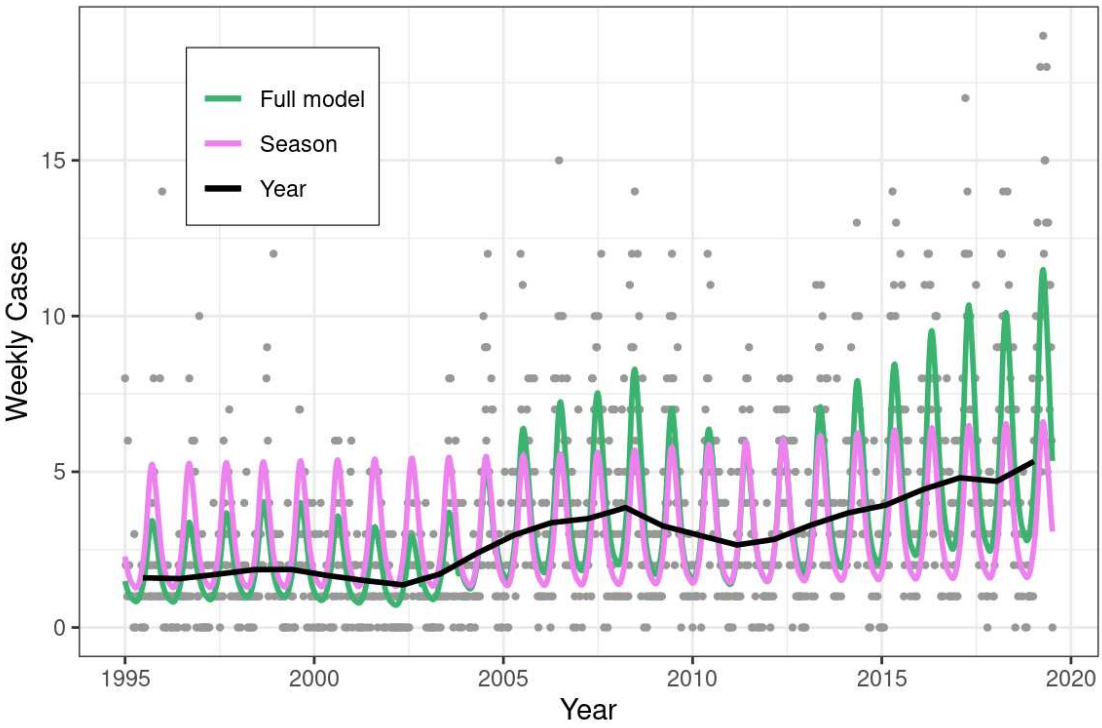

Figure S7: Predicted weekly cases over the study period based on the second alternative model with fixed seasonal effects, using the full model (green), only the seasonal component (magenta), or only the year component (black). Case data are shown as grey points.

4.2 Long-term trends

```
LTdfMAIN <- data.frame(year = unique(dfa$year),
                   region = "National",
                   meanyear = exp(fitMAIN$summary.random$year$mean),
                   upper = exp(fitMAIN$summary.random$year$`0.975quant`),
                   lower = exp(fitMAIN$summary.random$year$`0.025quant`)
                   )

LTdfSOUTH <- data.frame(year = unique(dfa$year),
                   region = "South",
                   meanyear = exp(fitSOUTH$summary.random$year$mean),
                   upper = exp(fitSOUTH$summary.random$year$`0.975quant`),
                   lower = exp(fitSOUTH$summary.random$year$`0.025quant`)
                   )
LTdfWEST <- data.frame(year = unique(dfa$year),
                   region = "West",
                   meanyear = exp(fitWEST$summary.random$year$mean),
                   upper = exp(fitWEST$summary.random$year$`0.975quant`),
                   lower = exp(fitWEST$summary.random$year$`0.025quant`)
                   )

LTdfEAST <- data.frame(year = unique(dfa$year),
                   region = "East",
                   meanyear = exp(fitEAST$summary.random$year$mean),
                   upper = exp(fitEAST$summary.random$year$`0.975quant`),
                   lower = exp(fitEAST$summary.random$year$`0.025quant`)
                   )

LTdf <- rbind(LTdfMAIN, LTdfSOUTH, LTdfWEST, LTdfEAST)

cols <- c("#000000", "#56B4E9","#E69F00", "#9b67a1")
names(cols) <- c("National", "South", "West", "East")

TrendPlot1 = ggplot(LTdf) +
  geom_line(aes(x=year,y=meanyear, color=region),size=1) +
  geom_ribbon(aes(x=year,ymax=upper, ymin=lower, fill=region), alpha= 0.2)+
  ylab("Relative Intensity of Weekly Cases") +
  xlab("Year") +
  scale_colour_manual(values=cols) +
  scale_fill_manual(values=cols)+
  theme_bw() +
  scale_x_continuous(limits=c(1995,2020), breaks=seq(1995,2020,5), labels=seq(19
95,2020,5)) +
  theme(plot.title= element_text(hjust = 0.5),
        legend.position = c(.25, .8),
        legend.title=element_blank(),
        legend.background = element_rect(color="black", fill="white",linetype =
"solid", size=.2, col="grey60")
        ) +
  labs(color="Region",fill="Region")
```

```
TrendPlot1
```

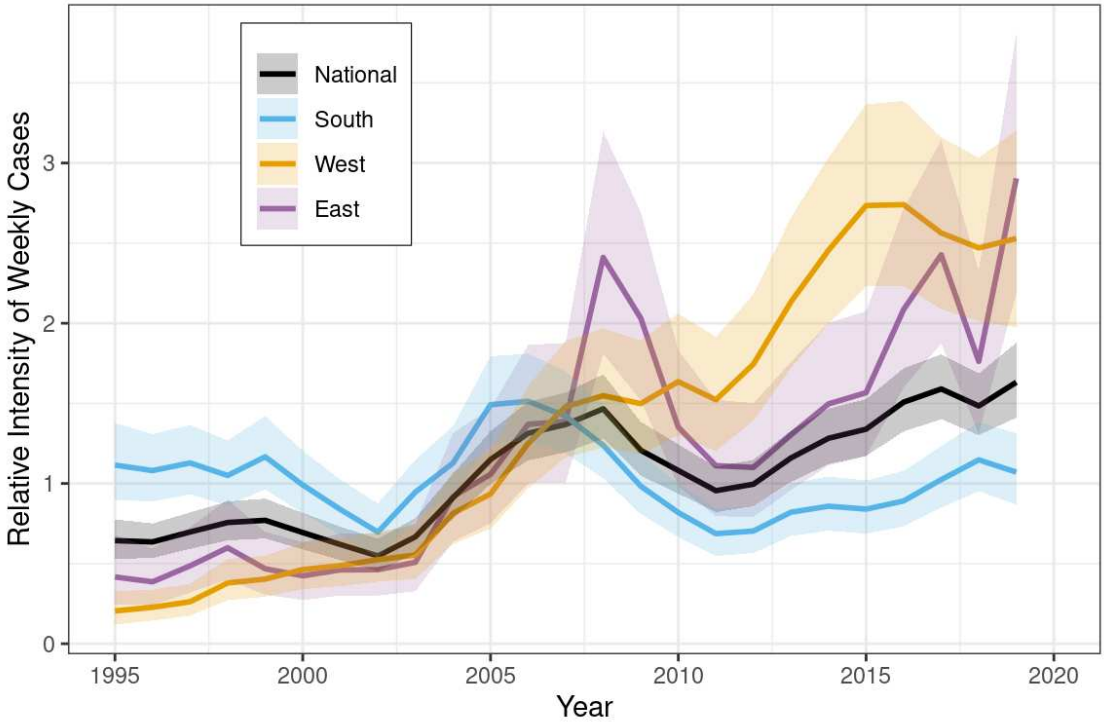

Figure S8: The long term trend component from the main national model and the models fitted to the regions South, West and East independently, illustrating the relative change in cases per week over years when the seasonal component is set to zero. Because the intercept and population offset are also not included, the trends estimated for different regions are not comparable to each other on an absolute scale.

The code below generates a figure similar to Figure S8 above, but the inclusion of the intercept makes it an absolute measure of case intensity rather than relative, so that the predictions for each region can be compared quantitatively. Per capita estimates are adjusted to a per 100,000 adults scale.

```
interMain = fitMAIN$summary.fixed$mean[1] + log(100000)
interSouth = fitSOUTH$summary.fixed$mean[1] + log(100000)
interWEST = fitWEST$summary.fixed$mean[1] + log(100000)
interEAST = fitEAST$summary.fixed$mean[1] + log(100000)

# remake the dataframe adding the intercept
LTdf2MAIN <- data.frame(year = unique(dfa$year),
                        region="National",
                        pred = exp(fitMAIN$summary.random$year$mean + interMai
n),
                        upper = exp(fitMAIN$summary.random$year$`0.975quant` + i
nterMain),
                        lower = exp(fitMAIN$summary.random$year$`0.025quant` + i
nterMain))

LTdf2SOUTH <- data.frame(year = unique(dfa$year),
                         region="South",
                         pred = exp(fitSOUTH$summary.random$year$mean + interSou
th),
                         upper = exp(fitSOUTH$summary.random$year$`0.975quant` +
interSouth),
                         lower = exp(fitSOUTH$summary.random$year$`0.025quant` +
interSouth))

LTdf2WEST <- data.frame(year = unique(dfa$year),
                        region="West",
                        pred = exp(fitWEST$summary.random$year$mean + interWES
T),
                        upper = exp(fitWEST$summary.random$year$`0.975quant` + i
nterWEST),
                        lower = exp(fitWEST$summary.random$year$`0.025quant` + i
nterWEST))

LTdf2EAST <- data.frame(year = unique(dfa$year),
                        region="East",
                        pred = exp(fitEAST$summary.random$year$mean + interEAS
T),
                        upper = exp(fitEAST$summary.random$year$`0.975quant` + i
nterEAST),
                        lower = exp(fitEAST$summary.random$year$`0.025quant` + i
nterEAST))

LTdf2 <- rbind(LTdf2MAIN, LTdf2SOUTH, LTdf2WEST, LTdf2EAST)

TrendPlot2 <- ggplot(LTdf2) +
  geom_ribbon(aes(x=year,ymax=upper, ymin=lower, fill=region),  alpha= 0.2) +
  geom_line(aes(x=year,y=pred, color=region),size=1) +
  ylab("Weekly Incidence (Cases per 100,000)") +
  xlab("Year") +
  theme_bw() +
  theme(legend.position = c(.7, .8), legend.title=element_blank(),
```

```
        legend.background = element_rect(color="black", fill="white",linetype =
"solid", size=.2, col="grey60")
  )+
  labs(color="Region",fill="Region") +
  scale_colour_manual(values=cols)+
  scale_fill_manual(values=cols)

TrendPlot2
```

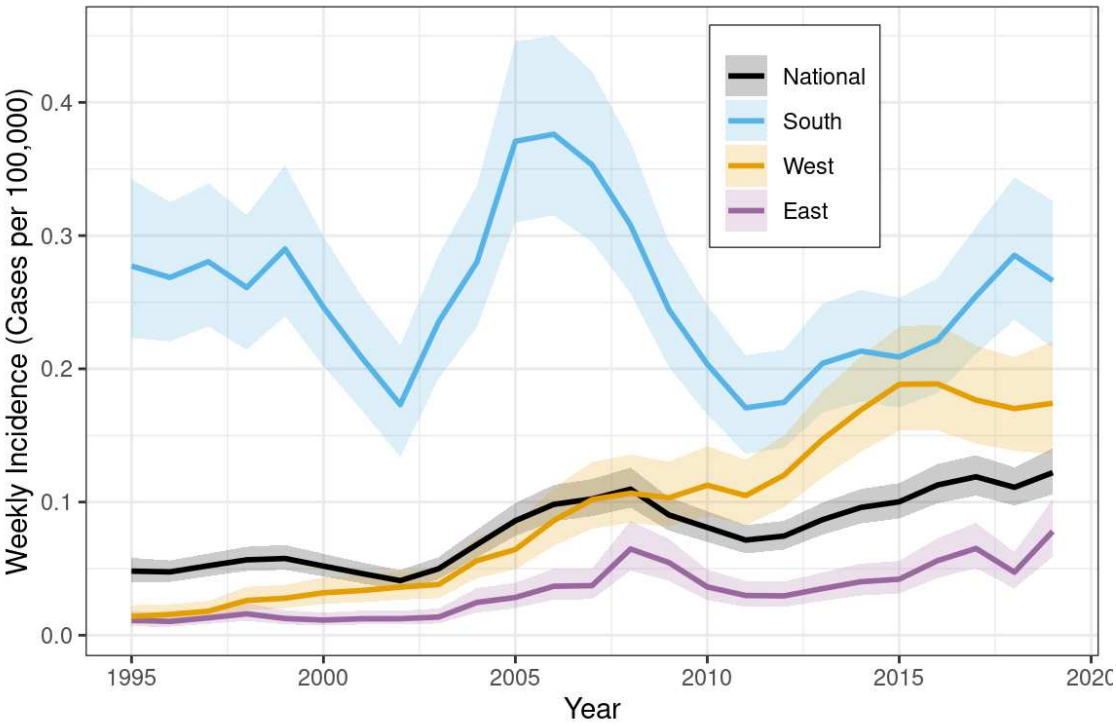

Figure S9: Predicted weekly cases per 100,000 adults from the main model and the regional models with the seasonal effect estimates set to zero. This figure captures the same long-term trends as in Figure S8 above, but on a different scale, highlighting the higher incidence in the region South compared to the other regions.

4.3 Extract peaks

The goal of the analysis was to evaluate whether and how seasonality has changed over the study period. To accomplish this, we extracted the seasonal peak, i.e. the week in which the seasonality component is at a maximum, from the model each year. Because the seasonal component is modeled with a periodic sine function, there is only one peak each year, and it uniquely describes the year's seasonality. This means any shift in the peak also applies to the onset of the season, or any other point of interest on the fitted sinusoidal curve.

The R function below extracts the annual peaks from the fitted models with flexible seasonality (i.e. the main model and regional models) by repeated sampling from the posterior distribution. We generated $n = 1000$ samples to ensure the peak extracted from each year is representative and that we can estimate a credible interval for the peak. INLA has built-in functionality for sampling from the posterior distribution.

```
#sampling n=1000 samples from the posterior distribution of model 'myfit'

peak_sampling_function <- function(myfit, nsample=1000) {

  samples = inla.posterior.sample(n=nsample, result = myfit)

  contents = myfit$misc$configs$contents
  tid = "t"
  t2id = "t2"
  predid = "Predictor"

  id1 = which(contents$tag==tid)
  id2 = which(contents$tag==t2id)
  idP = which(contents$tag==predid)

  ix1 = contents$start[id1]-1 + (1:contents$length[id1])
  ix2 = contents$start[id2]-1 + (1:contents$length[id2])
  ixP = contents$start[idP]-1 + (1:contents$length[idP])

  samt = lapply(samples, function(x) x$latent[ix1])
  samt2 = lapply(samples, function(x) x$latent[ix2])
  samP = lapply(samples, function(x) x$latent[ixP])

  iidid = "iid"
  idI = which(contents$tag==iidid)
  ixI = contents$start[idI]-1 + (1:contents$length[idI])
  samI = lapply(samples, function(x) x$latent[ixI])

  maxpeakw<-array(NA,dim=c(1000,length(Y)))
  maxpeakw=data.frame(maxpeakw)
  names(maxpeakw)<-Y

  #get the peaks from just the cyclic part of the model
  for(i in 1:1000){
    cyc2 = samt[[i]] * dfa$cos_i
    cyc3 = samt2[[i]]* dfa$sin_i
    cyc_sc = cyc2+cyc3
    for (j in 1:length(Y)){
      yy<-Y[j]
      wX<-which(dfa$year==yy)
      subcyc<- cyc_sc[dfa$t2 %in% wX]
      #takes the maximum week after week 12
      maxpeakw[i,j]<-wnr[subcyc==max(subcyc[-c(1:12)])]
    }
  }

  #make a data frame with summary stats for the peak week each year as output
  gdf <- data.frame(Year= Y, mean = round(apply(maxpeakw,2,mean),1), med= apply
(maxpeakw,2,median),
                        sd = round(apply(maxpeakw,2,sd),2), upper=round(apply(ma
xpeakw,2,quantile,prob=c(0.975)),1),
```

```
                        lower=round(apply(maxpeakw,2,quantile,prob=c(0.025)),1))

  return(gdf)
}
```

Apply the sampling function

This function is applied to extract the peaks for the national model, and the regional (South, West, and East fit independently) models:

```
peaksMAIN <- peak_sampling_function(fitMAIN, nsample=1000)
peaksMAIN$Region <- "National"
peaksSOUTH <- peak_sampling_function(fitSOUTH, nsample=1000)
peaksSOUTH$Region <- "South"
peaksWEST <- peak_sampling_function(fitWEST, nsample=1000)
peaksWEST$Region <- "West"
peaksEAST <- peak_sampling_function(fitEAST, nsample=1000)
peaksEAST$Region <- "East"

#Store all the sampled peaks in a dataframe for plotting:
plotDF <- rbind(peaksMAIN, peaksSOUTH, peaksWEST, peaksEAST)
```

Selecting a spline

We used AIC to compare different splines fitted to the sampled peaks (for visualization). The spline with $df = 4$ had the lowest AIC and was used for plotting.

```
fit1 <- lm(mean~Year, dat=plotDF)
fits <- lm(mean~splines::bs(Year,df=4), dat=plotDF)
fits3 <- lm(mean~splines::bs(Year,df=3), dat=plotDF)
AIC(fit1, fits3, fits)
```

```
##       df      AIC
## fit1   3 337.7273
## fits3  5 301.1475
## fits   6 289.0575
```

Plot the peaks

The following code plots the peaks from the main model and the models fitted to other regions, along with 95% credible intervals and the selected spline.

```
pPOT = ggplot(plotDF) +
  geom_linerange(aes(x=Year, y=mean, ymin=lower, ymax=upper), color=1, data=peak
sMAIN)+
  geom_point(aes(x=Year, y=mean, col=Region), size=2)+
  geom_point(aes(x=Year, y=mean), color=1, data=peaksMAIN)+
  stat_smooth(aes(x=Year, y=mean),data=peaksMAIN,  fill=1, col=1, alpha=.2, meth
od = "lm", formula=y~splines::bs(x,df=4), se=TRUE, size=1, show.legend = FALSE)
+
  scale_x_continuous(limits=c(1995,2020),breaks=seq(1995,2020,5), labels=seq(199
5,2020,5)) +
  theme_bw() +
  scale_colour_manual(values=cols)+
  scale_fill_manual(values=cols)+
  ylab("Peak Week") +
  scale_y_continuous(limits=c(30,52), breaks=seq(30,52,2)) +
  theme(plot.title= element_text(hjust = 0.5),
        legend.position = c(.85, .78),
        legend.title = element_blank(),
        legend.background = element_rect(color="black", fill="white",linetype =
"solid", size=.2, col="grey60")
        )


pPOT
```

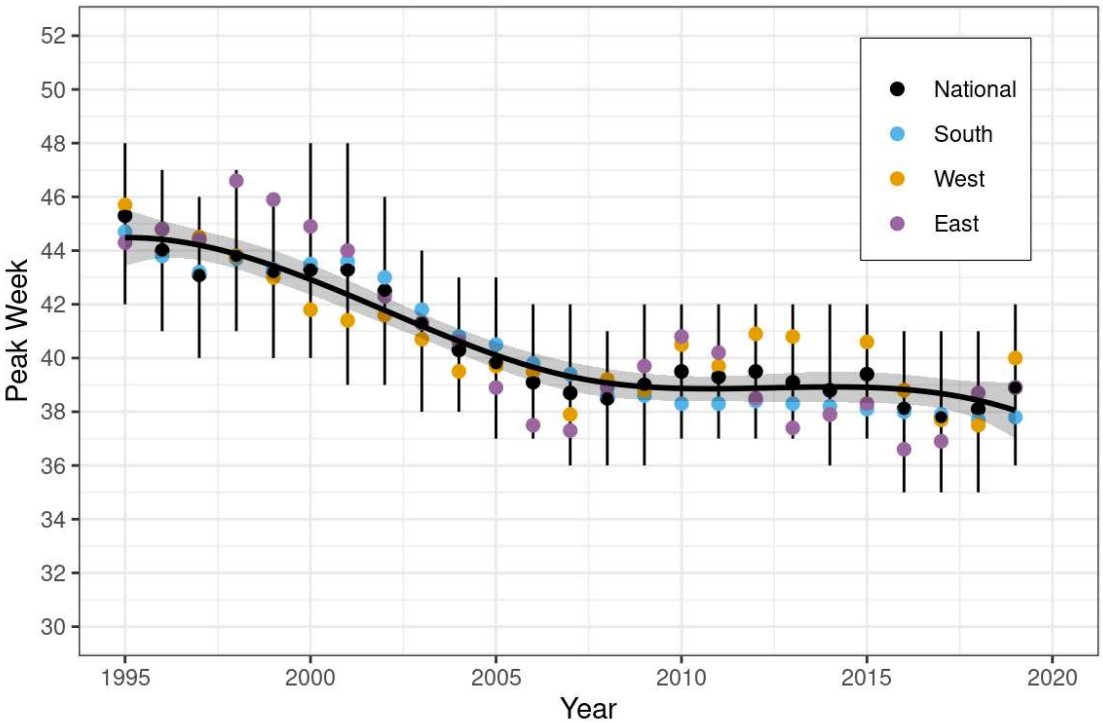

Figure S10: Extracted peaks from the models fitted to different regions. The 95% credible intervals and fitted spline represent the national model. Note that the estimated peaks from the South, West and East regions are all within the error bars for the national model peaks.

The code below generates a figure showing that the different regions have a similar overall pattern in the peaks as the spline visualized in Figure S10 above.

```
#Comparison of Splines between Regions

pPOT2 = ggplot(plotDF) +
  geom_linerange(aes(x=Year, y=mean, ymin=lower, ymax=upper), color="grey60", da
ta=peaksMAIN) +
  stat_smooth(aes(x=Year, y=mean, color=Region, fill=Region), alpha=0.2,method =
"lm", formula=y~splines::bs(x,df=4), se=TRUE, size=1) +
  ylab("Peak Week") +
  scale_x_continuous(breaks=seq(1995,2020,5), labels=seq(1995,2020,5)) +
  scale_y_continuous(limits=c(30,52), breaks=seq(30,52,2)) +
  theme_bw() +
  labs(color="Region", fill="Region") +
   scale_colour_manual(values=cols) +
  scale_fill_manual(values=cols)+
  theme(plot.title= element_text(hjust = 0.5),
        legend.position = c(.85, .78),
        legend.title = element_blank(),
        legend.background = element_rect(color="black", fill="white",linetype =
"solid", size=.2, col="grey60")
        )

pPOT2
```

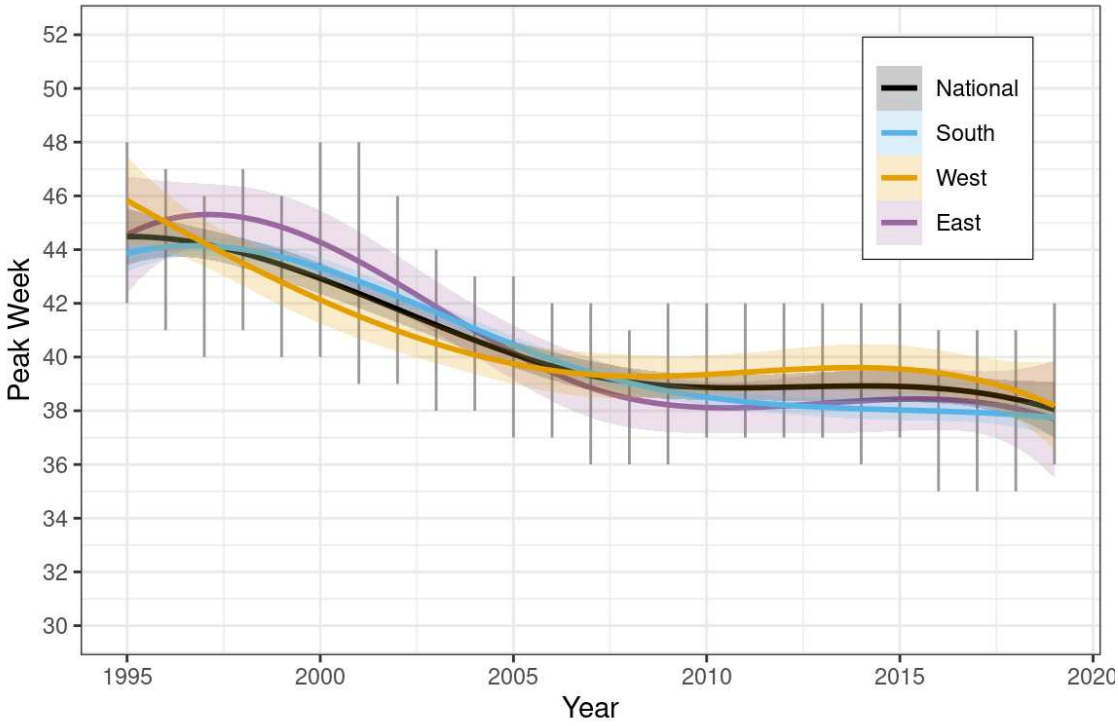

Figure S11: Comparison of the splines fit to regional peaks with the national spline from above. The error bars represent the error on the national peak week number, as in the figure above.

Below we take a closer look at the trend in peaks of the region East. The region East has quite few cases per year in the early part of the study period, yielding larger error bars (95% credible intervals) on the peak week than the national, South, and West models. The figure below compares the error regions for the East and national models to help interpret the trends above. The slightly earlier peaks at the start of the study period for the region East are within the time frame where peak estimation is most uncertain because of low case numbers.

```
plotDF2 <- rbind(peaksEAST, peaksMAIN)

pPOT3cols <- c("#9b67a1", "black")
names(pPOT3cols) <- c("East", "National")

pPOT3 <- ggplot(plotDF2) +
  geom_linerange(aes(x=Year, y=mean, ymin=lower, ymax=upper, color=Region), size
=1, data=peaksEAST)+
  geom_linerange(aes(x=Year+0.2, y=mean, ymin=lower, ymax=upper, color=Region),
size=1, data=peaksMAIN)+
  geom_point(aes(x=Year, y=mean, col=Region), size=2, data=peaksEAST)+
  geom_point(aes(x=Year+0.2, y=mean, col=Region), size=2, data=peaksMAIN)+
  scale_x_continuous(limits=c(1995,2020),breaks=seq(1995,2020,5), labels=seq(199
5,2020,5)) +
  theme_bw() +
  scale_colour_manual(values=pPOT3cols)+
  scale_fill_manual(values=pPOT3cols)+
  ylab("Peak Week") +
  scale_y_continuous(limits=c(27,52), breaks=seq(26,52,2)) +
  theme(plot.title= element_text(hjust = 0.5),
        legend.position = c(.87, .84),
        legend.title = element_blank(),
        legend.background = element_rect(color="black", fill="white",linetype =
"solid", size=.2, col="grey60"))

pPOT3
```

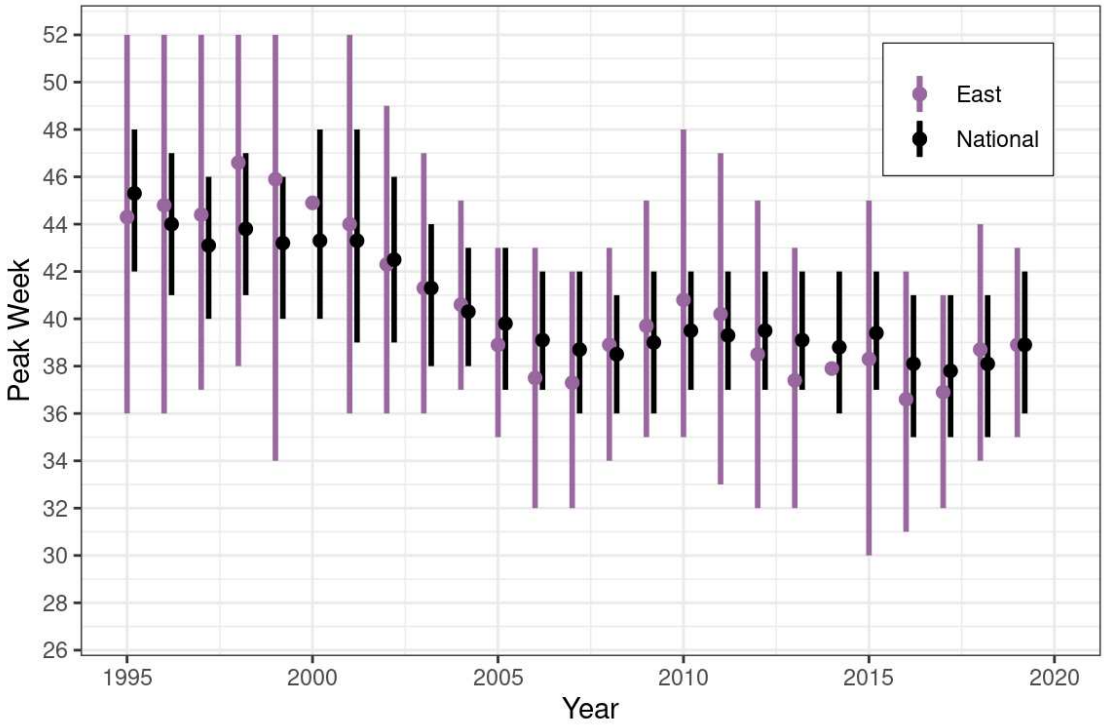

Figure S12: Comparison between 95% credible intervals on extracted peaks from the model fitted to the region East and the national model. The buffering on the x-axis between the series is a visualization aid only and does not represent any difference in the sampling.

4.4 Random effects properties

Table of medians and credible intervals for the standard deviations of the random effects in the main model:

```
table1 <- data.frame(
  Component = c("Year effect", "Seasonal parameter 1", "Seasonal parameter 2", "
Overdispersion parameter"),
  Median= signif(fitMAIN$summary.hyperpar[,4]^-0.5, 2),
  Lower0.025= signif(fitMAIN$summary.hyperpar[,3]^-0.5, 2),
  Upper0.975= signif(fitMAIN$summary.hyperpar[,5]^-0.5, 2)
)
```

Table S1: Point estimates and 95% credible intervals for the standard deviations of the random effects in the model fitted to the national data set.

Component	Median	Lower0.025	Upper0.975
Year effect	0.160	0.240	0.1100
Seasonal parameter 1	0.014	0.032	0.0062
Seasonal parameter 2	0.017	0.035	0.0071
Overdispersion parameter	0.210	0.270	0.1600

Table showing the estimated variance of each main model component, relative to the total variance:

```
seasonal <- mfDFYR$cyc2 + mfDFYR$cyc3 # seasonal effect
denominator <- sd(fitMAIN$summary.linear.predictor$mean - fitMAIN$summary.rando
m$iid$mean) #remove the iid part D

table2 <- data.frame(
  Component = c("Year effect", "Seasonal effect", "Population"),
  Proportional_Variance = c(sd(fitMAIN$summary.random$year$mean) / denominator,
  sd(seasonal) / denominator,
  sd(log(dfa$pop))/ denominator)
)
table2[,2] <- signif(table2[,2],2)

names(table2)<- c("Component", "Variance proportion")
```

Table S2: Estimated variance for each model component, relative to the total model variance.

Component	Variance proportion
Year effect	0.53
Seasonal effect	0.79
Population	0.11

4.5 Residuals

In this section we examine the residuals of the main national model to determine how well it fits the data.

Temporal autocorrelation

We checked for temporal autocorrelation in the residuals and found it to be very low:

```
par(mfrow=c(2,2))
acf(fitMAIN$summary.random$iid$mean, main="National")
acf(fitSOUTH$summary.random$iid$mean, main="South")
acf(fitWEST$summary.random$iid$mean, main="West")
acf(fitEAST$summary.random$iid$mean, main="East")
```

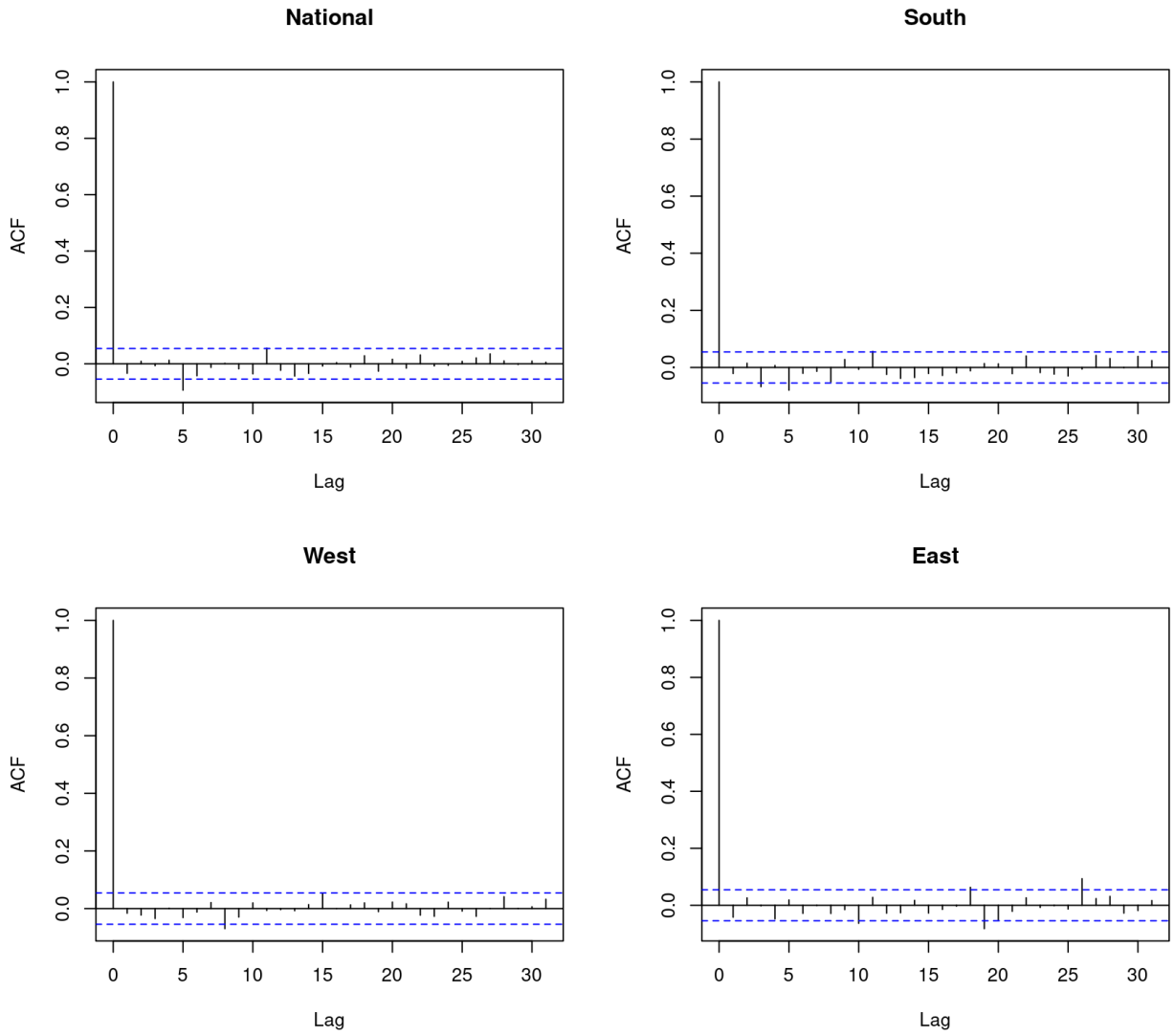

Figure S13: Autocorrelation functions for the residuals from the fitted models with flexible seasonal component, for the different regional data sets.

Residual effects of week number

Below is a graph of residuals from the main national model over the weeks of the year. The model is able to describe in the intra-annual variation well. The residuals are small and do not show a trend within the year.

```
resid0 = fitMAIN$summary.random$iid$mean # Residuals from the over-dispersion co
mponent
fitted = fitMAIN$summary.fitted.values$mean

## Pearson residuals
resid2 = (dfa$cases - fitted) / sqrt(fitted)

## Total residuals
resid1 = resid0 + resid2

## Plot of residuals across week numbers
wkres <- data.frame(week=rep(c(1:52),25))
wkres$resid1 <- resid1
wkres <- wkres %>% group_by(week) %>% summarize(resid1 = quantile(resid1, c(0.2
5, 0.5, 0.75)), q = c("q0.25", "q0.5", "q0.75"), mean=mean(resid1))
wkres <- pivot_wider(wkres, names_from = q, values_from = resid1)

pwkres <- ggplot(wkres) +
  geom_point(aes(x=week, y=q0.5)) +
  geom_ribbon(aes(x=week, ymax=q0.75, ymin=q0.25), alpha=0.2) +
  theme_bw() + xlab("Week Number") + ylab("Residuals")

pwkres
```

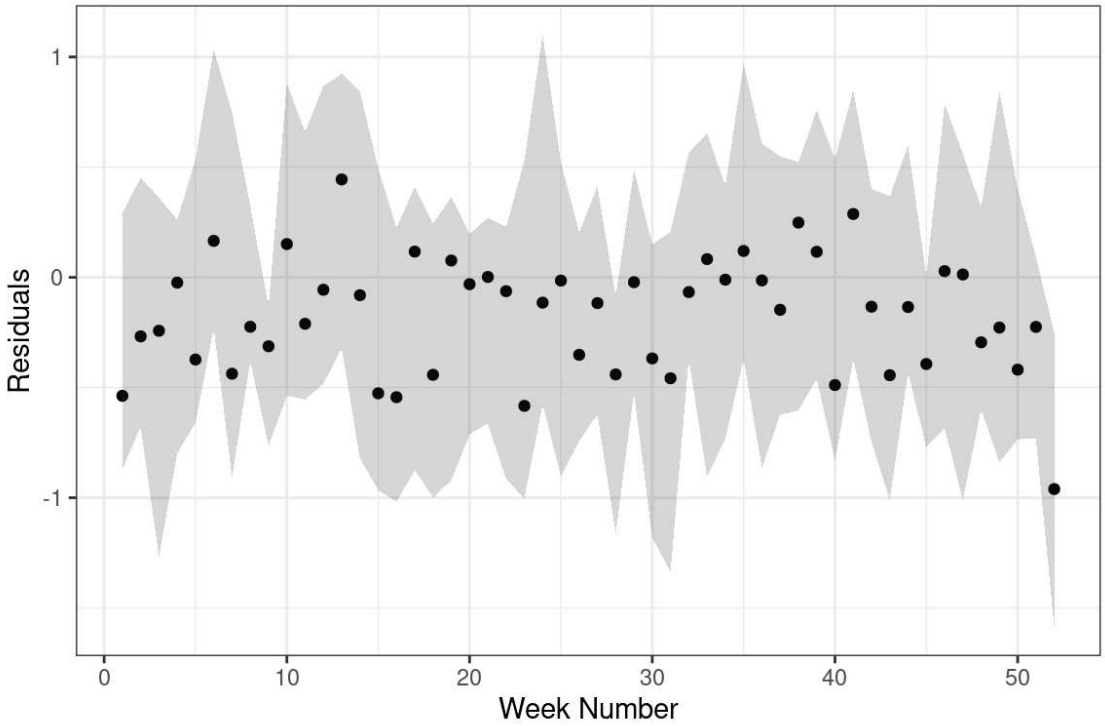

Figure S14: Residuals from the main national model summarized over weeks. The black points represent the median residuals over the study period at a given week number. The shaded area is bounded by the first and third quartiles of the residuals at each week number.

Proportion of cases in the peak season

We defined the duration of the peak season as the 4 week period centered on the peak week. The two weeks on either side of the mean peak is based on the standard deviation from the repeated sampling from the posterior distribution, which is on average 1.5 weeks over the time series, and maximum 2.15 weeks.

```
peaksMAIN$peakStart <- round(peaksMAIN$mean)-2
peaksMAIN$peakEnd <- round(peaksMAIN$mean)+2
summary(peaksMAIN$peakEnd-peaksMAIN$peakStart)
```

```
##    Min. 1st Qu.  Median    Mean 3rd Qu.    Max.
##       4       4       4       4       4       4
```

```
yrsums$NinPeak<-0
for(i in Y){
  start <- peaksMAIN[peaksMAIN$Year==i,]$peakStart
  end <- peaksMAIN[peaksMAIN$Year==i,]$peakEnd
  a<- dfa[dfa$year==i,]
  a<- a[a$week >= start & a$week <= end,]
  yrsums[yrsums$year==i,]$NinPeak <- sum(a$cases)
}

summary(yrsums$NinPeak/yrsums$n*100)
```

```
##    Min. 1st Qu.  Median    Mean 3rd Qu.    Max.
##   9.278  15.942  17.105  17.982  20.197  26.000
```

We visualize the percent of national cases in the peak season over the study period, and observe no systemic trend and high inter-annual variability.

```
p4wkpeak <- ggplot() +
  geom_point(aes(x=Y, y=yrsums$NinPeak/yrsums$n*100)) +
  geom_line(aes(x=Y, y=yrsums$NinPeak/yrsums$n*100)) + theme_bw() +
  ylab("Percent of Cases in Peak Season") + xlab("Year")

p4wkpeak
```

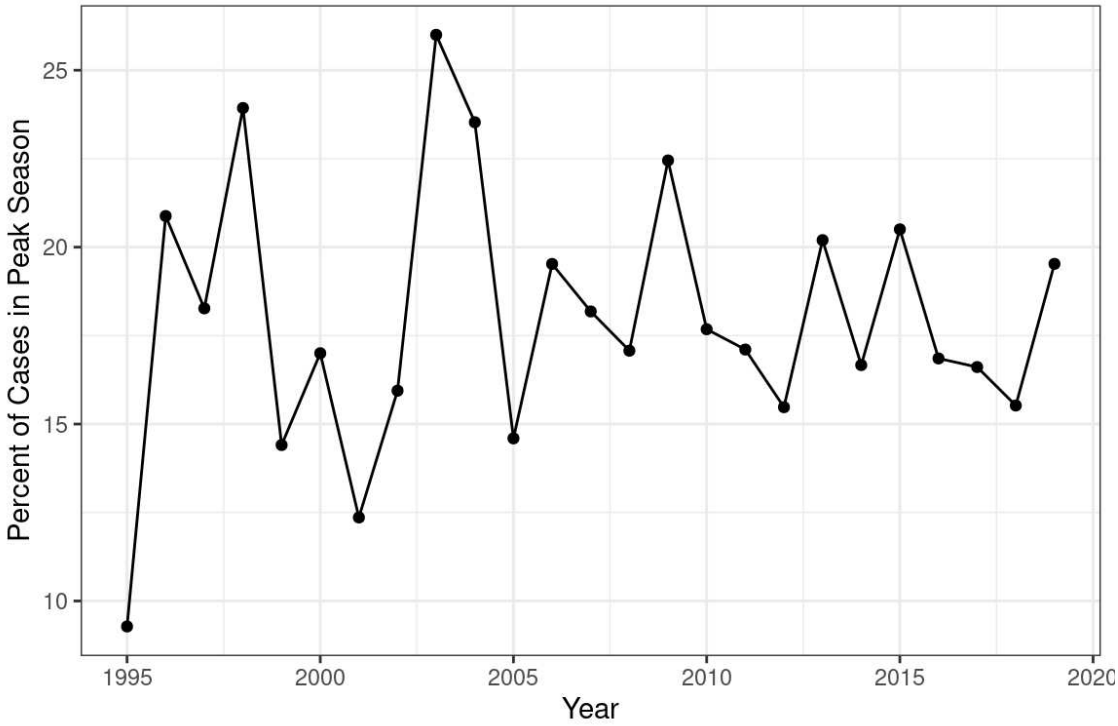

Figure S15: The percent of national Lyme borreliosis cases occurring during the peak season, defined as a 4-week period centered on the peak week.

5. Model comparisons

This section generates Table 1 in the main text. The purpose is to compare performance between the main model with flexible seasonality and the two alternative models with fixed seasonality.

5.1 Extract DIC's

The following code extracts the DIC (Deviance Information Criterion) value for each fitted model, which is included in the main manuscript in Table 1.

Note that the DIC values will change slightly every time the code is run, because of slight variability in the estimated posteriors.

```
DIC_MAIN <- fitMAIN$dic$dic
DIC_CSFIX <- fitCSFIX$dic$dic
DIC_RWFIX <- fitRWFIX$dic$dic
```

5.2 Cross validation

The cross validation script below uses 90% of the data as a training set, and measures model

performance based on predicting the remaining 10% of the data. The script iterates through the data randomly assigning different points to the test and training sets so that model performance is considered across the whole time series. This provides a way to compare model performance between the main and alternative models in addition to DIC. Predictive accuracy is measured by RMSE (root mean square error), MAE (mean absolute error), and negative log-likelihood.

```
forms=c(formMAIN, formCSFIX, formRWFIX)
forms.names = c("formMAIN", "formCSFIX", "formRWFIX")
crossval.results=data.frame()


## Use N crossvalidation sets:
n.cv.sets = 10
## Choose to do random subsets for the CV or not:
do.random.allocation = TRUE

for(j in 1:length(forms)){
  myform = forms[[j]]

  ## Step 1: Hide parts of the dataset in the test set and fit model
  rind = 1:nrow(dfa)
  CV = list()

  for (i in 1:n.cv.sets){
    if (i==n.cv.sets) {
      ids = rind
      rind = NA
    } else {
      number.of.ind = floor(nrow(dfa)/n.cv.sets)
      if (do.random.allocation){
        ## Sample randomly
        ids = sample(rind, number.of.ind, replace = F)
      } else {
        ## Use the first part of sequence
        ids = rind[1:number.of.ind]
      }
      rind = setdiff(rind, ids)
    }

    CV[[i]] = list(holdout=ids, formula=myform)

    tempdata = dfa
    tempdata$cases[ids] = NA

    myfit = inla(myform, data=tempdata, family="poisson",
                 control.predictor = list(compute=T, link=1),
                 control.compute = list(config=T,dic=T,waic=T))

    CV[[i]]$fit = myfit
    CV[[i]]$eta = myfit$summary.linear.predictor$mean

    if (any(is.na(CV[[i]]$eta))) stop("Some NAs found!")
  }

  ## Step 2: Compute summaries of how good the predictions are

  dfa$cv.eta.1 = NA
```

```
  all.ids = c()

  for (i in 1:n.cv.sets){
    ho.ids = CV[[i]]$holdout
    dfa$cv.eta.1[ho.ids] = CV[[i]]$eta[ho.ids]
    all.ids = c(all.ids, ho.ids)
  }

  error = dfa$cases-exp(dfa$cv.eta.1)
  RMSE = sqrt(mean((error)^2))
  MAE = mean(abs(error))
  negloglik = -1*sum(dpois(dfa$cases, lambda=exp(dfa$cv.eta.1), log=TRUE))

  new.results = data.frame(j=j, RMSE=RMSE, MAE=MAE, negloglik=negloglik)
  crossval.results = rbind(crossval.results, new.results)
}

crossval.results$names = forms.names
```

Combine results from DIC and cross validation in a table:

```
crossval.results$DIC <- c(DIC_MAIN, DIC_CSFIX, DIC_RWFIX)
table3 <- crossval.results[,c(2,3,4,6)]
colnames(table3)<-c("RMSE", "MAE", "NLL", "DIC")
rownames(table3)<-c("Main model", "Fixed season sinusoidal",  "Fixed season RW")

table3[,c(1,2)] <- signif(table3[,c(1,2)],3)
table3[,c(3,4)] <- signif(table3[,c(3,4)],5)
```

Table S3: Corresponding to Table 1 from main text, note that outputs vary slightly each time the crossvalidation code is run. Model performance metrics from cross-validation for comparing the three candidate models with different structures for the seasonality component. The main model includes a flexible seasonal component, while the other two models include a fixed seasonal component, either as a cyclic random walk or as a sinusoidal wave. The metrics compared are Root-Mean-Square Error (RMSE), Mean Absolute Error (MAE), Negative Log-Likelihood (NLL), and Deviance Information Criterion (DIC).

	RMSE	MAE	NLL	DIC
Main model	2.08	1.53	2560.5	5065.5
Fixed season sinusoidal	2.13	1.57	2599.2	5104.2
Fixed season RW	2.12	1.56	2589.6	5096.0

The code below creates a figure to show how the model performs on a test set after being fitted to the

training set:

```
dfaGAPS = dfa
startna = 1144
dfaGAPS$cases[startna:1300] = NA

forecastMAIN= inla(formMAIN, data=dfaGAPS, family="poisson",
                     control.predictor = list(compute=T, link=1),
                     control.compute = list(dic=1, waic=1, cpo=1))

pforecast <- ggplot() +
  geom_point(aes(x=dfa$X, y=dfa$cases), size=0.6, color="blue") +
  geom_point(aes(x=dfa$X, y=dfaGAPS$cases), color="grey40", size=0.6) +
  geom_line(aes(x=dfa$X, y=forecastMAIN$summary.fitted.values$mean), size=1, col
or="black") +
  geom_vline(xintercept = startna) +
  theme_bw() +
  theme(legend.position = "bottom") +
  xlab("Running Week Number") +
  ylab("Weekly Cases")

pforecast
```

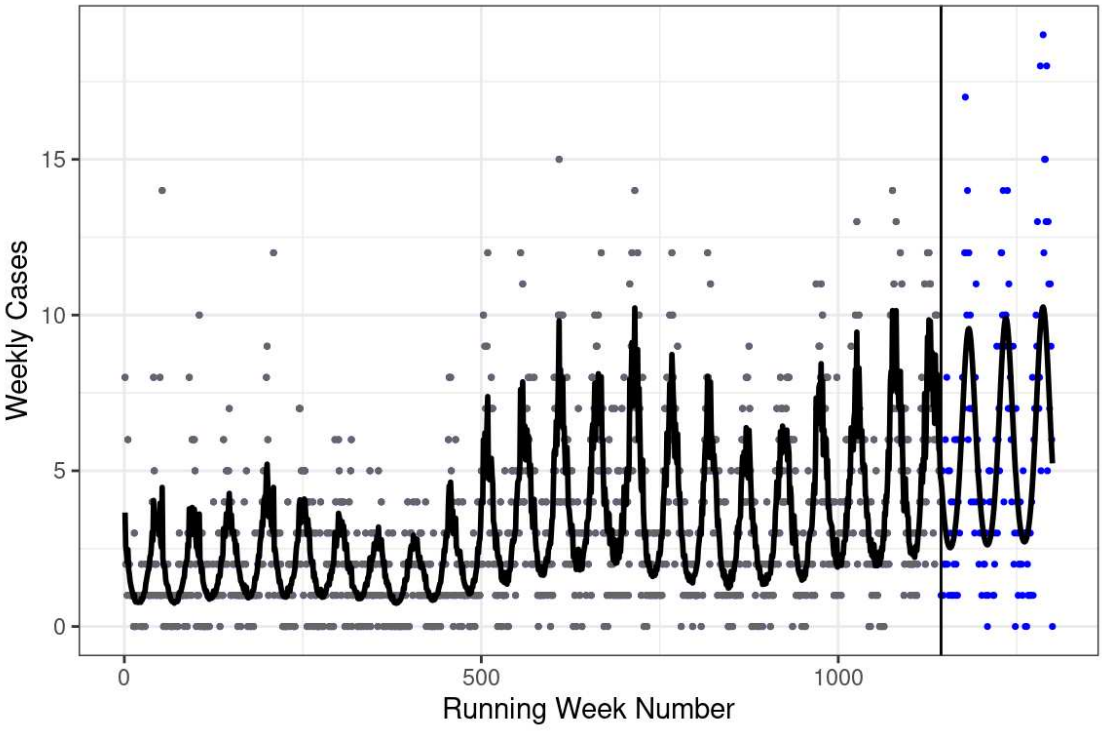

Figure S16: The main model forecasting for data in a test set (right of the vertical line) after being fitted to a training set (left of the vertical line).

6. NDVI

The week with maximum increase in greenness, or peak spring greening, is modeled to visualize changes seasonality over the study period. NDVI data was processed for areas below 200 m above sea level in the West, East, and South regions combined.

```
# Model the change in NDVI peak over time using lm
lmWeek<-lm(week~year, peak.spring)
summary(lmWeek)
```

```
##
## Call:
## lm(formula = week ~ year, data = peak.spring)
##
## Residuals:
##     Min      1Q  Median      3Q     Max
## -1.9546 -1.0415  0.1131  0.6492  2.9246
##
## Coefficients:
##             Estimate Std. Error t value Pr(>|t|)
## (Intercept) 257.1839    70.6392   3.641  0.00137 **
## year         -0.1208     0.0352  -3.431  0.00228 **
## ---
## Signif. codes:  0 '***' 0.001 '**' 0.01 '*' 0.05 '.' 0.1 ' ' 1
##
## Residual standard error: 1.269 on 23 degrees of freedom
## Multiple R-squared:  0.3386, Adjusted R-squared:  0.3098
## F-statistic: 11.77 on 1 and 23 DF,  p-value: 0.002279
```

```
# check global significance of lm
anova(lmWeek,test="Chisq")
```

```
## Analysis of Variance Table
##
## Response: week
##           Df Sum Sq Mean Sq F value   Pr(>F)
## year       1 18.961 18.9608  11.774 0.002279 **
## Residuals 23 37.039  1.6104
## ---
## Signif. codes:  0 '***' 0.001 '**' 0.01 '*' 0.05 '.' 0.1 ' ' 1
```

```
#Generate the B-spline basis matrix for a polynomial spline.
splineWeek.df3 <- lm(week~splines::bs(year,df=3),dat=peak.spring)
splineWeek.df4 <- lm(week~splines::bs(year,df=4),dat=peak.spring)
splineWeek.df5 <- lm(week~splines::bs(year,df=5),dat=peak.spring)

#Compare the models with AIC
AIC(lmWeek, splineWeek.df3, splineWeek.df4, splineWeek.df5)
```

```
##                df      AIC
## lmWeek          3 86.77447
## splineWeek.df3  5 83.03135
## splineWeek.df4  6 84.41240
## splineWeek.df5  7 85.94544
```

```
#df=3 yields the lowest AIC

anova(splineWeek.df3,test="Chisq")
```

```
## Analysis of Variance Table
##
## Response: week
##                            Df Sum Sq Mean Sq F value   Pr(>F)
## splines::bs(year, df = 3)  3 28.826  9.6087  7.4257 0.001423 **
## Residuals                  21 27.174  1.2940
## ---
## Signif. codes:  0 '***' 0.001 '**' 0.01 '*' 0.05 '.' 0.1 ' ' 1
```

```
pndviweek = ggplot(peak.spring) +
  ylab("Peak week of spring greening") +
  xlab("Year")+ theme_bw() +
  stat_smooth(aes(x=year, y=week), method = "lm", formula=y~splines::bs(x,df=3),
se=TRUE, size=1, show.legend = FALSE, color="#008631", fill="#008631", alpha=.
2)+
   scale_x_continuous(limits=c(1995,2020),breaks=seq(1995,2020,5), labels=seq(19
95,2020,5)) +
  geom_point(aes(x=year, y=week), size=2, color="#008631")
pndviweek
```

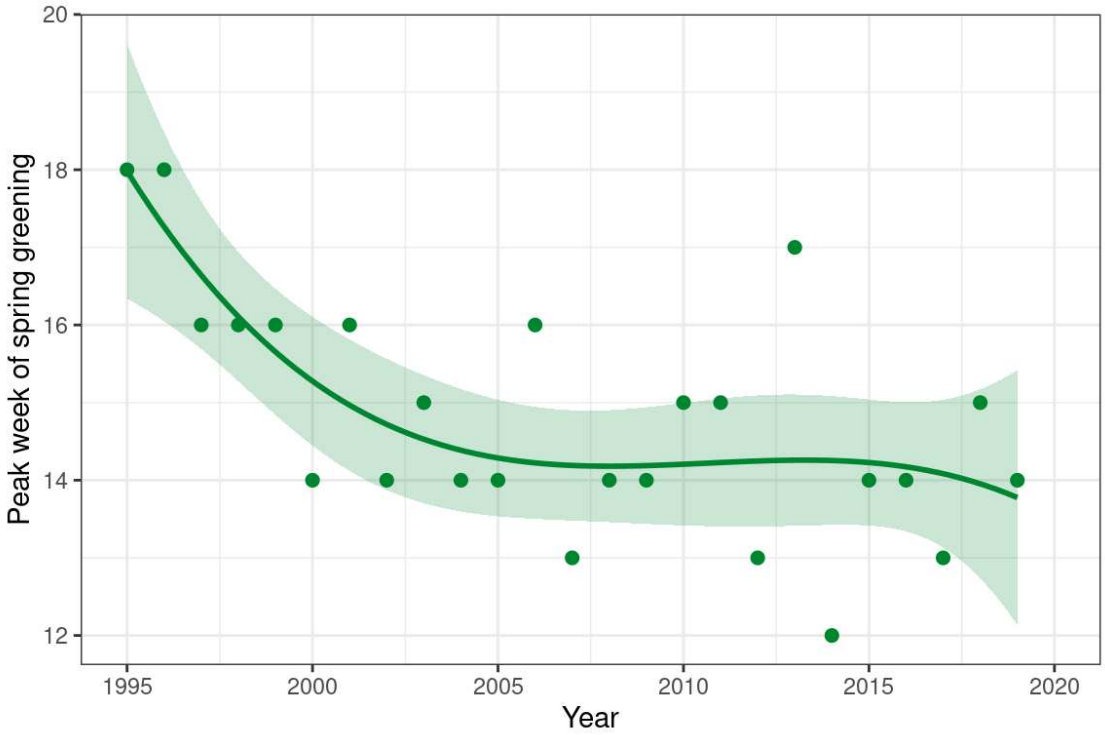

Figure S17: The week with maximum increase in greenness, or peak spring greening, is modeled to visualize changes seasonality over the study period.

Combined plot

```
FigA <- map_plot + labs(tag = "(a)") + theme(plot.tag = element_text())

FigB <- TrendPlot1 + labs(tag = "(b)") + theme(plot.tag = element_text())

FigC <- pndviweek + labs(tag = "(c)") + ylim(9,25) + theme(plot.tag = element_te
xt())

FigD <- pPOT + ylim(34,50) + labs(tag = "(d)") + theme(plot.tag = element_text
())

plot_grid(FigA, FigB, FigC, FigD, nrow=2, align="hv", axis="l", rel_heights = c
(1,1, 1,1))
```

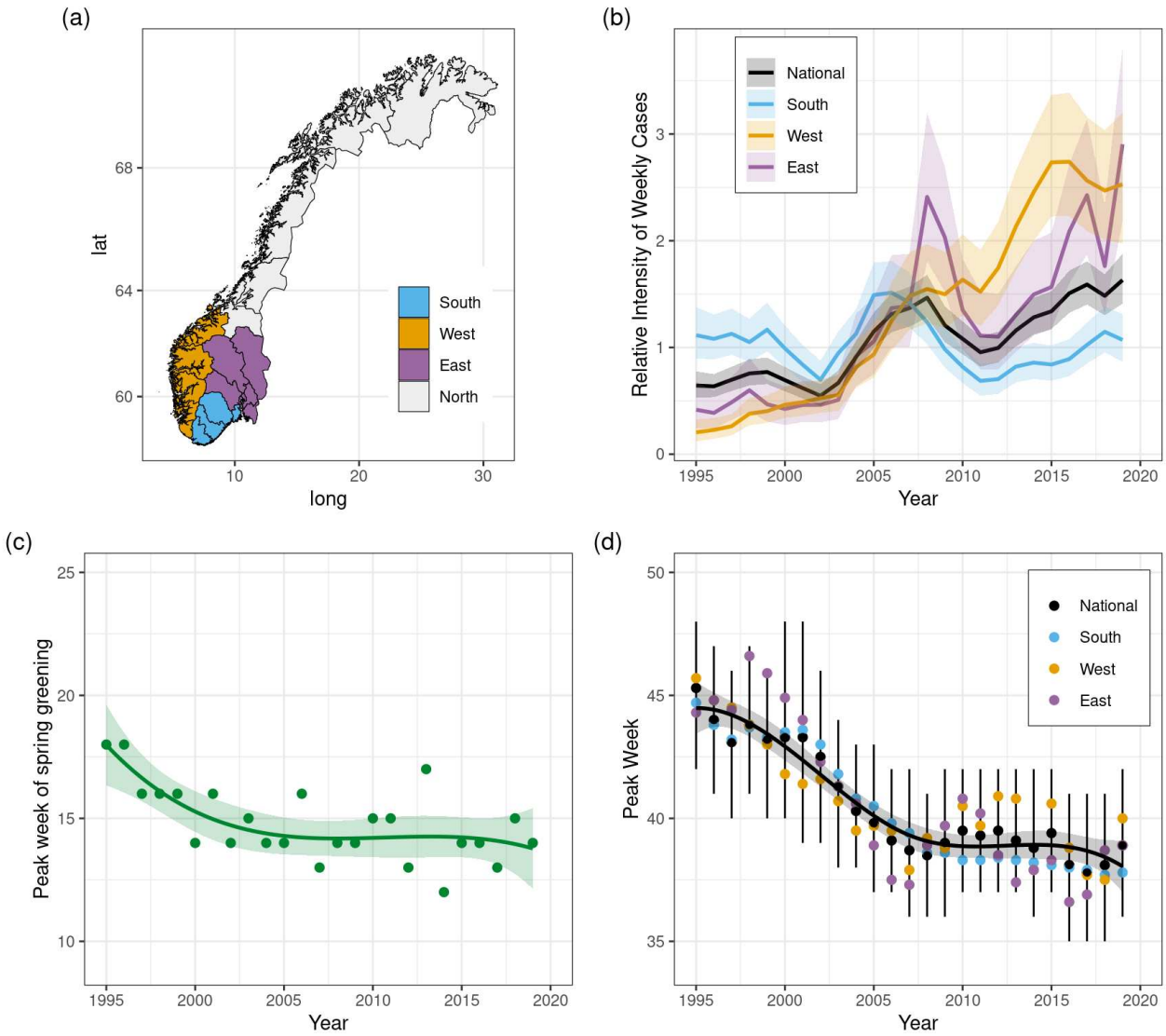

Figure S18: Figure 1 from the main text, showing key model outputs of changes in the seasonal and long-term trends of Lyme borreliosis cases in the regions.

References

- Simpson, D. P., H. Rue, A. Riebler, T. G. Martins, and S. H. Sørbye. 2017. “Penalising Model Component Complexity: A Principled, Practical Approach to Constructing Priors.” Statistical Science 32 (1): 1–28.
- Gómez-Rubio, Virgilio (2020). Bayesian Inference with INLA. Chapter 5. Chapman & Hall/CRC Press. Boca Raton, FL.

2

Received: 7 March 2023 | Revised: 14 June 2023 | Accepted: 30 June 2023

DOI: 10.1111/zph.13073

ORIGINAL ARTICLE

WILEY

Demographic patterns in Lyme borreliosis seasonality over 25 years

Asena Goren[1] | Atle Mysterud[1] | Solveig Jore[2] | Hildegunn Viljugrein[1,3] | Haakon Bakka[3] | Yngvild Vindenes[1]

[1]Department of Biosciences, Centre for Ecological and Evolutionary Synthesis (CEES), University of Oslo, Oslo, Norway

[2]Zoonotic, Food & Waterborne Infections, The Norwegian Public Health Institute, Oslo, Norway

[3]Norwegian Veterinary Institute, Ås, Norway

Correspondence
Asena Goren, Department of Biosciences, Centre for Ecological and Evolutionary Synthesis (CEES), University of Oslo, P.O. Box 1066 Blindern, Oslo NO-0316, Norway.
Email: asena.goren@ibv.uio.no

Funding information
Research Council of Norway, Grant/Award Number: 313286; University of Oslo

Abstract

Lyme borreliosis, the most common vector-borne disease in Europe and North America, is attracting growing concern due to its expanding geographic range. The growth in incidence and geographic spread is largely attributed to climate and land-use changes that support the tick vector and thereby increase disease risk. Despite a wide range of symptoms displayed by Lyme borreliosis patients, the demographic patterns in clinical manifestations and seasonal case timing have not been thoroughly investigated and may result from differences in exposure, immunity and pathogenesis. We analysed 25 years of surveillance data from Norway, supplemented by population demography data, using a Bayesian modelling framework. The analyses aimed to detect differences in case seasonality and clinical manifestations of Lyme borreliosis across age and sex differentiated patient groups. The results showed a bimodal pattern of incidence over age, where children (0–9 years) had the highest incidence, young adults (20–29 years) had low incidence and older adults had a second incidence peak in the ages 70–79 years. Youth (0–19 years) presented with a higher proportion of neuroborreliosis cases and a lower proportion of arthritic manifestations compared to adults (20+ years). Adult males had a higher overall incidence than adult females and a higher proportion of arthritis cases. The seasonal timing of Lyme borreliosis consistently occurred around 4.4 weeks earlier in youth compared to adults, regardless of clinical manifestation. All demographic groups exhibited a shift towards an earlier seasonal timing over the 25-year study period, which appeared unrelated to changes in population demographics. However, the disproportionate incidence of Lyme borreliosis in seniors requires increased public awareness and knowledge about this high-risk group as the population continues to age concurrently with disease emergence. Our findings highlight the importance of considering patient demographics when analysing the emergence and seasonal patterns of vector-borne diseases using long-term surveillance data.

KEYWORDS
demography, Lyme borreliosis, Lyme disease, seasonality, surveillance, vector-borne diseases

1 | INTRODUCTION

Lyme borreliosis, also known as Lyme disease, is the most common vector-borne disease in the northern hemisphere (Steinbrink et al., 2022). There is increasing evidence of the geographic expansion of Lyme borreliosis, particularly into higher latitude and elevation areas in Europe and North America (Jore et al., 2011; Mysterud et al., 2017; van Oort et al., 2020; Vandekerckhove et al., 2019). This tick-vectored bacterial (spirochete) infection is caused by several genospecies in the *Borrelia burgdorferi* sensu lato (sl) complex, with *B. burgdorferi* sensu stricto most common in North America and *Borrelia afzelii* and *Borrelia garinii* in Europe (Nelder et al., 2016; Steere et al., 2016). The emergence and geographic expansion of Lyme borreliosis have primarily been attributed to climate and land-use changes impacting the tick vector and thereby increasing disease hazard (Brownstein et al., 2005; Couper et al., 2021; Li et al., 2019; Lindgren & Jaenson, 2006; Simon et al., 2014). While many studies focus on spatial changes in Lyme borreliosis cases linked to climate change, far fewer explore long-term temporal and seasonal changes in the disease system (Goren et al., 2023; Monaghan et al., 2015; Moore et al., 2014). Little is known about how human demography impacts Lyme borreliosis incidence and seasonality through differences in exposure, immunity and pathogenesis among age and sex groups. Demographic changes in the population could impact the future burden of Lyme borreliosis and other vector-borne diseases, and a deeper understanding of disease demography is necessary for managing the risk of emerging diseases.

The pathogenesis of Lyme borreliosis is highly variable among individuals, but the typical presentation of a localized infection is an initially expanding skin lesion, termed *erythema migrans*, located at the site of the bite of an infected tick. The lesion usually appears around 2–30 days after the bite and may be accompanied by flu-like symptoms (Johnson et al., 2018; Steinbrink et al., 2022). If left untreated, a localized infection can progress into a disseminated form of disease (Steere et al., 2016). Early disseminated infections can result in neurological manifestations involving the central and/or peripheral nervous systems (Cadavid et al., 2016; MacDonald et al., 2016; Steere et al., 2016; Steinbrink et al., 2022). Late dissemination can result in long-term sequelae and can include arthritis, *acrodermatitis chronica atrophicans* and carditis (Cadavid et al., 2016; Coburn et al., 2021). It has been estimated that 15%–20% of untreated localized infections progress to the early disseminated form (Koedel et al., 2015; Ornstein et al., 2001; Strnad & Rego, 2020). Age- and sex-based differences in immune markers have been found to impact *Borrelia* sp. seroconversion and pathogenesis in patients, but little is known about how this impacts disease trends on a population scale (Carlsson et al., 2018; Steere et al., 2003; Woudenberg et al., 2020).

To better understand the causes of population-level trends in Lyme borreliosis over time, we need a deeper understanding of the role of patient demography. The goal of this study is to investigate demographic differences in clinical manifestations, as well as in temporal trends of annual incidence and seasonal case timing. We take advantage of a unique dataset encompassing 25 years of Norwegian Lyme borreliosis surveillance data, at the expanding northern limit of the disease's biogeographical range in Europe.

Impacts

- Analysis of 25 years of Lyme borreliosis surveillance data from Norway revealed differences across age and sex groups in annual incidence, seasonal timing and clinical manifestations.
- Youth (0–19 years old) exhibited a 4.4 weeks earlier seasonal timing of cases compared to adults (20+ years), irrespective of clinical manifestation. There was a higher proportion of neuroborreliosis and a lower proportion of arthritis cases among youth compared to adults.
- There was a bimodal incidence pattern across age, with children (0–9 years) having the highest incidence, low incidence in young adults (20–29 years) and a second incidence peak in older adults aged 70–79 years. In adults (20+ years), males had a higher overall incidence compared to females and a higher proportion of arthritic manifestations.

2 | METHODS

2.1 | Surveillance data

This study is based on Lyme borreliosis surveillance data from Norway, which is curated by the Norwegian Institute of Public Health through the Norwegian Surveillance System for Communicable Diseases (MSIS). Since 1991, Lyme borreliosis has been a notifiable disease in Norway, with consistent notification criteria since 1995 (MacDonald et al., 2016). For this reason, this analysis covers the 25 year period from 1995 to 2019. There have been a few changes in case reporting and diagnostic testing methods for Lyme borreliosis during this time. Only disseminated forms of Lyme borreliosis are notifiable in Norway, by both clinicians and medical laboratories. Notification is based on a clinically compatible case with laboratory confirmation of *B. burgdorferi* sl by isolation, polymerase chain reaction (PCR) nucleic acid test or enzyme-linked immunosorbent assay (ELISA) antibody test (Mysterud et al., 2019; Norwegian Public Health Institute, 2023). Some notable changes in diagnostics over the study period include the introduction of improved ELISA methods in 2005–2008 and the introduction of standardized use of spinal puncture for diagnosis in children under 9 years old since 2011 (Berstad et al., 2017; Hunfeld et al., 2005; Mysterud et al., 2019). These changes in diagnostics, combined with increased disease awareness, could have resulted in higher overall detection rates as these new methods were implemented. A more detailed account of

reporting criteria can be found elsewhere (MacDonald et al., 2016; Mysterud et al., 2019).

The timing of cases in this study is determined by the date of diagnostic testing, which is available for every patient. This date usually occurs several weeks after the tick bite when symptoms of disseminated disease have emerged (Coburn et al., 2021). Clinical manifestations were grouped into three categories: neuroborreliosis, arthritis or other. Neuroborreliosis was defined as any neurological manifestation of the disease, while arthritis was categorized as all clinical manifestations affecting the joints. Any other manifestations, such as *acrodermatitis chronica atrophicans*, carditis and multiple *erythema migrans*, were categorized as 'other'. The incidence comparisons among demographic groups were based on cases per 100,000 persons (per year or week, depending on the model) in the population, where population data (Statistics Norway, 2022) were differentiated by sex and age. Initial explorations of Lyme borreliosis incidence trends across age and sex groups were based on 10-year age intervals for ages 0–80, with the oldest individuals pooled into the '80–99 years' group (Figure 1). Because of the bimodal incidence distribution over age (Figure 1c), temporal trends in incidence were analysed by comparison of three demographic groups: youth, adult males and adult females, with youth defined as individuals aged 0–19 years old and adults as individuals aged 20 years old or more.

2.2 | Statistical analysis

The statistical R package INLA (http://www.r-inla.org) was used to fit Bayesian models to investigate differences in case timing, incidence, and clinical manifestations across demographic groups, as well as explore differences in temporal trends within and between years (Rue et al., 2009). We first fitted a set of models to annual incidence rates stratified by demographic groups. We then fitted another set of models to annual values for the proportion of cases in each demographic group presenting with neurological, arthritic or other clinical manifestations. A third set of models was fitted to weekly incidence rates, accounting for seasonal effects. Incidence rates were defined as the number of cases per 100,000 persons in the selected demographic group for the specified time period (week or year). The R code for fitting the models and defining priors is provided as Appendix S2, without the underlying data as these are restricted.

To estimate differences in clinical manifestation (neuroborreliosis, arthritis or other) within each demographic group (youth, adult males, and adult females), a Poisson distribution was used to model the number of cases y_{jk} in year j and clinical manifestation type k,

$$y_{jk} \sim Poisson(\lambda_{jk}), \tag{1}$$

where λ_{jk} is the expected annual number of cases with manifestation k. The annual incidence was modelled with a logarithmic link function, including a population offset (size of demographic group) and year as an autoregressive term:

$$\ln(\lambda_{jk}) = \beta_0 + G_k + \ln(N_j) + Y_j + \epsilon_{jk}. \tag{2}$$

Here β_0 is the intercept (reference level representing neuroborreliosis), and G_k is a fixed effect factor representing the effect of clinical manifestation (arthritis or other, compared to the reference), $\ln(N_j)$ is the population offset, Y_j is the year effect, and ϵ_{jk} is a Gaussian random effect used to account for overdispersion (Bakka et al., 2019; Goren et al., 2023). The population offset accounts for any changes in the number of observed cases due to changes in population size. The year effects are modelled as random intercepts following an autoregressive model of order 1 constrained to mean zero to avoid confounding with the reference level β_0. The model was run separately for each demographic group.

Differences in clinical manifestation were also quantified based on the proportion of cases within each demographic group. Letting y_{jk} be the number of cases in year j of manifestation type k, this variable has a binomial distribution

$$y_{jk} \sim Binomial(y_j, p_{jk}), \tag{3}$$

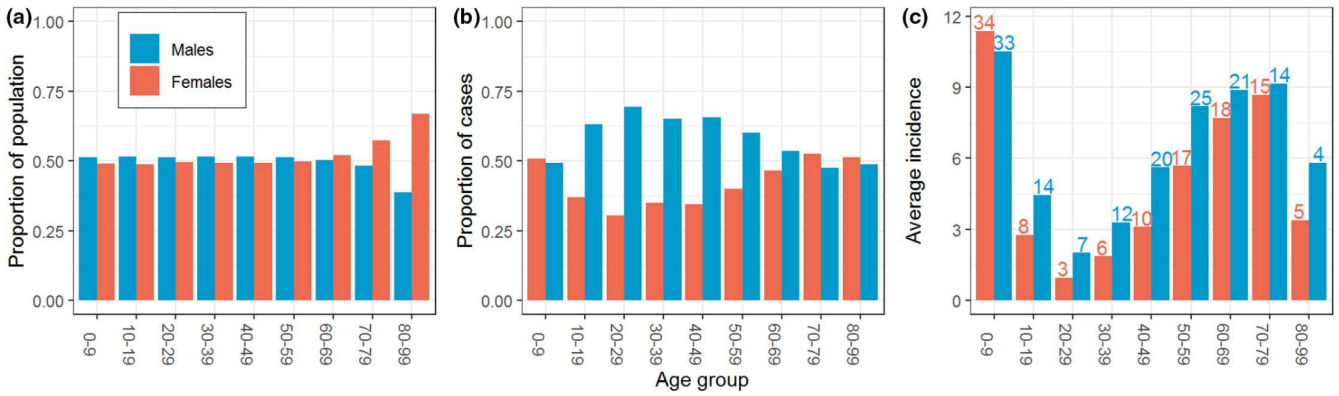

FIGURE 1 (a) Proportion of males and females in each age group in the population data over the study period. (b) Proportion of males and females in each age group in the Lyme borreliosis surveillance data over the study period. (c) Annual incidence (per 100,000) of Lyme borreliosis averaged over the study period, for each sex and age group. The numbers above the bars represent average annual case numbers.

where p_{kj} is the probability that each of the y_j cases in the demographic group presents with the clinical manifestation k. This probability was modelled on the logit scale as

$$\text{logit}(p_{kj}) = \beta_0 + G_k + Y_j + \varepsilon_{jk} \quad (4)$$

with the same interpretation and definition of the model components ($\beta_0, G_k, Y_j, \varepsilon_{jk}$) as for the model in Equation (2) (defined on another scale). The model was run separately for each demographic group. Results of the models are presented as point estimates of incidence or proportion in each group with the corresponding 95% credible intervals calculated from the posterior distributions. We consider two point estimates to be significantly different if each lies outside the credible interval of the other.

To compare seasonal case timing between demographic groups and clinical manifestations, the above models for incidence (Equations 1 and 2) were expanded to a weekly scale, adding a seasonal component following the approach of Goren et al. (2023). This weekly model captures changes in seasonality over time by separating long term (inter-annual) from seasonal trends (intra-annual). A Poisson distribution was used to model the number of cases y_{ij} in week i (from 1 to 52) and year j,

$$y_{ij} \sim Poisson(\lambda_{ij}) \quad (5)$$

where λ_{ij} is the expected number of cases, described by a logarithmic link function:

$$\ln(\lambda_{ij}) = \beta_0 + \ln(N_j) + Y_j + W_{ij} + \varepsilon_{ij}. \quad (6)$$

Here β_0 is the intercept, Y_j is the year effect estimated for year j, W_{ij} is the seasonal effect modelled using a sinusoidal wave function, $\ln(N_j)$ is the population offset and ε_{ij} is a Gaussian random effect used to account for overdispersion (Bakka et al., 2019; Goren et al., 2023). By including the population offset term $\ln(N_j)$, we are in effect modelling the weekly incidence rate (per capita). The sinusoidal wave function used to model the seasonal effect ensures that case seasonality is uniquely described by the week in which cases peak. Changes in within-year case timing are measured by extracting the annual peak week from the fitted models, and any shifts observed apply to all seasonal features (Goren et al., 2023). The year trend and seasonal effects were modelled using a first-order random walk to (i) account for autocorrelations in the time series and (ii) allow for the seasonal pattern to change (slowly) over the years.

A seasonal model was fit independently to the number of weekly cases for each demographic group, for weekly cases of all clinical manifestations together and for neuroborreliosis cases only. The seasonal model was also fit independently to the total number of weekly cases for each clinical manifestation. For arthritis cases and other clinical manifestations, there were too few cases to fit a model with flexible seasonality. Instead, the seasonal part of the model (W_{ij} in Equation (6) above) was modelled using fixed effects for the sinusoidal wave function so that the seasonality was restricted to be the same for each year (Goren et al., 2023). The model with fixed seasonality outperformed the flexible seasonality model by DIC for arthritis and other clinical manifestations, but not for neuroborreliosis (see Appendix S2). All analyses were done using the statistical software R version 4.0.3 (R Core Team, 2022).

3 | RESULTS

Over the study period, there was a demographic shift towards an ageing population in Norway (Figure S1). The sex ratio did not change much across age groups during the study period, except in the oldest age groups that had an initially high but decreasing proportion of females (Figure S2). Overall, the age groups had slightly more males in the younger and intermediate age groups and more females in the older age groups (Figure 1a). The overall Lyme disease annual incidence distribution, expressed as annual incidence (per 100,000) averaged over the study period, was bimodal over age both for males and females (Figure 1c), with the highest incidence at age 0–9 years (11 per 100,000), and a smaller peak at age 70–79 years (9 per 100,000). Although the 70–79 years group had the highest incidence of adults, the majority of adult cases were in the 50–59 years group (Figure 1c).

The proportion of youth compared to adults in the population of Norway showed a minimal decrease during the study period (Figure S3). Geographic patterns were not investigated in this study, but the proportions of the youth and adult populations in different regions remained relatively unchanged over the study period (Figure S4). The youth had a higher incidence of Lyme borreliosis than adults, and adult males had a higher incidence compared to adult females (Figure 1c). Males had a higher incidence than females in all except the youngest age group (0–9 years old), where there was a higher incidence in females (Figure 1c). Compared to the proportion of males in each age group in the underlying population, there was an excess of male cases in all age groups except the youngest (Figure S5).

The statistical models fitted to annual data showed that patterns of clinical manifestation were significantly different between youth and adults, and more similar among adult males and females (Figure 2). In all demographic groups, neuroborreliosis was the most common clinical manifestation, with the highest incidence as well as the proportion of cases. Adult males had a higher annual incidence (per 100,000) of neuroborreliosis (3.67 [3.47, 3.87]) and arthritis (1.12 [0.94, 1.30]) compared to adult females (neuroborreliosis: 2.61 [2.45, 2.78]; arthritis: 0.59 [0.48, 0.73]; Figure 2a, Table S1). The proportion of neuroborreliosis cases was very similar in adult males (0.55 [0.53, 0.57]) and females (0.56 [0.53, 0.58]), while the proportion of arthritis cases was estimated to be somewhat higher (0.17 [0.14, 0.20]) compared to adult females (0.13 [0.10, 0.16]; Figure 2b, Table S1). The youth had a higher proportion of neuroborreliosis (0.79 [0.78, 0.81]) and a lower proportion of arthritis (0.08 [0.06, 0.10]) and other manifestations (0.08 [0.06, 0.10]) compared to adult males and females (Figure 2b, Table S1).

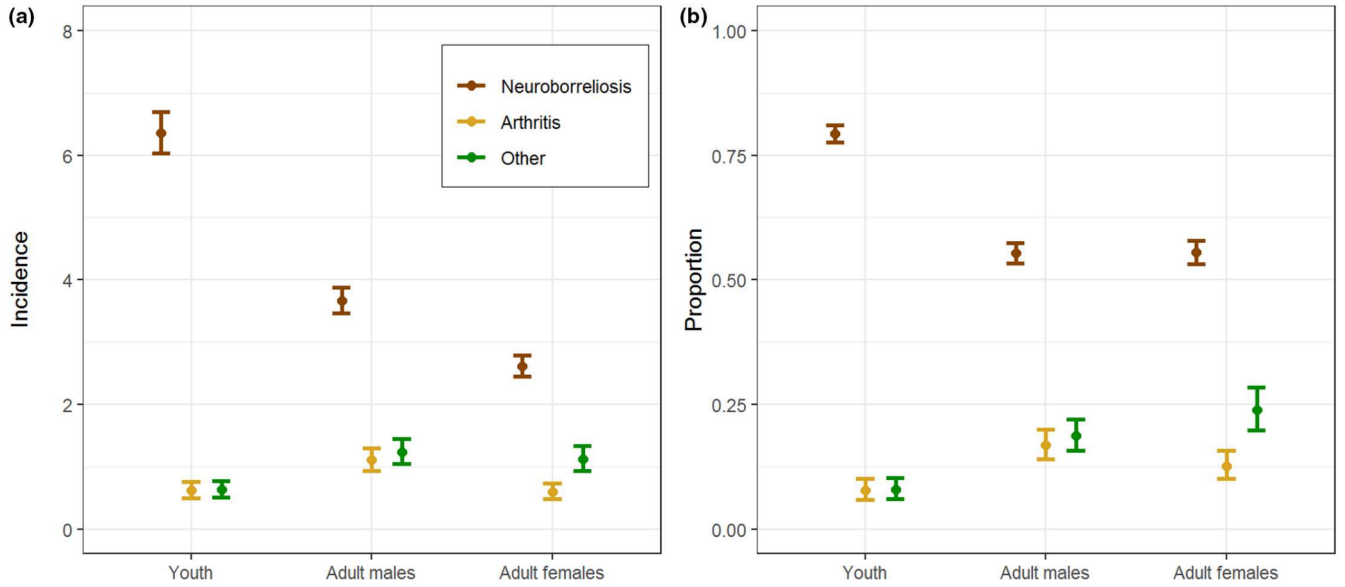

FIGURE 2 Comparison of Lyme borreliosis clinical manifestations between demographic groups, based on INLA models fitted to annual data for each clinical manifestation, with a random effect year component and no seasonal component. (a) Mean annual incidence (per 100,000) with 95% credible intervals. (b) Per cent of cases with each clinical manifestation within each demographic group, with 95% credible intervals.

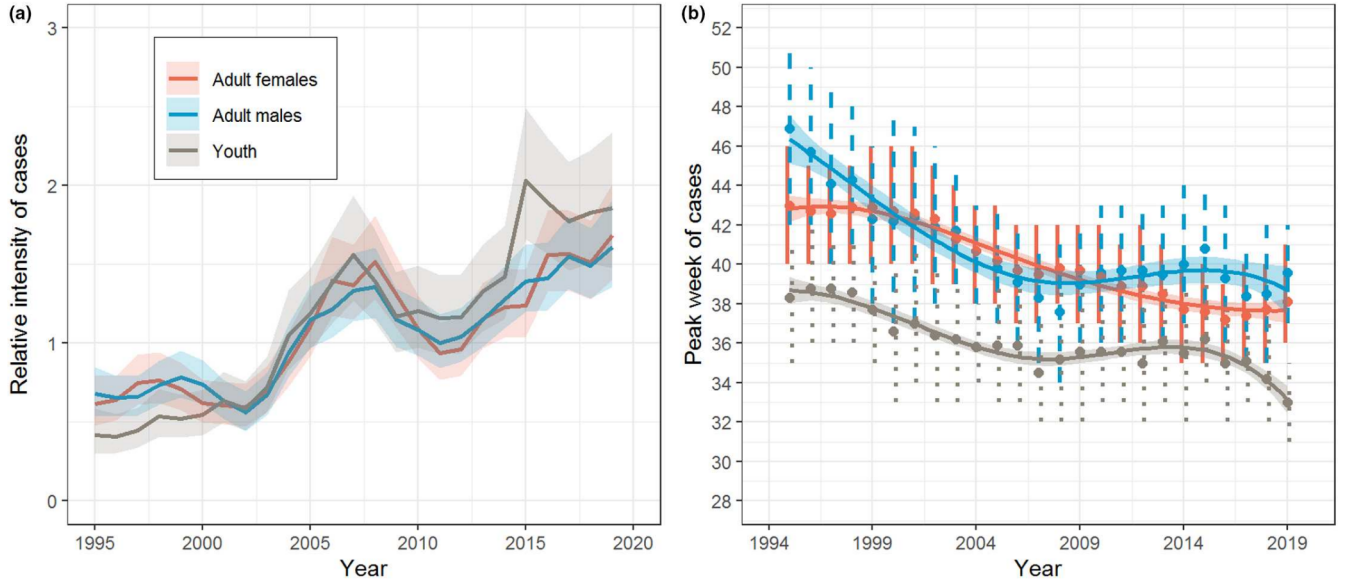

FIGURE 3 Temporal trends in Lyme borreliosis cases for demographic groups (youth, adult females, and adult males) based on seasonal INLA models. (a) Inter-annual trend comparison based on the annual components of the models, with shaded 95% credible intervals. The annual components describe the relative intensity of cases (not incidence) over the study period. (b) Comparison of changing seasonality measured by predicted seasonal incidence peak. The ribbons represent the 95% confidence intervals on the fitted splines, while the vertical lines represent error margins on the estimated peak incidence weeks based on repeated sampling from the posterior distribution.

The inter-annual trends were similar across demographic groups, with youth exhibiting a slightly greater increase in incidence over the study period (Figure 3a). The inter-annual trends were also similar across clinical manifestations, with neuroborreliosis showing a slightly greater increase in incidence than arthritis over the study period (Figure 4a). Differences in case seasonality were larger between youth and adults than between adult males and females (Figure 3b), with the seasonal incidence peak on average 4.4 weeks earlier in youth than adults. The difference in case timing between youth and adults was also observed when the analysis was restricted to neuroborreliosis cases (Figure S6), indicating the difference is not driven by differences in clinical manifestation. There was limited difference in case seasonality across clinical manifestations, however, low annual case numbers for arthritis resulted in large error margins for the seasonal peaks and necessitated the use of a simplified model with fixed seasonality across years.

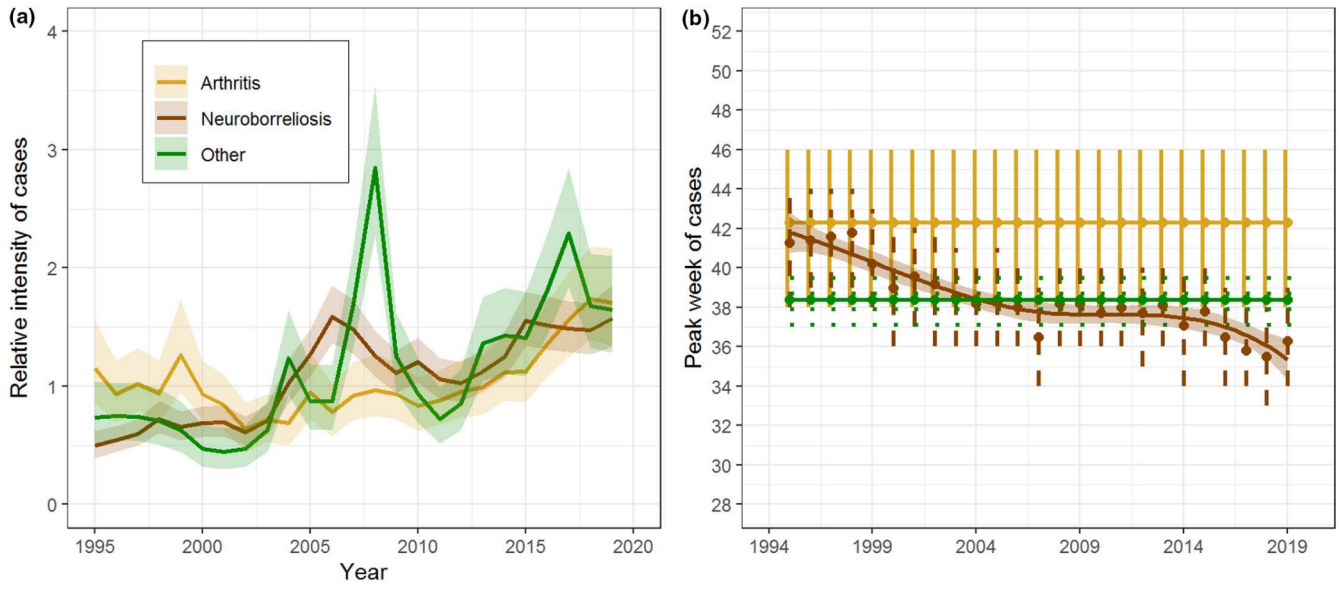

FIGURE 4 Temporal trends in Lyme borreliosis cases for different clinical manifestations (neuroborreliosis, arthritis and other) based on seasonal INLA models. (a) Inter-annual trend comparison based on annual components of the seasonal models, with 95% credible intervals. The annual components describe the relative intensity of cases (not incidence) over the study period. (b) Comparison of the seasonality of the different clinical manifestations of Lyme borreliosis measured by the seasonal incidence peak. The ribbons represent the 95% confidence intervals on the fitted splines, while the vertical lines represent error margins on the estimated peak weeks based on repeated sampling from the posterior distribution. Note that due to low case numbers, arthritis and other clinical manifestations were modelled with a fixed seasonal effect across years, while neuroborreliosis was modelled with a flexible seasonality that can vary across years.

4 | DISCUSSION

Based on long-term surveillance data from Norway, we analysed demographic differences in incidence, clinical manifestation, and seasonality of Lyme borreliosis using a Bayesian framework for statistical analysis. We found that youth (0–19 years) had a higher overall incidence, a larger proportion of neuroborreliosis cases, and an earlier seasonal peak by 4.4 weeks compared to adults. Adult males had a higher overall incidence of Lyme borreliosis with a higher proportion of arthritis compared to adult females. The overall demographic trends identified in this analysis, including the bimodal incidence distribution over age and overrepresentation of males in most age groups, are predominantly in concordance with prior studies in Norway and other countries (Berglund et al., 1995; Eliassen et al., 2017; Nygård et al., 2005; Schwartz et al., 2017; Skufca et al., 2022; Stanek & Strle, 2018; Steere et al., 2016; Sundheim et al., 2021; Tulloch et al., 2019, 2020; Tveitnes & Øymar, 2015). This study is the first to provide insight into how the seasonality of Lyme borreliosis varies among demographic groups.

The bimodal distribution of incidence over patient age suggests that children and older adults are at higher risk of developing disseminated Lyme borreliosis, compared to young adults in the age range 18–30. The reasons for these differences are not yet clear and may be due to a combination of factors such as exposure to vectors, care-seeking behaviour and biological and immunological differences. In Norway, youth tend to have a higher proportion of neurological manifestations compared to other forms of the disease (Figure 2), which is typical in Europe but contrasts with North America, where arthritis is commonly seen in both youth and adult patients (Christen et al., 1993; Marques et al., 2021; Stanek et al., 2012).

While it is known from prior studies that the seasonal timing of Lyme borreliosis cases has shifted significantly over the study period (Goren et al., 2023), this analysis demonstrated consistent differences in case seasonality between demographic groups (Figure 3b). The current analysis demonstrated that the overall shift in case seasonality observed prior was unlikely to be caused by changes in patient or population demography. The 4.4 weeks earlier case timing in youth compared to adults was not attributable to adults having a higher incidence of arthritis and other late disseminated clinical manifestations compared to youth (Stanek & Strle, 2018), as the difference persisted even when restricting the analysis to only neuroborreliosis cases (Figure 3, Figure S6). The difference in case timing between youth and adults could indicate that youth have more rapid pathogenesis of Lyme borreliosis than adults. While there is evidence of some differences in pathogenesis between adults and children (Feder Jr, 2008), there is yet insufficient clinical evidence to determine if more rapid pathogenesis actually occurs in youth. Differences in Lyme borreliosis trends between adults and children could also be related to behavioural factors resulting in differential tick exposure (Cull et al., 2020). A combination of other factors could also impact case timing, such as differences in healthcare-seeking behaviour between youth and adults and patient handling in hospitals. Demographic differences in healthcare-seeking behaviour and patient handling have not been sufficiently investigated for Lyme borreliosis, in particular, but have been broadly acknowledged in public health literature (Giasson & Chopik, 2020; Thompson

et al., 2016). Further investigation into infection dynamics between the *Borrelia* genospecies and the immune system across ages could yield deeper insight into the observed trends.

This study found an overrepresentation of males in the Lyme borreliosis surveillance data, which is expected because only disseminated cases are reported in the national surveillance data in Norway. Gender differences in accessing healthcare are well recognized (Dias et al., 2022; Govender & Penn-Kekana, 2008). For Lyme borreliosis, females typically represent a higher proportion of localized infections and *erythema migrans*, whereas males comprise a higher proportion of disseminated disease cases (Eliassen et al., 2017; Nygård et al., 2005; Skufca et al., 2022; Tulloch et al., 2019, 2020). A prior study in an overlapping time period in Norway used general practitioner data instead of surveillance data and found an overrepresentation in females presenting with *erythema migrans*, indicating early localized Lyme borreliosis infection (Eliassen et al., 2017). This trend has been attributed to gender-related differences in healthcare-seeking behaviour (Bennet et al., 2007; Doyal, 2001; Eliassen et al., 2017), but insufficient investigation has been conducted into whether there could also be a biological explanation for the increased incidence of disseminated Lyme borreliosis in males (Schwarzwalder et al., 2010; Strle et al., 2013). In this study, some of the elevated overall incidence in adult males compared to females was attributable to a higher incidence of Lyme arthritis. More research is needed to confirm this pattern and disentangle the causes. It is known that females have a higher incidence of auto-immune rheumatoid arthritis than males (Kvien et al., 2006), but little research has been done into sex differences in non-rheumatoid arthritides to determine if other types of septic arthritis show a similar trend as Lyme arthritis of elevated incidence in males.

This study explores demographic patterns in Lyme borreliosis clinical manifestation and is the first study to investigate differences in the seasonality of Lyme borreliosis case timing across demographic groups. Further research into disease pathogenesis is needed to understand the causal explanations of the demographic patterns observed in surveillance data.

FUNDING INFORMATION

This project is funded by the University of Oslo (PhD grant) and the Research Council of Norway (project TimeLyme, 313286).

CONFLICT OF INTEREST STATEMENT

The authors declare that they have no conflict of interest.

DATA AVAILABILITY STATEMENT

The data used for this analysis are maintained by the Norwegian Institute of Public Health and cannot be made publicly available due to patient confidentiality. The R script for analyses is provided as Appendix S2.

ETHICS STATEMENT

The project was approved by the Regional Committee for Medical and Health Research Ethics (REK sør-øst B; Reference 115365).

ORCID

Asena Goren https://orcid.org/0000-0003-1042-3413
Atle Mysterud https://orcid.org/0000-0001-8993-7382
Solveig Jore https://orcid.org/0000-0001-8527-4892
Hildegunn Viljugrein https://orcid.org/0000-0002-3798-5267
Haakon Bakka https://orcid.org/0000-0001-8272-865X
Yngvild Vindenes https://orcid.org/0000-0003-1197-5818

REFERENCES

Bakka, H., Vanhatalo, J., Illian, J. B., Simpson, D., & Rue, H. (2019). Non-stationary gaussian models with physical barriers. *Spatial Statistics*, *29*, 268–288. https://doi.org/10.1016/j.spasta.2019.01.002

Bennet, L., Stjernberg, L., & Berglund, J. (2007). Effect of gender on clinical and epidemiologic features of Lyme borreliosis. *Vector-Borne and Zoonotic Diseases*, *7*(1), 34–41. https://doi.org/10,1089/vbz.2006.0533

Berglund, J., Eitrem, R., Ornstein, K., Lindberg, A., Ringnér, Å., Elmrud, H., Carlsson, M., Runehagen, A., Svanborg, C., & Norrby, R. (1995). An epidemiologic study of Lyme disease in southern Sweden. *New England Journal of Medicine*, *333*(20), 1319–1324. https://doi.org/10.1056/NEJM199511163332004

Berstad, A. K. H., Døllner, H., & Eikeland, R. (2017). *Generell veileder i pediatri, 3.7 Borreliose*. Norsk barnelegeforening. January 01. First published 2006, updated 2011 and 2017. https://www.helsebiblioteket.no/innhold/retningslinjer/pediatri/generell-veileder-i-pediatri/3.infeksjoner-vaksiner-og-undersokelse-av-adoptivbarn/3.7-borreliose#-helsebiblioteket-innhold-retningslinjer-pediatri-generell-veileder-i-pediatri-3infeksjoner-vaksiner-og-undersokelse-av-adoptivbarn-37-borreliose

Brownstein, J. S., Holford, T. R., & Fish, D. (2005). Effect of climate change on Lyme disease risk in North America. *EcoHealth*, *2*(1), 38–46. https://doi.org/10.1007/s10393-004-0139-x

Cadavid, D., Auwaerter, P. G., Rumbaugh, J., & Gelderblom, H. (2016). Antibiotics for the neurological complications of Lyme disease. *Cochrane Database of Systematic Reviews*, *2016*(12), CD006978. https://doi.org/10.1002/14651858.cd006978.pub2

Carlsson, H., Ekerfelt, C., Henningsson, A. J., Brudin, L., & Tjernberg, I. (2018). Subclinical Lyme borreliosis is common in South-Eastern Sweden and may be distinguished from Lyme neuroborreliosis by sex, age and specific immune marker patterns. *Ticks and Tick-Borne Diseases*, *9*(3), 742–748. https://doi.org/10.1016/j.ttbdis.2018.02.011

Christen, H. J., Hanefeld, F., Eiffert, H., & Thomssen, R. (1993). Epidemiology and clinical manifestations of Lyme borreliosis in childhood: A prospective multicentre study with special regard to neuroborreliosis. *Acta Paediatrica*, *82*, 1–76. https://doi.org/10.1111/j.1651-2227.1993.tb18082.x

Coburn, J., Garcia, B., Hu, L. T., Jewett, M. W., Kraiczy, P., Norris, S. J., & Skare, J. (2021). Lyme disease pathogenesis. *Current Issues in Molecular Biology*, *42*, 473–518. https://doi.org/10.21775/cimb.042.473

Couper, L. I., MacDonald, A. J., & Mordecai, E. A. (2021). Impact of prior and projected climate change on US Lyme disease incidence. *Global Change Biology*, *27*(4), 738–754. https://doi.org/10.1111/gcb.15435

Cull, B., Pietzsch, M. E., Gillingham, E. L., McGinley, L., Medlock, J. M., & Hansford, K. M. (2020). Seasonality and anatomical location of human tick bites in the United Kingdom. *Zoonoses and Public Health*, *67*(2), 112–121. https://doi.org/10.1111/zph.12659

Dias, S. P., Brouwer, M. C., & van de Beek, D. (2022). Sex and gender differences in bacterial infections. *Infection and Immunity*, *90*(10), e0028322. https://doi.org/10.1128/iai.00283-22

Doyal, L. (2001). Sex, gender, and health: The need for a new approach. *BMJ*, *323*(7320), 1061–1063. https://doi.org/10.1136/bmj.323.7320.1061

Eliassen, K. E., Berild, D., Reiso, H., Grude, N., Christophersen, K. S., Finckenhagen, C., & Lindbæk, M. (2017). Incidence and antibiotic treatment of erythema migrans in Norway 2005–2009. *Ticks and Tick-Borne Diseases*, *8*(1), 1–8. https://doi.org/10.1016/j.ttbdis.2016.06.006

Feder, H. M., Jr. (2008). Lyme disease in children. *Infectious Disease Clinics of North America*, *22*(2), 315–326. https://doi.org/10.1016/j.idc.2007.12.007

Giasson, H. L., & Chopik, W. J. (2020). Geographic patterns of implicit age bias and associations with state-level health outcomes across the United States. *European Journal of Social Psychology*, *50*(6), 1173–1190. https://doi.org/10.1002/ejsp.2707

Goren, A., Viljugrein, H., Rivrud, I. M., Jore, S., Bakka, H., Vindenes, Y., & Mysterud, A. (2023). The emergence and shift in seasonality of Lyme borreliosis in northern Europe. *Proceedings of the Royal Society B. Biological Sciences*, *290*, 20222420. https://doi.org/10.1098/rspb.2022.2420

Govender, V., & Penn-Kekana, L. (2008). Gender biases and discrimination: A review of health care interpersonal interactions. *Global Public Health*, *3*(S1), 90–103. https://doi.org/10.1080/17441690801892208

Hunfeld, K., Fingerle, V., Stanek, G., Daghofer, E., Brade, V., Wilske, B., & Peters, H. (2005). *European multicenter study for evaluation of a new enzyme immunoassay for detection of IgG antibodies against Borrelia burgdorferi sensu lato*. 10th international conference on Lyme borreliosis and other tick-borne diseases.

Johnson, K. O., Nelder, M. P., Russell, C., Li, Y., Badiani, T., Sander, B., Sider, D., & Patel, S. N. (2018). Clinical manifestations of reported Lyme disease cases in Ontario, Canada: 2005–2014. *PLoS One*, *13*(6), e0198509. https://doi.org/10.1371/journal.pone.0198509

Jore, S., Viljugrein, H., Hofshagen, M., Brun-Hansen, H., Kristoffersen, A. B., Nygård, K., Brun, E., Ottesen, P., Sævik, B. K., & Ytrehus, B. (2011). Multi-source analysis reveals latitudinal and altitudinal shifts in range of *Ixodes ricinus* at its northern distribution limit. *Parasites & Vectors*, *4*(1), 84. https://doi.org/10.1186/1756-3305-4-84

Koedel, U., Fingerle, V., & Pfister, H.-W. (2015). Lyme neuroborreliosis—Epidemiology, diagnosis and management. *Nature Reviews Neurology*, *11*(8), 446–456. https://doi.org/10.1038/nrneurol.2015.121

Kvien, T. K., Uhlig, T., Ødegård, S., & Heiberg, M. S. (2006). Epidemiological aspects of rheumatoid arthritis: The sex ratio. *Annals of the new York Academy of Sciences*, *1069*(1), 212–222. https://doi.org/10.1196/annals.1351.019

Li, S., Gilbert, L., Vanwambeke, S. O., Yu, J., Purse, B. V., & Harrison, P. A. (2019). Lyme disease risks in Europe under multiple uncertain drivers of change. *Environmental Health Perspectives*, *127*(6), 67010. https://doi.org/10.1289/EHP4615

Lindgren, E., & Jaenson, T. G. (2006). *Lyme borreliosis in Europe: Influences of climate and climate change, epidemiology, ecology and adaptation measures*. World Health Organization, Regional Office for Europe. https://apps.who.int/iris/handle/10665/107800

MacDonald, E., Vestrheim, D. F., White, R. A., Konsmo, K., Lange, H., Aase, A., Nygård, K., Stefanoff, P., Aaberge, I., & Vold, L. (2016). Are the current notification criteria for Lyme borreliosis in Norway suitable? Results of an evaluation of Lyme borreliosis surveillance in Norway, 1995-2013. *BMC Public Health*, *16*(1), 729. https://doi.org/10.1186/s12889-016-3346-9

Marques, A. R., Strle, F., & Wormser, G. P. (2021). Comparison of Lyme disease in the United States and Europe. *Emerging Infectious Diseases*, *27*(8), 2017–2024. https://doi.org/10.3201/eid2708.204763

Monaghan, A. J., Moore, S. M., Sampson, K. M., Beard, C. B., & Eisen, R. J. (2015). Climate change influences on the annual onset of Lyme disease in the United States. *Ticks and Tick-Borne Diseases*, *6*(5), 615–622. https://doi.org/10.1016/j.ttbdis.2015.05.005

Moore, S. M., Eisen, R. J., Monaghan, A., & Mead, P. (2014). Meteorological influences on the seasonality of Lyme disease in the United States. *The American Journal of Tropical Medicine and Hygiene*, *90*(3), 486–496. https://doi.org/10.4269/ajtmh.13-0180

Mysterud, A., Heylen, D. J. A., Matthysen, E., Garcia, A. L., Jore, S., & Viljugrein, H. (2019). Lyme neuroborreliosis and bird populations in northern Europe. *Proceedings of the Royal Society B: Biological Sciences*, *286*(1903), 20190759. https://doi.org/10.1098/rspb.2019.0759

Mysterud, A., Jore, S., Østerås, O., & Viljugrein, H. (2017). Emergence of tick-borne diseases at northern latitudes in Europe: A comparative approach. *Scientific Reports*, *7*(1), 16316. https://doi.org/10.1038/s41598-017-15742-6

Nelder, M. P., Russell, C. B., Sheehan, N. J., Sander, B., Moore, S., Li, Y., Johnson, S., Patel, S. N., & Sider, D. (2016). Human pathogens associated with the blacklegged tick *Ixodes scapularis*: A systematic review. *Parasites & Vectors*, *9*(1), 265. https://doi.org/10.1186/s13071-016-1529-y

Norwegian Public Health Institute. (2023). *Meldingskriterier for Sykdommer i MSIS*. https://www.fhi.no/publ/informasjonsark/meldingskriterier-for-sykdommer-i-msis/

Nygård, K., Brantsæter, A. B., & Mehl, R. (2005). Disseminated and chronic Lyme borreliosis in Norway, 1995–2004. *Eurosurveillance*, *10*(10), 1–2. https://doi.org/10.2807/esm.10.10.00568-en

Ornstein, K., Berglund, J., Nilsson, I., Norrby, R., & Bergström, S. (2001). Characterization of Lyme borreliosis isolates from patients with erythema Migrans and neuroborreliosis in southern Sweden. *Journal of Clinical Microbiology*, *39*(4), 1294–1298. https://doi.org/10.1128/jcm.39.4.1294-1298.2001

R Core Team. (2022). *R: A language and environment for statistical computing*. Foundation for Statistical Computing.

Rue, H., Martino, S., & Chopin, N. (2009). Approximate Bayesian inference for latent gaussian models by using integrated nested Laplace approximations. *Journal of the Royal Statistical Society: Series B (Statistical Methodology)*, *71*(2), 319–392. https://doi.org/10.1111/j.1467-9868.2008.00700.x

Schwartz, A. M., Hinckley, A. F., Mead, P. S., Hook, S. A., & Kugeler, K. J. (2017). Surveillance for Lyme disease—United States, 2008–2015. *MMWR Surveillance Summaries*, *66*(22), 1–12. https://doi.org/10.15585/mmw.ss6622a1

Schwarzwalder, A., Schneider, M. F., Lydecker, A., & Aucott, J. N. (2010). Sex differences in the clinical and serologic presentation of early Lyme disease: Results from a retrospective review. *Gender Medicine*, *7*(4), 320–329. https://doi.org/10.1016/j.genm.2010.08.002

Simon, J. A., Marrotte, R. R., Desrosiers, N., Fiset, J., Gaitan, J., Gonzalez, A., Koffi, J. K., Lapointe, F. J., Leighton, P. A., & Lindsay, L. R. (2014). Climate change and habitat fragmentation drive the occurrence of *Borrelia burgdorferi*, the agent of Lyme disease, at the northeastern limit of its distribution. *Evolutionary Applications*, *7*(7), 750–764. https://doi.org/10.1111/eva.12165

Skufca, J., De Smedt, N., Pilz, A., Vyse, A., Begier, E., Blum, M., Riera-Montes, M., Gessner, B., Skovdal, M., & Stark, J. H. (2022). Incidence of Lyme neuroborreliosis in Denmark: Exploring observed trends using public surveillance data, 2015–2019. *Ticks and Tick-Borne Diseases*, *13*(6), 102039. https://doi.org/10.1016/j.ttbdis.2022.102039

Stanek, G., & Strle, F. (2018). Lyme borreliosis–from tick bite to diagnosis and treatment. *FEMS Microbiology Reviews*, *42*(3), 233–258. https://doi.org/10.1093/femsre/fux047

Stanek, G., Wormser, G. P., Gray, J., & Strle, F. (2012). Lyme borreliosis. *The Lancet*, *379*(9814), 461–473. https://doi.org/10.1016/S0140-6736(11)60103-07

Statistics Norway. (2022). https://www.ssb.no/en

Steere, A. C., Sikand, V. K., Schoen, R. T., & Nowakowski, J. (2003). Asymptomatic infection with *Borrelia burgdorferi*. *Clinical Infectious Diseases*, *37*(4), 528–532. https://doi.org/10.1086/376914

Steere, A. C., Strle, F., Wormser, G. P., Hu, L. T., Branda, J. A., Hovius, J. W. R., Li, X., & Mead, P. S. (2016). Lyme borreliosis. *Nature Reviews Disease Primers*, *2*(1), 16090. https://doi.org/10.1038/nrdp.2016.90

Steinbrink, A., Brugger, K., Margos, G., Kraiczy, P., & Klimpel, S. (2022). The evolving story of *Borrelia burgdorferi* sensu lato transmission in Europe. *Parasitology Research*, *121*(3), 781–803. https://doi.org/10.1007/s00436-022-07445-3

Strle, F., Wormser, G. P., Mead, P., Dhaduvai, K., Longo, M. V., Adenikinju, O., Soman, S., Tefera, Y., Maraspin, V., & Lotrič-Furlan, S. (2013). Gender disparity between cutaneous and non-cutaneous manifestations of Lyme borreliosis. *PLoS One*, *8*(5), e64110. https://doi.org/10.1371/journal.pone.0064110

Strnad, M., & Rego, R. O. (2020). The need to unravel the twisted nature of the *Borrelia burgdorferi* sensu lato complex across Europe. *Microbiology*, *166*(5), 428–435. https://doi.org/10.1099/mic.0.000899

Sundheim, K. M., Levas, M. N., Balamuth, F., Thompson, A. D., Neville, D. N., Garro, A. C., Kharbanda, A. B., Monuteaux, M. C., & Nigrovic, L. E. (2021). Seasonality of acute Lyme disease in children. *Tropical Medicine and Infectious Disease*, *6*(4), 196. https://doi.org/10.3390/tropicalmed6040196

Thompson, A. E., Anisimowicz, Y., Miedema, B., Hogg, W., Wodchis, W. P., & Aubrey-Bassler, K. (2016). The influence of gender and other patient characteristics on health care-seeking behaviour: A QUALICOPC study. *BMC Family Practice*, *17*(1), 1–7. https://doi.org/10.1186/s12875-016-0440-0

Tulloch, J. S., Christley, R. M., Radford, A. D., Warner, J. C., Beadsworth, M. B., Beeching, N. J., & Vivancos, R. (2020). A descriptive epidemiological study of the incidence of newly diagnosed Lyme disease cases in a UK primary care cohort, 1998–2016. *BMC Infectious Diseases*, *20*(1), 1–13. https://doi.org/10.1186/s12879-020-05018-2

Tulloch, J. S., Semper, A. E., Brooks, T. J., Russell, K., Halsby, K. D., Christley, R. M., Radford, A. D., Vivancos, R., & Warner, J. C. (2019). The demographics and geographic distribution of laboratory-confirmed Lyme disease cases in England and Wales (2013–2016): An ecological study. *BMJ Open*, *9*(7), e028064. https://doi.org/10.1136/bmjopen-2018-028064

Tveitnes, D., & Øymar, K. (2015). Gender differences in childhood Lyme neuroborreliosis. *Behavioural Neurology*, *2015*, 1–6. https://doi.org/10.1155/2015/790762

van Oort, B. E. H., Hovelsrud, G. K., Risvoll, C., Mohr, C. W., & Jore, S. (2020). A mini-review of *Ixodes* ticks climate sensitive infection dispersion risk in the Nordic region. *International Journal of Environmental Research and Public Health*, *17*(15), 5387. https://doi.org/10.3390/ijerph17155387

Vandekerckhove, O., Buck, E. D., & Wijngaerden, E. V. (2019). Lyme disease in Western Europe: An emerging problem? A systematic review. *Acta Clinica Belgica*, *76*(3), 244–252. https://doi.org/10.1080/17843286.2019.1694293

Woudenberg, T., Böhm, S., Böhmer, M., Katz, K., Willrich, N., Stark, K., Kuhnert, R., Fingerle, V., & Wilking, H. (2020). Dynamics of *Borrelia burgdorferi*-specific antibodies: Seroconversion and Seroreversion between two population-based, cross-sectional surveys among adults in Germany. *Microorganisms*, *8*(12), 1859. https://doi.org/10.3390/microorganisms8121859

SUPPORTING INFORMATION

Additional supporting information can be found online in the Supporting Information section at the end of this article.

How to cite this article: Goren, A., Mysterud, A., Jore, S., Viljugrein, H., Bakka, H., & Vindenes, Y. (2023). Demographic patterns in Lyme borreliosis seasonality over 25 years. *Zoonoses and Public Health*, *70*, 647–655. https://doi.org/10.1111/zph.13073

Selected Figures and Tables from Supplementary Materials

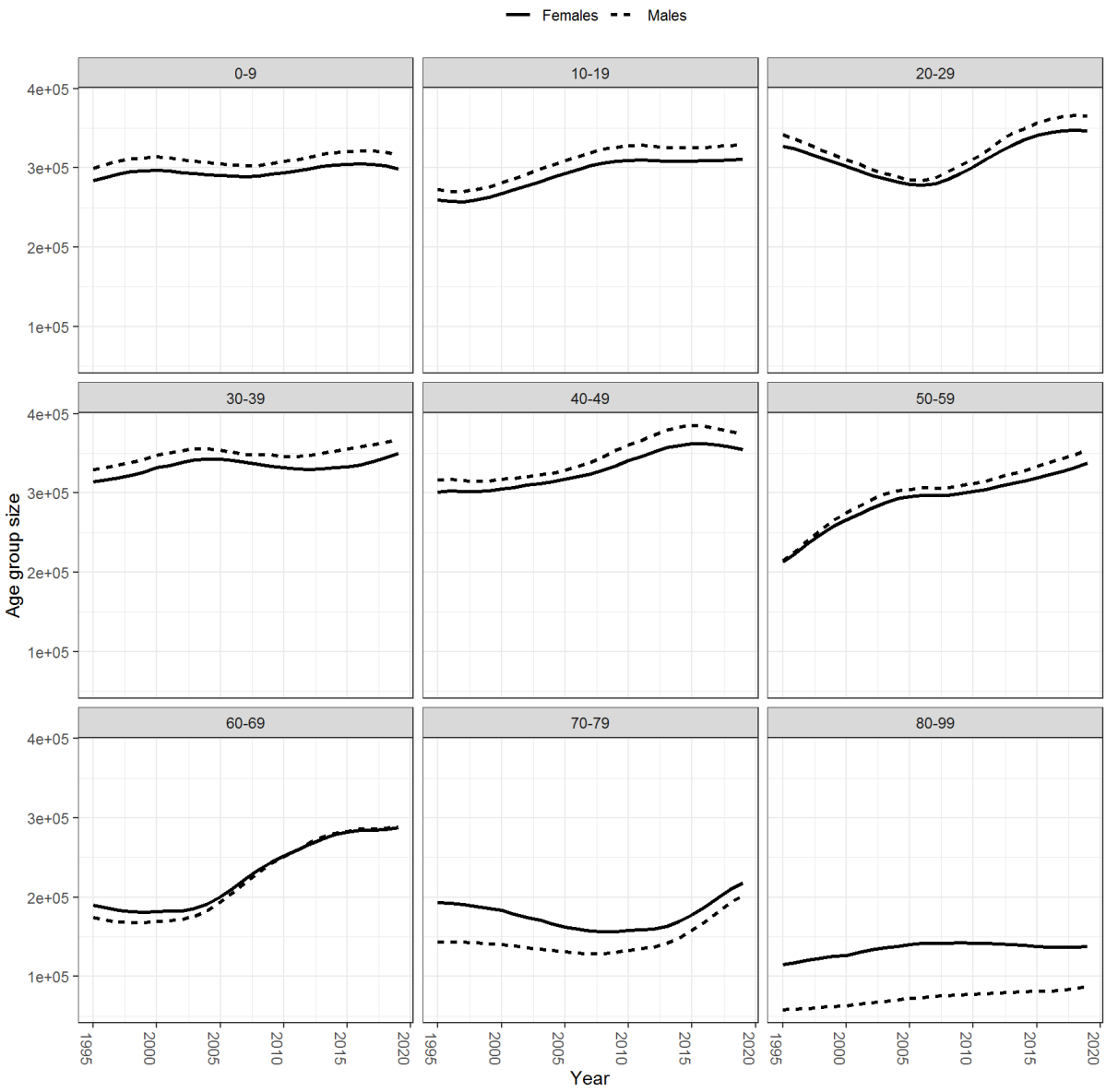

Figure S1. Number of individuals in different demographic age groups (10-year intervals for all groups except the oldest which has a 20-year interval) in Norway over the study period, shown for males and females. Data source: Statistics Norway.

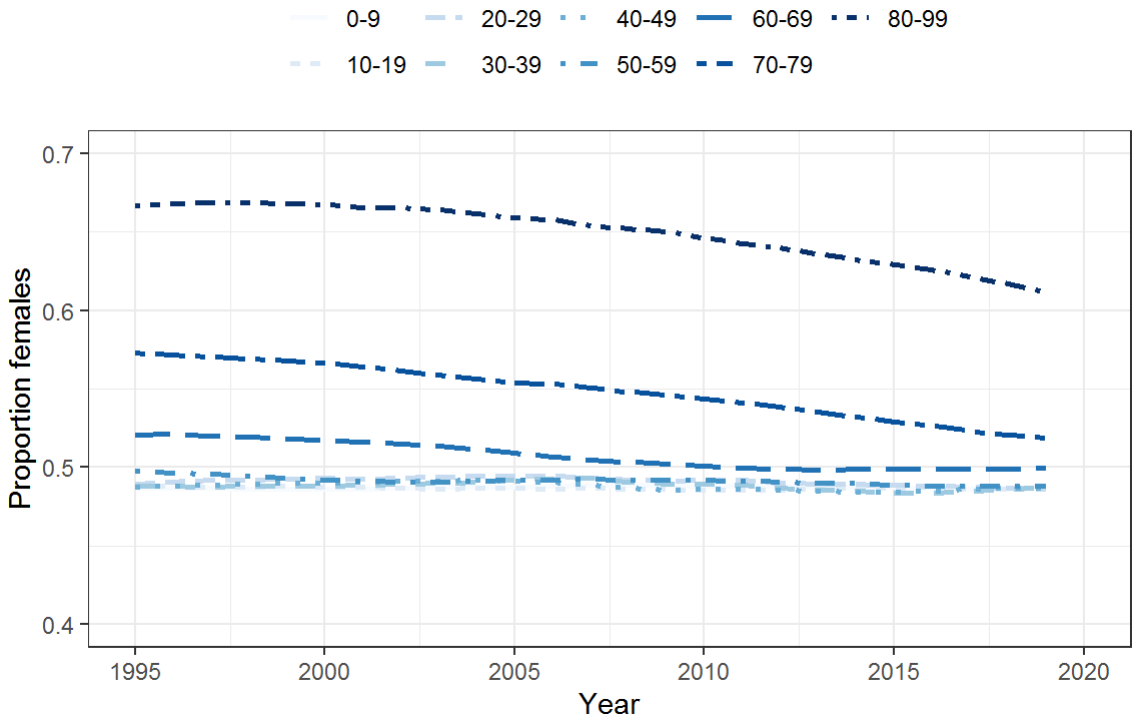

Figure S2. Changing proportion of females in each demographic age group in Norway over time (10-year intervals for all groups except the oldest which has a 20-year interval). Data source: Statistics Norway.

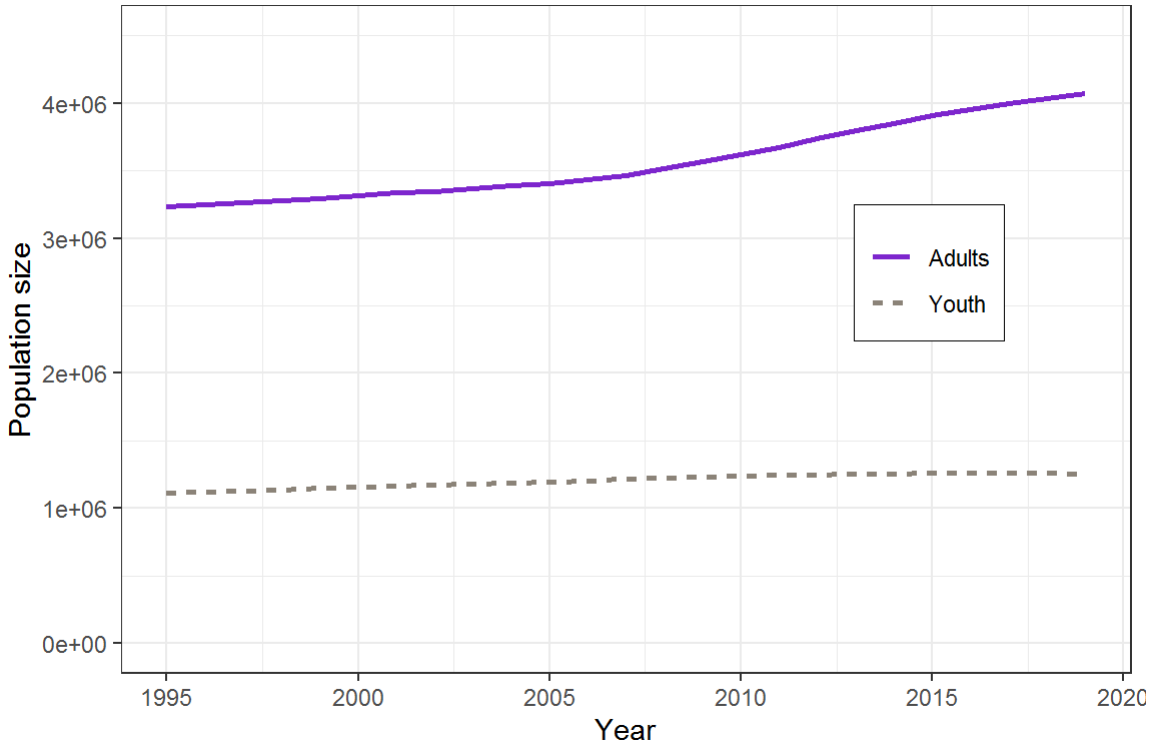

Figure S3. Changes in the population of youth (0-19 years) and adults (20-99 years) during the study period. Data source: Statistics Norway.

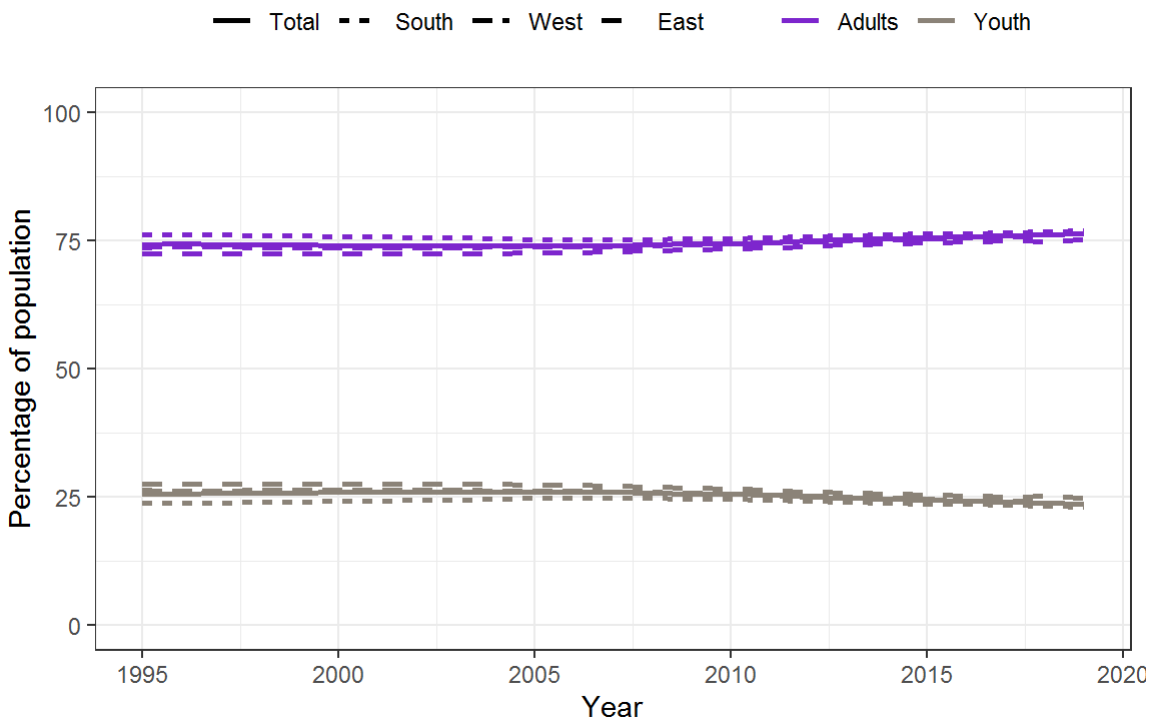

Figure S4. Changing percentage of youth (0-19 years) and adults (20-99) in different regions of Norway over time (South, West and East, see Goren et al. 2023 for definitions of each region). Data source: Statistics Norway.

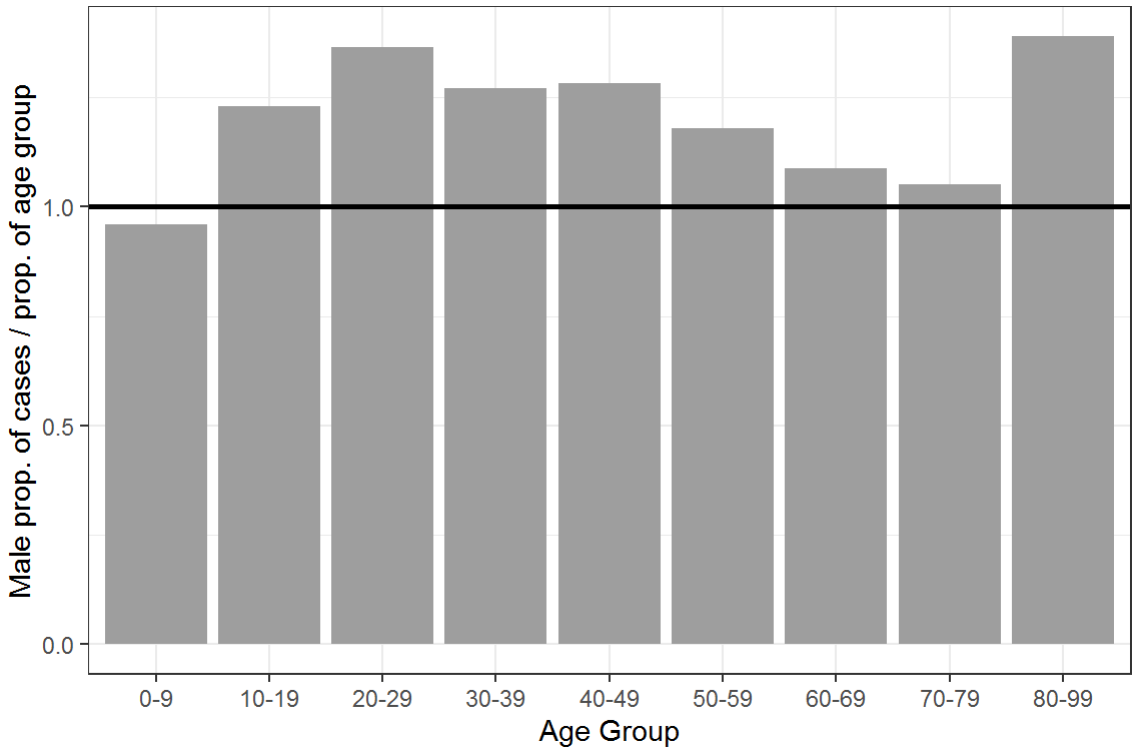

Figure S5. Average male proportion of Lyme borreliosis cases divided by average male proportion in the population data for each age group. A number above 1 indicates an excess of males in the case data relative to the underlying population.

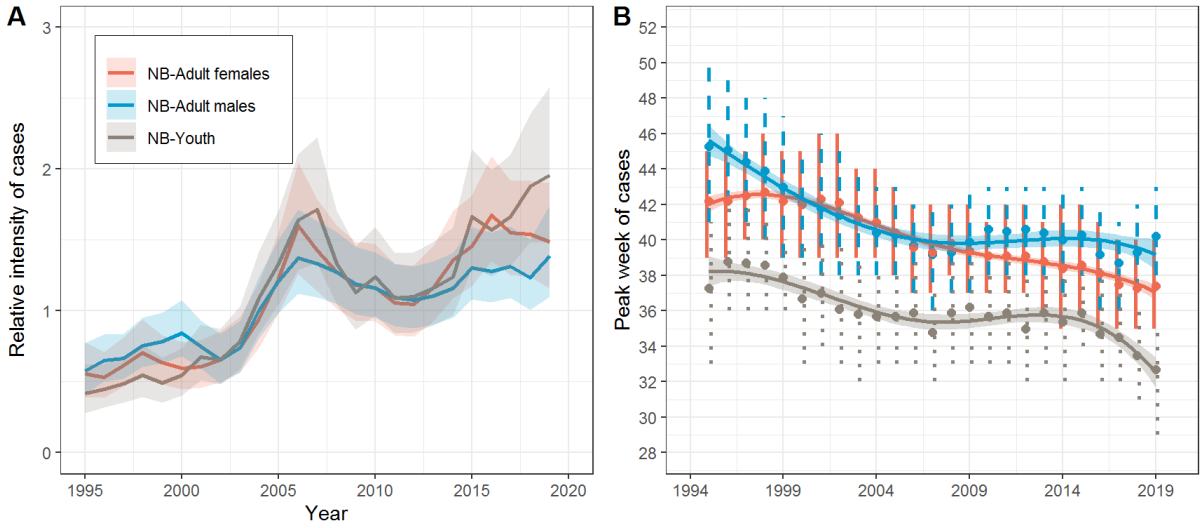

Figure S6. Temporal trends in Lyme neuroborreliosis cases for demographic groups (youth, adult females, and adult males) based on seasonal INLA-models. (A) Inter-annual trend comparison based on the annual components of the models, with shaded 95% credible intervals. The annual components describe relative changes in average weekly cases, not incidence, over the study period. (B) Comparison of changing seasonality measured by predicted seasonal incidence peak. The ribbons represent the 95% confidence intervals on the fitted splines, while the vertical lines represent error margins on the estimated peak incidence weeks based on repeated sampling from the posterior distribution. This figure is the same as Figure 3 in the main text but includes only cases of neuroborreliosis and no other clinical manifestations.

Table S1. Estimated incidences and proportions of clinical manifestations within each demographic group, from annual INLA-models without seasonality.

Demographic Group	Clinical Manifestation	Incidence	Proportion of Cases
Adult Males	Neuroborreliosis	3.67 [3.47, 3.87]	0.55 [0.53, 0.57]
Adult Males	Arthritis	1.11 [0.94, 1.30]	0.17 [0.14, 0.20]
Adult Males	Other	1.23 [1.05, 1.44]	0.19 [0.16, 0.22]
Adult Females	Neuroborreliosis	2.61 [2.45, 2.78]	0.56 [0.53, 0.58]
Adult Females	Arthritis	0.59 [0.48, 0.73]	0.13 [0.10, 0.16]
Adult Females	Other	1.12 [0.94, 1.33]	0.24 [0.20, 0.28]
Youth	Neuroborreliosis	6.36 [6.03, 6.70]	0.79 [0.78, 0.81]
Youth	Arthritis	0.61 [0.50, 0.76]	0.08 [0.06, 0.10]
Youth	Other	0.63 [0.51, 0.77]	0.08 [0.06, 0.10]

3

Modeling the effects of seasonality in tick questing behavior and host demographic turnover on Lyme disease hazard

Asena Goren[1*], Atle Mysterud[1], and Yngvild Vindenes[1]

[1]Centre for Ecological and Evolutionary Synthesis (CEES), Department of Biosciences, University of Oslo, P.O. Box 1066 Blindern, NO-0316 Oslo, Norway.

* author for correspondence: asenag@uio.no

Keywords: *Ixodes ricinus*, Lyme disease, seasonality, disease ecology, compartmental disease model